TABLE OF CONTENTS

THE EFFECTS OF REGIONAL DEVELOPMENT ON THE ILLINOIS RIVER ENVIRONMENT

By

Richard N. DeVries and Don F. Kincannon

ABSTRACT

Little water-quality data exists for the scenic and popular Illinois River Basin in Oklahoma and Arkansas, making it impossible to predict the impact of regional developments on the basin. In this research preliminary studies were made to determine the water quality and quantity characteristics of the river and its tributaries, the assimilative capacity of the river, and the present land use pattern. A statistical analysis of the low flows at gaging stations on the Illinois River, Flint Creek and the Barron Fork were made. Allowable organic waste loadings were investigated and modeled. The National Weather Service River Forecast System's streamflow simulation model was fit to the existing basin data. This model will be used in future studies to determine the correlation between quality and quantity. All of the available water quality data was analyzed along with additional field quality data obtained in 1975 at selected locations. Land use information was obtained using ERTS

The conclusions reached are that the present water quality of the basin is excellent and in order to maintain this quality, models must be developed to predict environmental changes that result from development within the basin.

Keywords: Water Quality Data, Hydrologic Models, Land Use, Illinois River, Stream assimilation capacity

INTRODUCTION

The Illinois River originates in northwest Arkansas as Osage Creek and flows westward until it meets with Muddy Fork, which in turn drains Clear and Goose Creeks. The Muddy Fork system drains the southern portion of the tributary area of the Illinois River in the state of Arkansas while Osage Creek and the upper reaches of Flint Creek drain the northern portion of the tributary area. The Illinois River then crosses the Oklahoma-Arkansas state line and continues running westward. It drains tributaries such as Wedington Creek and Ballard Creek. After Flint Creek joins the Illinois River, the river flows in a southerly direction into the Tenkiller Ferry Reservoir. The major tributaries joining the river in this reach are Barren Fork and Caney Creek. After leaving the Tenkiller Ferry Reservoir, the Illinois River flows southward for a distance of approximately seven miles and drains into the Arkansas River just upstream of the Robert S. Kerr Lock and Dam. The drainage area of the subbasin is 1,660 square miles.

The Illinois River is one of the most scenic rivers in Oklahoma. A fairly large industry providing float trips on this river has developed above Tenkiller Ferry Reservoir. Below the reservoir the river is stocked with trout, providing one of the few trout streams in Oklahoma.

Recently announcements have been made of industrial, municipal, and recreational developments in the basin. The location of a new power generation plant on Little Flint Creek in Arkansas has been proposed. A regional wastewater treatment plant has also been proposed for Siloam Springs, Arkansas. A 600-acre development of retirement and second homes has been proposed in Oklahoma. Individuals also continue to build

homes along the Illinois River. If this type of development continues, the quality of the river could deteriorate.

Very little is actually known about the water-quality characteristics of the Illinois River or its assimilative capacity. Therefore, it is basically impossible to predict the impact of regional developments on the Illinois River.

The objectives of this study were: (1) Determine the hydrologic characteristics of the Illinois River, (2) Determine what field measurements are required, (3) Determine what water-quality data are presently available, and (4) Determine the present land use of the basin.

The following sections detail the research results to meet these objectives.

ANALYSIS OF DROUGHT FLOWS AND OF METHODS FOR DETERMINING THE SELF-PURIFICATION CAPACITY OF THE ILLINOIS RIVER

Low Flow Analysis

General

The design flow for pollution control is usually based on statistical analysis of historical records of drought flow, for it is at low flow that the stream will have the least capacity to assimilate organic waste materials and maintain an acceptable DO concentration. A year is the basic time unit when dealing with streamflow, and the year is usually defined as from March to April for drought flow analysis in order to include the dry part of the year as a whole. The extreme low flow for the year is determined as the average daily flow for drought flows of various durations, with the low 1-day, 7-day, or 30-day average low flow sufficing for many practical applications.

For flood flows, the base time unit of one year yields extreme values which are independent events, but this condition may not hold for drought flows. Hydrological factors influencing drought flow may extend the period through which completely independent minima may occur to over two years for some drainage basins. Therefore, some drought flows determined from records of single years may not truly be drought flows, or completely independent minima from year to year.

Plotting data on probability paper is the most common engineering treatment of statistical data, and requires ranking the occurrences for determining plotting positions. Weibull's plotting position formula is used for many statistical distributions and has also been recommended for extreme value distributions. This formula to determine the probability of an occurrence being less than or equal to a given value is

$$p(x) = \frac{m}{n+1} \tag{1}$$

where m is the rank of the occurrence, n is the total number of occurrences, and p(x) is the probability of an occurrence being less than or equal to x. By ranking occurrences in increasing order of magnitude, using this plotting position formula and plotting on probability paper, the magnitude of an occurrence for any given recurrence interval may be obtained by

$$T(x) = \frac{1}{1-p(x)} \tag{2}$$

where T(x) is the recurrence interval, or the average return period (in years) for an occurrence of a given magnitude.

Since drought flows are a set of extreme values, the applicability of extreme value theory to drought flows is in order. This theory assumes that

the more extreme values deviate from the mean to a greater extent than the values below the mean-a skewed distribution exists for the data.

Gumbel (14) has modified the extreme value theory developed for floods for drought flows. Gumbel's extremal value theory for flood flows is based on the equation:

$$p(x) = e^{-e^{-y}} \tag{3}$$

where e is the base of natural logarithms, and y is a function of the streamflow.

For drought flows, the extreme value distribution developed by Gumbel becomes a three-parameter distribution of the form:

$$p(x) = \exp -\left[\left(\frac{x-\varepsilon}{u-\varepsilon}\right)^{\alpha}\right] \tag{4}$$

where ε is the minimum flow approached and is greater than or equal to zero, while u, x, and α are calculated from the mean ($\overline{X}$), standard deviation (s), and skewness (a) of the distribution.

A test for whether a set of low flow observations conforms to the extreme value theory for low flows is given by Gumbel:

$$\varepsilon \geq 0 \text{ if } \overline{X} + s\left(A(\alpha) - B(\alpha)\right) \geq 0$$

Values of $A(\alpha)$ and $B(\alpha)$ are given in a table developed by Garabedian for observed coefficients of skewness (14). If from this test, ε assumes a negative value, the theory is not applicable for the data.

A result of application of this theory is that the logarithms of drought flows may be plotted versus the probability of the flow being less than or equal to a given severity of drought flow on extremal probability paper. The drought flows are ranked in decreasing order of magnitude for determining their plotting position. Gumbel's extreme value

theory for low flows is thus referred to as Gumbel's logextremal distribution.

The data will plot a straight line if the minimum low flow for the distribution is zero ($\varepsilon=0$), and will be concave downward if the minimum low flow approached is greater than zero ($\varepsilon>0$). A concave upward curve indicates that for the distribution of $\varepsilon<0$ and hence the data does not conform to Gumbel's logextremal distribution for low flows.

Other types of theoretical distributions that have been used to fit low flow data are log-normal and Log Pearson Type III. These distributions are based on three parameters, and are applicable to drought flows in that they assume a minimum value at one end of the distribution. The log-normal distribution can be easily applied graphically by plotting the logarithms of the data on normal probability. A straight line will be formed if the logarithms of the data are a normal distribution.

Fifty-five streams in the State of New York were statistically analyzed for drought flow distributions by log-normal, Log Pearson Type III, and Gumbel's logextremal value methods of theoretically fitting data in a study by O'Connor. The streams were selected on the criterion that the length of record must have been longer than twenty-five years, the stations were to be uniformly distributed throughout the state, and no significant diversions or controls on the streams could be present. The drought flows analyzed were based on the yearly minimum 7-day average low flows.

Conclusions of the study by O'Connor were that the parameters defining the log-normal distribution are more easily understandable and facilitated better understanding of the distribution. Also, the length of record on most of the streams was shorter than thirty years and was too short to draw any definite conclusions concerning the reliability of a fit defined

by any of the three methods. The log-normal method of fitting was recommended from the results of the study.

Matalas, in a study for the United States Geological Survey, analyzed the 7-day average low flow distribution of 40 gaging stations throughout the United States. This was done using theoretical statistical fits of the log-normal, Log Pearson Type III, and Gumbel's log-extremal value distributions. The Gumbel distribution and the Log Pearson Type III were found to best fit the data, and were almost synonomous in their fitting of the data.

Hardison and Martin did a low flow frequency analysis for the United States Geological Survey on 85 stream gaging stations in twenty-two states south of the Great Lakes and east of the Mississippi, but also including Arkansas, Oklahoma, Louisiana, Missouri, and Texas. The study was done using logextremal probability paper to define all of the distributions graphically. The data was plotted for several durations of low flow, varying from the 7-day average to the 274-day average low flow. The variability of the resulting curves indicated that much difficulty would be encountered in attempting to fit a single theoretical statistical distribution to all of the data at every station. The Mountain Fork River near Eagletown, Oklahoma, exhibited a very steeply sloping, concave upward curve that was not duplicated by any of the other streams in the study.

Some of the questions raised in the report by Hardison and Martin were to what extent the slope of the curves depended on the rate of base flow recession, and to what extent the frequency distribution was influenced by the length of dry periods. Also, to what extent the spacing

between curves of low flows at different duration periods depended upon the rainfall that falls during periods of low flow was asked by the report.

Valz recommends the use of Gumbel's logextremal probability paper and explains in detail the application of this method. His work was done principally on predicting low flows for various water courses in the State of Michigan. From the results of these studies, he presented a method for graphically analyzing the case of a concave downward curve on logextremal probability paper. This is for the case when the minimum flow approached is greater than zero from Gumbel's theory. This method can also be applied to certain cases of flow regulation.

Riggs in a survey of the results from various theoretical statistical and logextremal graphical analyses of drought flows, including those cited in this literature review, concluded that:

1) A long streamflow record is best for determining low flow characteristics in a basin. In the absence of a long period of record, correlation of the data with that of neighboring basins to extend the period of record is desirable if a good correlation of observed data exists.

2) Particular basin characteristics define the shape of the frequency curve; no one shape is generally applicable.

3) The effects of basin characteristics and sampling errors are much greater than errors in fitting a curve to plotted points; thus, the use of a theoretical distribution has little if any advantage over a graphical fit.

Kincannon, Kao, and Stover studied the low flow distributions of three gaging stations located on Bird Creek and the Arkansas River in northeastern Oklahoma. The distributions were fitted using the Johnson S_B distribution and Gumbel's extreme value distribution for low flows.

This was done for the 1, 3, 7, 14, 30, 60, and 90-day low flows for the streams. Nearly all of the flow distributions at the three stations had a lower flow limit of zero. Two cases, the 60 and 90-day low flows on the Arkansas River, had a lower flow limit greater than zero. The Johnson S_B distribution gave a better fit for the flows on the Arkansas River, while Gumbel's distribution gave the best fit for the small flow station on Bird Creek. It was concluded from this study that the Johnson S_B distribution, which assumes both an upper and lower limit for the drought flows, gave a better fit of the data.

A low flow analysis was done by the United States Geological Survey on the Barren Fork at Eldon, and the Illinois River at Tahlequah in 1959. This study was done by plotting the data on logextremal probability paper. The data was correlated with the White River in Arkansas in order to extend the period of record. The graphs presented in the report by the USGS show straight line plots at Eldon for the 7- and 30-day low flow durations, and presents two intersecting straight lines at an obtuse angle at Tahlequah for the 7- and 30-day average low flows. The first line was moderately sloping for probabilities less than 80 percent, and very steeply sloping for probabilities greater than 80 percent. The flows at the 10-year recurrence interval for the 7- and 30-day average low flow distributions were determined to be 12 cfs and 20 cfs, respectively, at Tahlequah and 4.2 cfs and 5.7 cfs at Eldon on the Barren Fork. No discussion was given concerning these plots, and no data points were plotted to define the lines.

The consensus of the work done on low flows is that Gumbel's log-extremal distribution is the most generally applicable for low flow data. Plotting the data on logextremal probability paper facilitates defining this distribution. This was done for the gaging stations at Tahlequah

and Eldon in the Illinois River basin by the United States Geological Survey, but was done using 16 years less data than is now available. An examination of the applicability of Gumbel's logextremal theory to stations in the Illinois River basin was made and will be further explained in the results section.

Methods of Study

There are six United States Geological Survey streamflow gaging stations in the Illinois River basin, and are located as shown on a map of the basin on Figure 1. Pertinent data concerning these gaging stations is given in the following table:

TABLE I

STREAMFLOW GAGING STATIONS FOR THE ILLINOIS RIVER BASIN IN OKLAHOMA

USGS Gaging Station	Location	Drainage Area	Period of Record
07195500	Illinois River, near Watts, Oklahoma	635 $mi.^2$	8/55 to 9/73
07196000	Flint Creek, near Kansas, Oklahoma	110	8/55 to 9/73
07196500	Illinois River, at Tahlequah, Oklahoma	959	10/35 to 9/73
07197000	Barren Fork, near Eldon, Oklahoma	307	10/48 to 9/73
07198000	Illinois River, near Gore, Oklahoma	1626	4/39 to 9/73

Daily records of streamflow are published by the United States Geological Survey in the annual series "Surface Water Supply of the United States, Part 7" (4), with more recent daily data available in "Water Resources Data for Oklahoma, Part 1" (5).

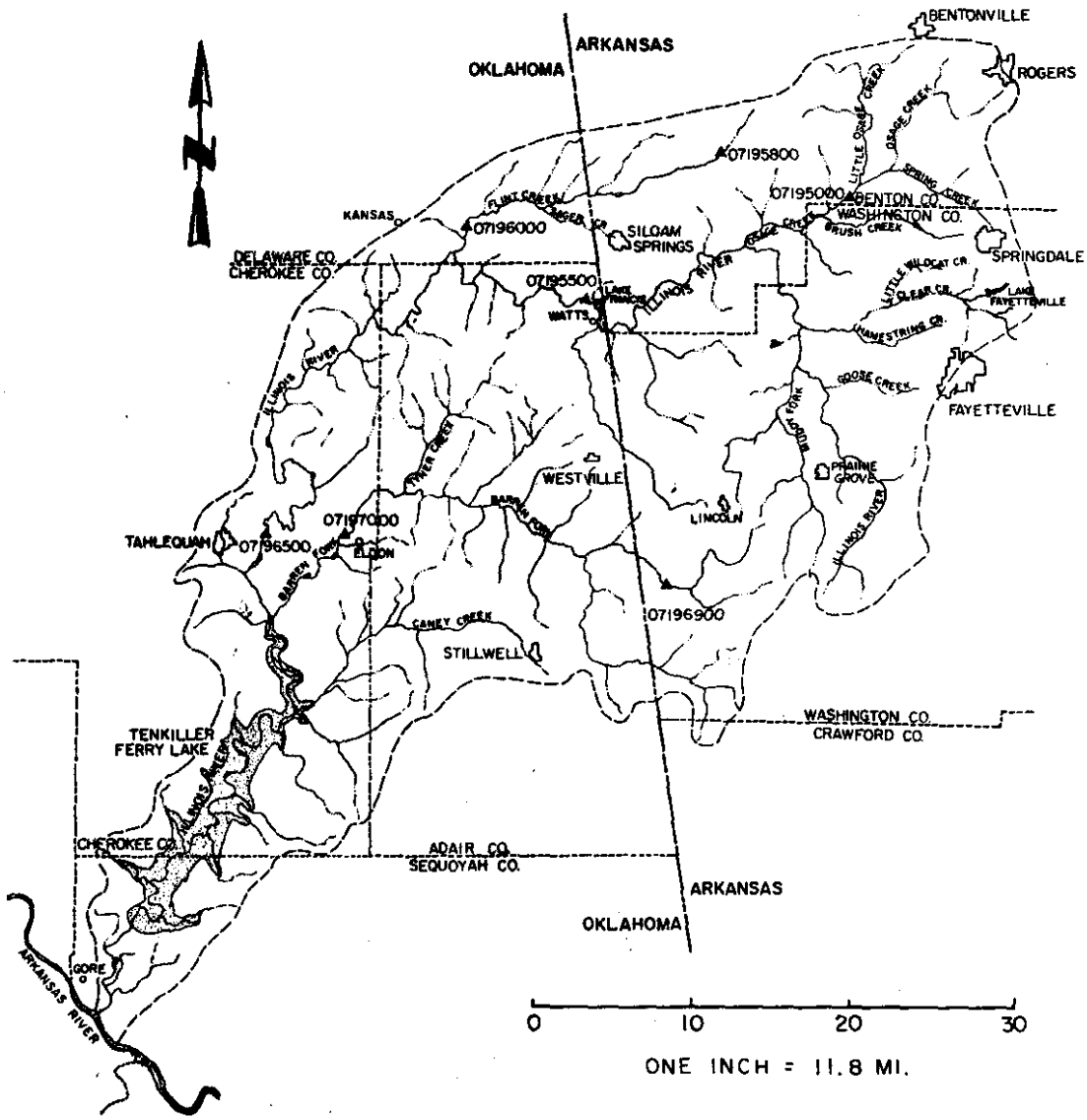
BENTONVILLE
ROGERS
OKLAHOMA
ARKANSAS
07195800
07195000
BENTON CO.
WASHINGTON CO.
KANSAS
07196000
SILOAM SPRINGS
SPRINGDALE
DELAWARE CO.
CHEROKEE CO.
07195500
ILLINOIS RIVER
WATTS
LAKE FAYETTEVILLE
FAYETTEVILLE
GOOSE CREEK
WEST VILLE
PRAIRIE GROVE
LINCOLN
TAHLEQUAH
07196500
07197000
ELDON
07196900
CANEY CREEK
STILLWELL
TENKILLER FERRY LAKE
WASHINGTON CO.
CRAWFORD CO.
CHEROKEE CO.
ADAIR CO.
SEQUOYAH CO.
ARKANSAS
OKLAHOMA
GORE
ARKANSAS RIVER
0
10
20
30
ONE INCH = 11.8 MI.

Figure 1.

The historical records for discharge measurements at gaging stations on the Illinois River near Watts (07195500) and near Tahlequah (07196500), Flint Creek near Kansas (07196000), and the Barren Fork at Eldon (07197000) were the stations analyzed for low flows. For each water year, rather than the period from March to April recommended for drought flows, the lowest 1-day, 7-day, and 30-day average flow was recorded. These values were then ranked in decreasing order of magnitude as recommended for drought flow analysis. The plotting positions for these ranked flows were obtained from the formula: plotting position = $m/(n+1)$. The values of flow and the logarithms of the values were then plotted versus their plotting positions on normal probability paper and extremal probability for the 7-day average low flows. This was done to find the best graphical definition of the drought flow distributions at the gaging stations. Parameters to further statistically define each distribution, such as the mean ($\bar{x}$), standard deviation (s), coefficient of variability (C_v), and coefficient of skewness (C_s) were then calculated from the data. This type of procedure was also carried out for the 1- and 30-day low flows, with the step of plotting on different types of probability paper eliminated since these distributions paralleled the 7-day average low flow distributions.

Results of Low Flow Analysis

The plots of the data revealed that at Watts, Tahlequah and Kansas, the yearly low flow distributions were nearly normal. The skewness that would be expected of a distribution bounded by a minimum value was not present.

Taking the coefficients of skewness calculated at the gaging stations for the 7-day low flows and testing them for fitting a logextremal distribution by using the test equation proposed by Gumbel, equation (5)

$$\varepsilon \geq 0 \text{ if } \bar{x} + S \quad A(\alpha) - B(\alpha) \quad \geq 0 \tag{5}$$

yields the results shown in Table II

TABLE II

TESTING FOR A LOGEXTREMAL DISTRIBUTION

Gaging Station	C_s	$\bar{X} + S\ A(\alpha) - B(\alpha)$
Watts 07195500	0.347	-20.0
Kansas 07196000	-0.206	-16.2
Tahlequah 07196500	0.193	-51.9
Eldon 07197000	5.22	11.5

According to Gumbel, since $\varepsilon<0$ for the low flows at Watts, Tahlequah and Kansas, the extreme value theory for drought flows is not applicable. The plotting of the logarithms of the drought flow on Gumbel extreme value probability paper yields a curve which is concave upward. This curve cannot be accurately fit by eye and indicates that Gumbel's theory is not applicable for the data. The same conclusion can be made for the log-normal fit of the distribution, as again a concave upward curve was found from the plotting of the logarithms of flow on normal probability paper.

Analyzing the low flows graphically on normal probability paper seems to be the best way to interpret the low flow distributions observed at Watts, Tahlequah, and Kansas. A possible reason that these distributions

are nearly normal is the high degree of flow variability of these streams in the Oklahoma hills--extreme drought flows in some years being very much below the mean drought flow, and a variable base flow that depends upon the severity of drought as well as the physical basin characteristics. These distributions do not conform to Gumbel's logextremal theory, and cannot accurately be treated graphically as distributions approaching a minimum flow greater than or equal to zero.

The graphs on normal probability paper for the 1-, 7-, and 30-day low flows at the four gaging stations studied are presented in Figures 4, 5, 6, and 7. Since the data fit a straight line for the stations at Watts, Kansas, and Tahlequah on normal probability paper, the mean and standard deviation were calculated, then compared to the mean and standard deviation that were observed from the best graphical fit of a straight line. The coefficient of variability was then calculated for both of these cases, and the coefficient of skewness was computed for the data sets of the 7-day average flows since the 7-day average is the most often used in decreeing a design low flow. These statistical parameters are given with the respective graphs.

For the gaging stations at Watts (Figure 2), the theoretical best fit from the mean and standard deviation did not seem to be as good as a line drawn to fit the points graphically. The graphical mean was determined to be lower than the computed mean for the 1- and 7-day low flows, while a good straight line fit of the data could not be observed with the 30-day average low flows. A best straight line fit on the graph yielded a mean which was higher by six cfs than the computed mean of the data. The standard deviations determined from these best straight line fits were higher for the three flow distributions than a theoretical

fit of the data would have determined. The coefficient of variability was thus higher from the graphical determination than that computed from the data. A high coefficient of variability of 0.60 for the 7-day average low flow was determined from the graphs, with coefficients of variability of 0.62 and 0.65 for the 1- and 30-day average low flows, respectively. The coefficient of skewness was found to be 0.347 for the 7-day average low flow data. This skewness toward the high flow side is probably attributable to the two high flows at the lowest probabilities that do not fit on the line of the drought flow trend. As discussed by Velz, these may not truly be drought flows.

The means calculated from the data for the gaging station at Kansas (Figure 3) closely define the observed fits on the graphs. The standard deviations, however, are observed to be greater by the lines formed from plotting the data than those calculated from the data for the 1- and 7-day average low flows--8.4 versus 7.1, and 8.1 versus 7.3, respectively. Two flows at the lowest frequencies for the 30-day average low flows are much greater than would seem in line with the rest of the data, and thus the standard deviation from the graph is much less than that computed from the data, 10.6 versus 12.8. Approximately the same variability of the flows at this gaging station is observed as was noted for the Watts gaging station, C_v being 0.67, 0.60, and 0.54 for the 1-, 7-, and 30-day average low flows, respectively. The coefficient of skewness was calculated to be -0.206, or the distribution was skewed to the low flow side for the 7-day average low flows.

Thirty-eight years of data have been collected at the Tahlequah gaging station (Figure 4), and the means and standard deviations calculated for the 1-, 7-, and 30-day average low flows are very close to those

graphically observed to be more representative of the trend of the major population of the data. The standard deviations again seemed to be slightly greater from a plot of the data than those calculated, so the greater slopes were used since this yields a slightly more conservative estimate of low flows for frequencies greater than 50 percent. The coefficients of variability were much like those for Watts and Kansas, being 0.66, 0.60, and 0.62 for the 1-, 7-, and 30-day average low flows. The data for the 7-day average low flows was skewed slightly right, C_s calculated to be 0.193. Like the stations at Watts and Kansas, the 1- and 7-day average low flows better defined a straight line than the 30-day average low flows. For all three gaging stations, the data points were most tightly knit about a line for the 7-day average low flows.

The Barren Fork at Eldon (Figure 5) exhibited a different type of plot in that the flows were noticeably skewed from the graphical analyses. The coefficient of skewness was calculated to be 5.22 from the 7-day average low flows. This data could have been fit by logextremal theory for drought flows as a limiting flow is approached at the lower magnitudes of flow for the distribution. Plotting these data on logextremal probability paper yielded approximately straight lines, unlike for the other three gaging stations. The graphs included are on normal probability paper. The coefficient of variability was calculated to be approximately 0.74 for all three flow distributions, but the meaning of this value is not the same as for the other three gaging stations, since the distribution is highly skewed.

Decisions related to drought flow usually center around a 10-year recurrence interval, and the Environmental Protection Agency has designated that a 7-day average 10-year recurrence low flow should be used

Figure 2. The 1-, 7-, and 30-day Average Low Flow Distributions for Watts (07195500), n = 18 years

1-day Average Low Flows

	Computed	Graphically Determined
$\bar{X}$	62.5	60.8
S	36.0	38.0
C_v	.58	.62

7-day Average Low Flows

	Computed	Graphically Determined
$\bar{X}$	73.4	70.2
S	39.4	42.5
C_v	.54	.60
C_s	.35	-

30-day Average Low Flows

	Computed	Graphically Determined
$\bar{X}$	109.2	115.0
S	62.2	75.0
C_v	.57	.65

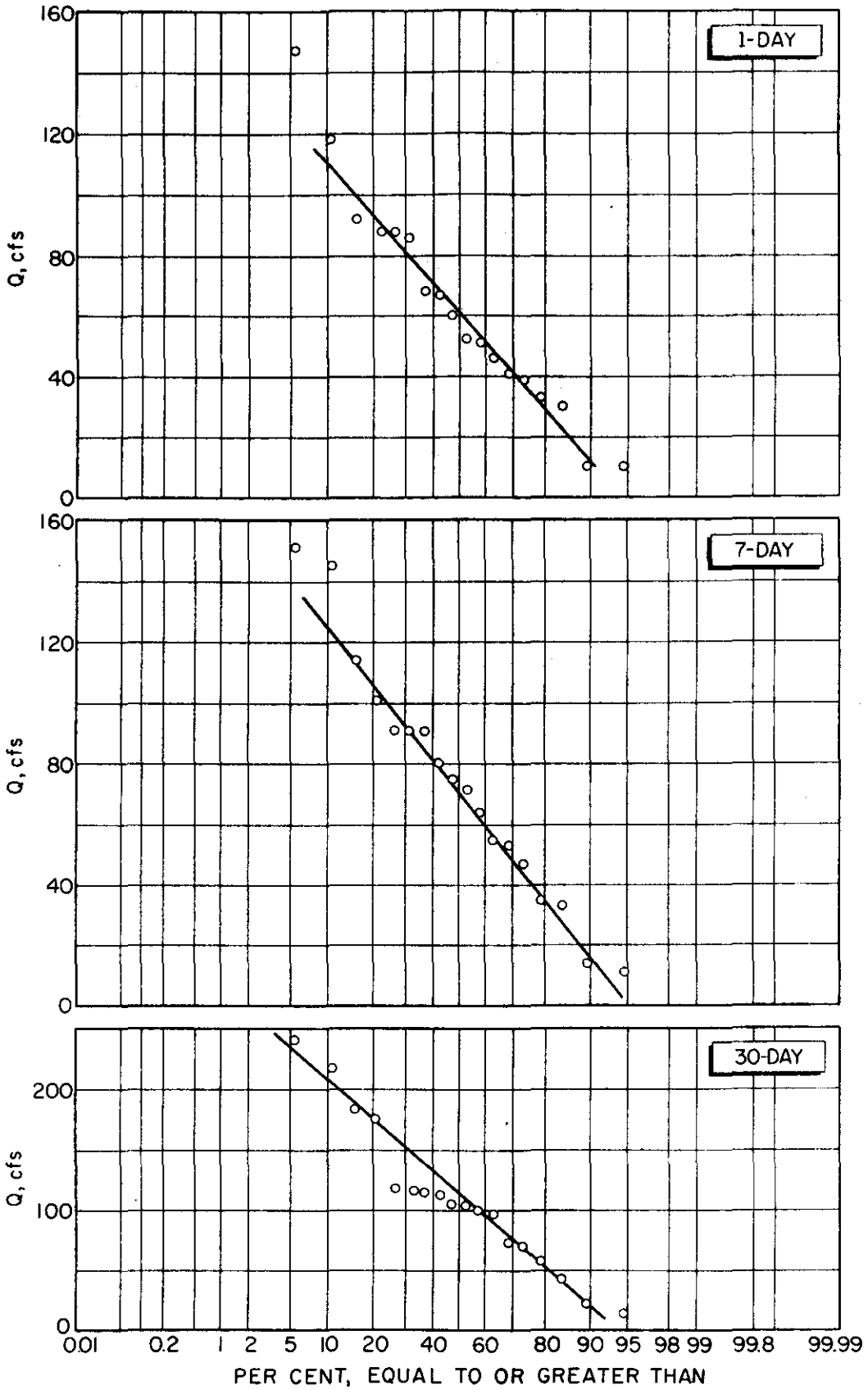
1-DAY
7-DAY
30-DAY
Q, cfs
160
120
80
40
0
200
100
0.001
0.2
1
2
5
10
20
40
60
80
90
95
98
99
99.8
99.99
PER CENT, EQUAL TO OR GREATER THAN

Figure 3. The 1-, 7-, and 30-day Average Low Flow Distributions for Kansas (07196000), n = 18 years

1-day Average Low Flows

	Computed	Graphically Determined
$\bar{X}$	12.6	12.5
S	7.1	8.4
C_v	.56	.67

7-day Average Low Flows

	Computed	Graphically Determined
$\bar{X}$	13.6	13.6
S	7.3	8.1
C_v	.54	.60
C_s	-.21	-

30-day Average Low Flows

	Computed	Graphically Determined
$\bar{X}$	20.8	19.5
S	12.8	10.6
C_v	.62	.54

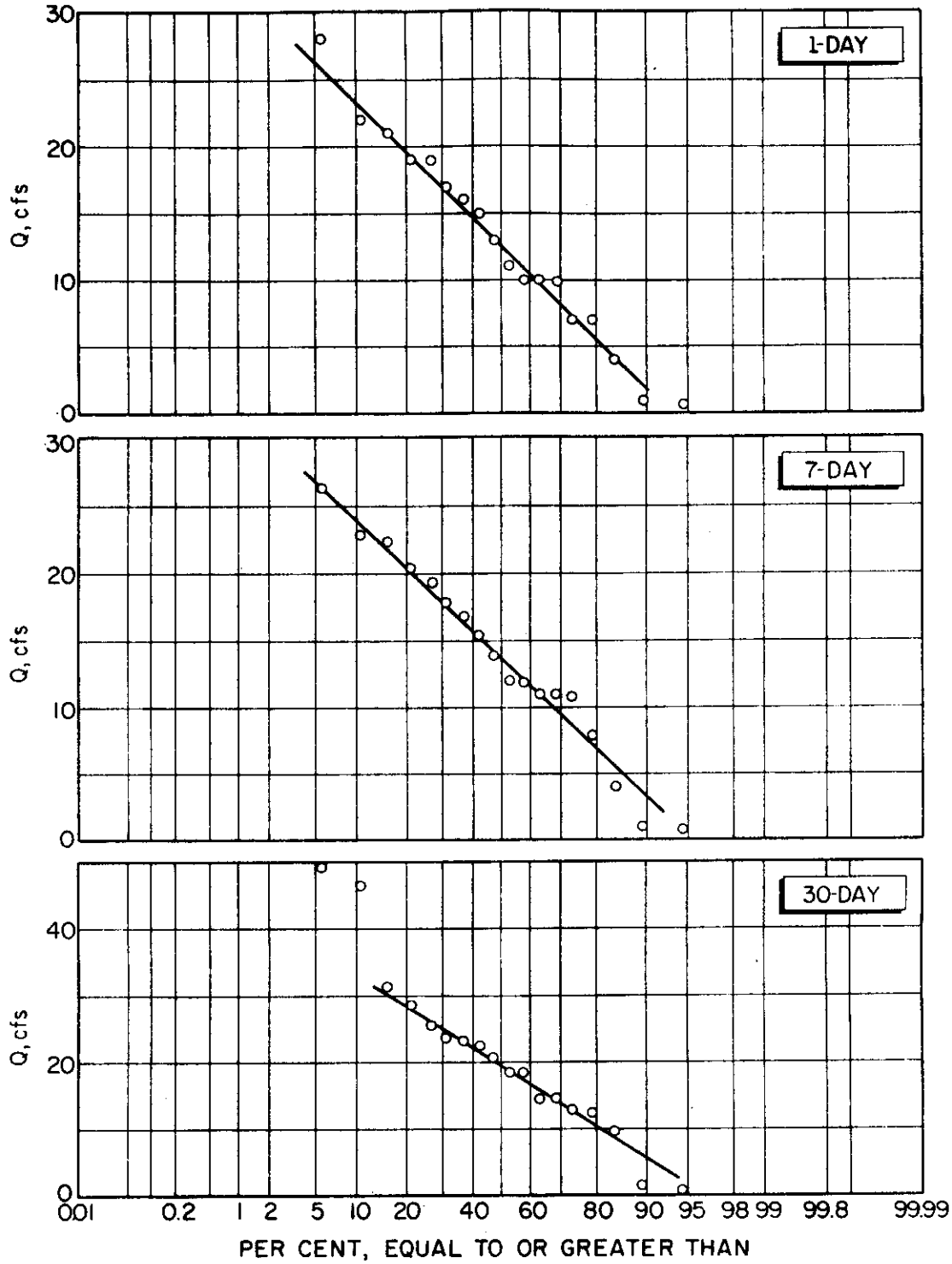
1-DAY
7-DAY
30-DAY
Q, cfs
30
20
10
0
40
0.001
0.2
1
2
5
10
20
40
60
80
90
95
98
99
99.8
99.99
PER CENT, EQUAL TO OR GREATER THAN

Figure 4. The 1-, 7-, and 30-day Average Low Flow Distributions for Tahlequah (07196500), n = 38 years

	Computed	Graphically Determined
1-day Average Low Flows		
$\bar{X}$	87.9	88.0
S	52.9	58.0
C_v	.60	.66
7-day Average Low Flows		
$\bar{X}$	95.0	94.0
S	55.3	57.0
C_v	.58	.60
C_s	.19	-
30-day Average Low Flows		
$\bar{X}$	133.8	133.0
S	82.3	82.0
C_v	.62	.62

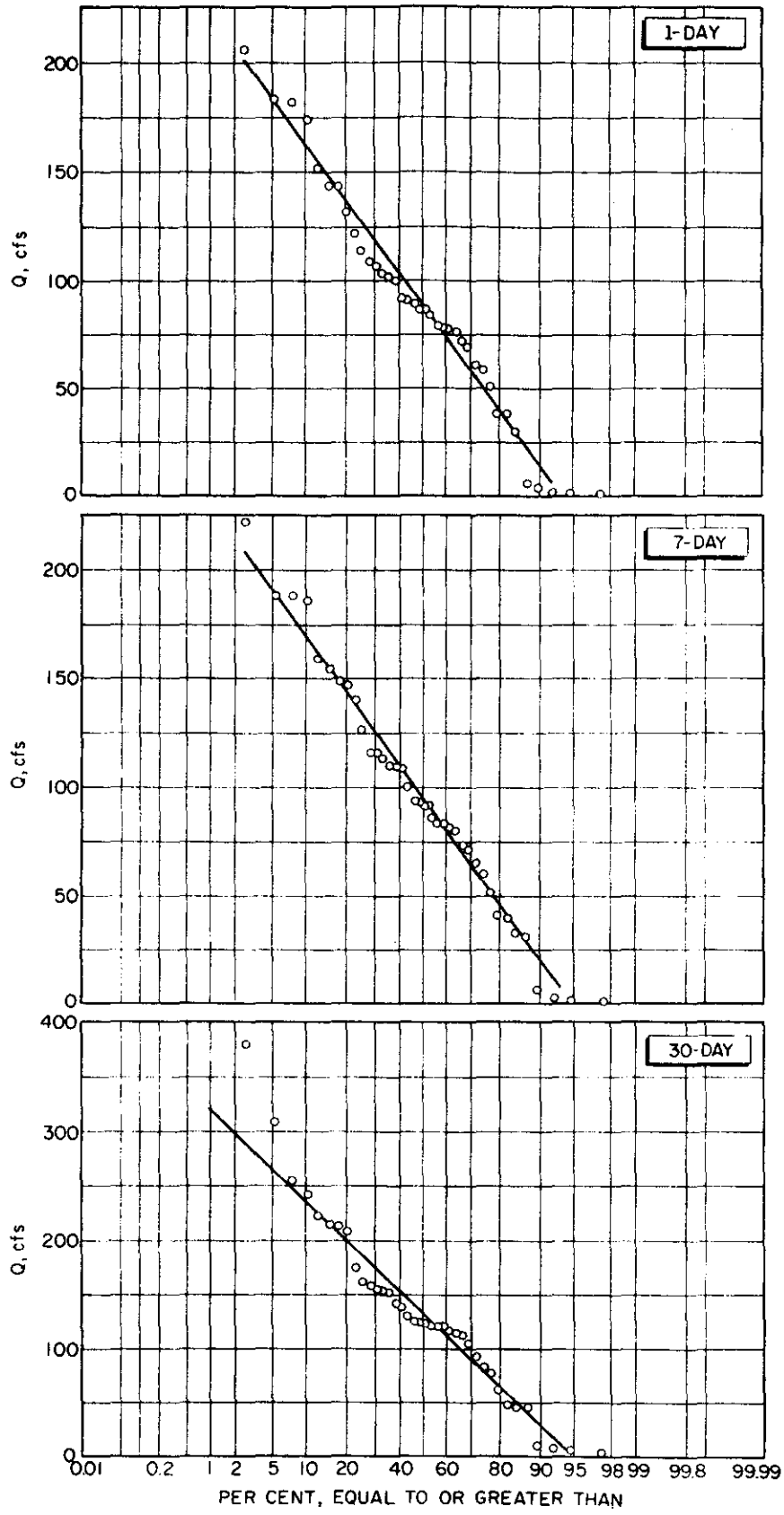
1-DAY
7-DAY
30-DAY
Q, cfs
200
150
100
50
0
400
300
0.01
0.2
1
2
5
10
20
40
60
80
90
95
98
99
99.8
99.99
PER CENT, EQUAL TO OR GREATER THAN

Figure 5. The 1-, 7-, and 30-day Average Low Flow Distributions for Eldon (07197000), n = 25 years

Computed from Data

	1-day Average Low Flows	7-day Average Low Flows	30-day Average Low Flows
$\bar{X}$	17.2	18.4	27.4
S	12.9	13.6	20.1
C_v	.75	.74	.73
C_s	-	5.22	

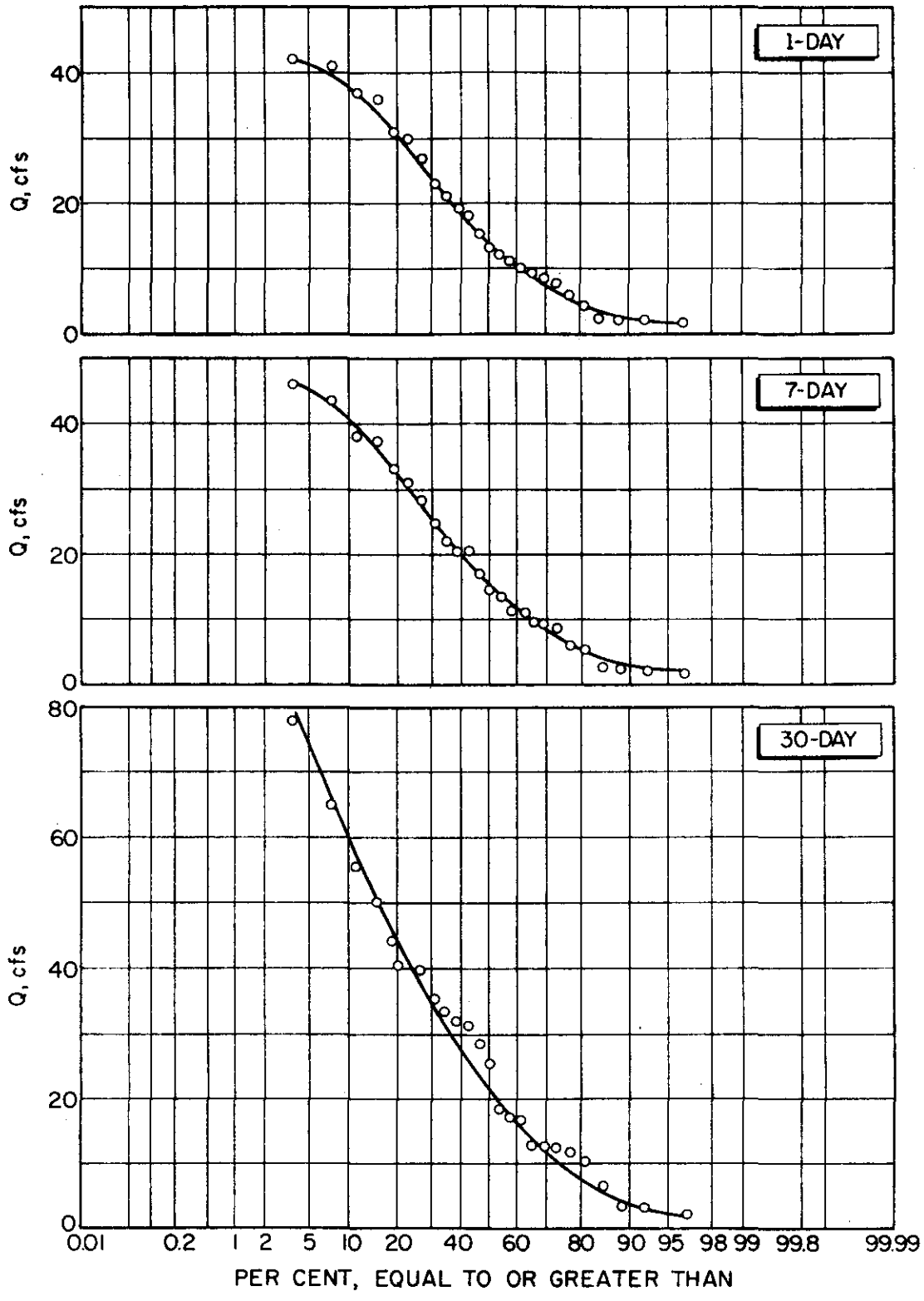
1-DAY
7-DAY
30-DAY
Q, cfs
0
20
40
60
80
0.01
0.2
1
2
5
10
20
40
60
80
90
95
98
99
99.8
99.99
PER CENT, EQUAL TO OR GREATER THAN

for design purposes. The 1-, 7-, and 30-day averages at a 10-year recurrence interval were taken from the graphs at the four gaging stations. These low flows are listed in Table III.

TABLE III

10-YEAR RECURRENCE INTERVAL LOW FLOWS (cfs)
(fraction of mean low flow in parentheses)

Station	1-day Average		7-day Average		30-day Average	
Watts 07195500	12	(0.20)	16	(0.23)	20	(0.17)
Kansas 07196000	1.8	(0.14)	3.3	(0.24)	5.8	(0.30)
Tahlequah 07196500	14	(0.16)	20	(0.21)	28	(0.21)
Eldon 07197000	2.3	(0.13)	2.8	(0.15)	3.5	(0.13)

The 10-year recurrence low flows at Tahlequah for the 7- and 30-day average low flows were determined to be 20 and 28 cfs, compared to 12 and 20 cfs determined in the 1959 United States Geological Survey study. The 1959 study was made using logextremal probability paper, and with sixteen fewer years of record, which explains the differences in the values obtained. The 10-year recurrence interval low flows computed in this report were very low compared to usual flows in these streams, being even less than one-quarter of the mean yearly low flow for all except the 30-day average low flows on Flint Creek. This characteristic was also indicated by the high coefficient of variability calculated for these low flow distributions.

A further quantitative analysis of the 10-year recurrence interval

low flows is made possible by comparing the yields listed in Table IV. The yield is defined as the ratio of the flow to the drainage area above the station and can be used to compare the different gaging stations. It can be seen that at the 7-day average low flows, the flow on Flint Creek shows the highest yield, 0.030. A higher yield is recorded at Watts (0.025) than at Tahlequah (0.021) for the 7-day average flow, with the Barren Fork showing a very poor yield of 0.009. The gaging stations at Watts and Tahlequah show approximately the same variability in yield for the different drought flow durations. The Flint Creek shows a wider variability in yield between the 1-, 7-, and 30-day low flows than Watts and Tahlequah, while the Barren Fork near Eldon shows little variation in yield between the different low flow durations. This is probably due to a reliable base flow being the 10-year recurrence flow for all three low flow durations on the Barren Fork. In studies done in Michigan, Velz considered 7-day average 10-year drought flow yields of 0.1 to be very low. The very low yields calculated at the four gaging stations in the Illinois River basin are indicative of the severe dry summer periods for which Oklahoma is noted.

TABLE IV

YIELD FOR 10-YEAR RECURRENCE INTERVAL LOW FLOWS

cfs/mi^2

Station	1-day Average	7-day Average	30-day Average
Watts 07195500	0.019 0.019	0.025 0.025	0.032 0.032
Kansas 07196000	0.016	0.030	0.053
Tahlequah 07196500	0.015	0.021	0.029
Eldon 07197000	0.007	0.009	0.011

Streeter-Phelps Equation and Busch's Five Minute Solution to Stream Assimilation Capacity

General

The understanding of the importance of dissolved oxygen in relation to the ability of a stream to oxidize organic matter owes much to the pioneer work in sewage biochemistry done in England near the end of the 19th Century, and continued in America after the turn of the century. Studies on the nature of organic stream self-purification were empirical in that recording stream conditions in analytical terms was made with no development made toward a set of general principles.

The first attempt at mathematically defining stream self-purification was made by Streeter and Phelps. The concepts and mathematical formulations which they presented are still being used with little modification in many instances even today although with much reservation.

Streeter and Phelps viewed the deoxygenation characteristics of a stream as the liabilities on a balance sheet, and reaeration as assets which must be related to time, temperature, and other physical characteristics of the stream. The governing law they presented for deoxygenation was "the rate of biochemical oxidation of organic matter is proportional to the remaining concentration of unoxidized substance, measured in terms of oxidizability" or

$$-\frac{dL}{dt} = K_1 L \tag{6}$$

where L is the oxygen demand of the organic substance remaining, t is the time elapsed, and K_1 is a constant defining the rate at which the reaction proceeds. On the reaeration side of the balance, the rate of oxygen

replenishment was found to be proportional to the oxygen deficit remaining at any time, or

$$-\frac{dD}{dt} = K_2 D \tag{7}$$

where D is the oxygen saturation deficit, t is the time elapsed, and K_2 is a constant affecting the rate of oxygen transfer across the interface. Taking these two factors, deoxygenation and reaeration, and adding them as on a balance sheet, yields the differential equation:

$$\frac{dD}{dt} = K_1 L - K_2 D \tag{8}$$

which, when solved, yields the classical Streeter-Phelps equation:

$$D = \frac{K_1 L_a}{K_2 - K_1} \left(e^{-K_1 t} - e^{-K_2 t} \right) + D_a e^{-K_2 t} \tag{9}$$

where D_a is the initial dissolved oxygen saturation deficit, D is the saturation deficit at time t, and L_a is the initial ultimate oxygen demand, all in mg/l; t is the time elapsed in days, and K_1 and K_2 are the coefficients of deoxygenation and reaeration in $days^{-1}$.

Though it is used in many practical problems, there are many problems associated with the concepts and usage of the Streeter-Phelps sag equation. The equation is based on the assumptions that

1) the flow is steady and uniform throughout the reach,

2) there is only one source of pollutant discharge per reach, a point discharge which upon mixing becomes constant in concentration throughout the cross-sectional area of flow,

3) there is only one type of oxygen demand in the reach, and that is caused by the point discharge,

4) oxygen transfer takes place only from the atmosphere to the stream,

5) reaeration and deoxygenation can be defined by first-order decreasing rate equations, and

6) the coefficients of deoxygenation and reaeration are constant for a given reach.

In the second assumption, the value of the initial oxygen demand will not properly define the amount of organic material in the reach if there are other inflows, channel scouring, or sedimentation adding or subtracting organic material. Also, there will be a time and distance involved in the complete mixing of the pollutant which will depend on stream characteristics such as cross-section and velocity.

The third assumption eliminates the existence of abnormal oxygen demands in the stream such as nitrification, benthnic and sludge deposits, immediate oxygen demands such as the oxidation of hydrogen sulfide, and biological extraction and accumulation on rocks and shorelines (12). Photosynthetic organisms can also cause an abnormal depletion of oxygen through respiration at night, then produce oxygen by photosynthesis, serving as a source of oxygen other than the atmosphere.

In the fifth assumption, experimentation verifies the expressing of reaeration as a first-order decreasing rate reaction, but serious doubts are present in the assumption that deoxygenation, or oxygen uptake, proceeds by first-order decreasing rate kinetics. Studies by Bhatla and Gaudy show that the kinetics of oxygen uptake in a BOD bottle (often used for determination of kinetics of oxygen uptake in the stream) are many times characterized by an early exponentially

increasing phase similar to a microbial growth curve, then followed by a plateau and another autocatalytic-type curve. These kinetics for oxygen uptake which vary for different situations, many times defy approximation by a first-order decreasing rate equation.

Another inconsistency in this assumption is that oxygen uptake has been found to vary with the concentration of waste. Jennelle and Gaudy have shown that a Monod-type relationship exists between waste concentration and the rate of oxygen uptake in the exponential phase of uptake. Thus, the bottle dilution technique of BOD determination should not be used to define the rate of oxygen uptake in the stream except at that concentration.

Another shortcoming in the BOD bottle technique is that deoxygenation may be affected by mixing. Work by Ali and Bewtra shows a definite indication that oxygen uptake was affected by mixing, while Jennelle and Gaudy noted that mixing played no significant effect in their studies. Thus, the coefficient of deoxygenation may not truly describe kinetics of oxygen uptake, and this, coupled with the shortcomings of determination in a BOD bottle, allows that only a compensating error in the determination of K_2 may describe the true dissolved oxygen profile in a stream.

The sixth assumption is weakened by the fact that in the dynamic and varying conditions of the environment, the constants will change with different hydrological conditions. In trust, K_1 and K_2 are not really constants, but vary with temperature, turbulence, waste loading, streamflow, weather, and other factors (24).

The use of the Streeter-Phelps equation requires evaluation of the coefficient of reaeration, K_2, and the coefficient of deoxygenation, K_1.

The modern methods for evaluating K_2 for stream conditions are empirical formulations expressing K_2 as a function of stream depth, temperature, and velocity, of the general form

$$K_2 = C\frac{V^a}{H^n} \tag{10}$$

where V is the velocity, H is the depth, a, n, and C are constants, and C depends upon the temperature. These equations have been developed by Streeter, O'Connor and Dobbins, Churchill, and Isaacs and Gaudy. Other methods and equations for determining K_2 are available.

The constant K_1 is evaluated either by the dilution BOD bottle technique and solving the equation

$$y_T = L\left(1 - e^{-K_1 t}\right) \longrightarrow \tag{11}$$

where y_T is the oxygen demand remaining at time t, and L is the ultimate BOD, or is evaluated by determining the ultimate BODs at two points on the stream and determining the time of travel between these points, then solving the integrated equation for first-order decreasing rate deoxygenation

$$L_b = L_a\, e^{-K_1 t} \tag{12}$$

where L_b is the downstream ultimate BOD, and L_a is the initial ultimate BOD and t is the travel time between the points.

A different approach has been taken by Busch in his method for stream assimilation capacity. His idea is that a stream's maximum assimilative capacity does not depend upon variable conditions, but depends only upon the minimum reaeration capacity of the stream. Thus, there is no reason to even consider the interrelationship of deoxygenation and reaeration in

a water quality management program. His solution uses the general expression for gas transfer to a liquid

$$\frac{dM}{dt} = K_{L\ min}\ D_{max}\ A_i \qquad (13)$$

where M is the mass of oxygen transferred, K_L is the mass transfer coefficient, A_i is the interfacial surface area, and D_{max} is the maximum allowable dissolved oxygen deficit.

The solution to Busch's equation yields the maximum uniform loading rate of an oxygen demand that can be applied and not cause a drop in the dissolved oxygen below that which is allowed, subject to the worst stream conditions of reaeration.

The simple concept for planning presented by Busch would seem to have much merit if it is a usable and practical concept. Comparing this model to the Streeter-Phelps equation will help in showing the differences between the two methods and the limits of applicability of Busch's method for stream assimilation capacity.

Assumptions for Comparison of Busch's Method to the Streeter-Phelps Equation

In the comparison of Busch's method for stream assimilation capacity with the Streeter-Phelps Sag Equation, the 12.8-mile reach of Flint Creek from the state line to its junction with the Illinois River was used for the computations. The cross-section of Flint Creek at the gaging station near Kansas, and the 1-, 7-, and 30-day, 10-year recurrence interval low flows were assumed to be valid throughout the length of the reach. The data used was thus the cross-sectional results for H, V, W, and A determined at these flows. Two more flows were picked at random and evaluated for

these parameters to aid in illustrative purposes. These results are presented in Table V.

TABLE V

CALCULATION OF K_2 AND K_L FOR THE CROSS-SECTION AT FLINT CREEK

$$k_2 = 2.833 \frac{V}{H^{1.5}}$$

Flow (cfs)	H (ft)	V (ft/sec)	K_2	K_L
1.8	0.06	0.19	110.0	6.6
3.3	0.11	0.19	44.1	4.8
5.8	0.17	0.22	26.7	4.5
67.0	0.88	0.47	4.6	4.0
133.0	1.27	0.64	3.6	4.6

As previously defined the Streeter-Phelps equation is

$$D = \frac{K_1 La}{K_2 - K_1}\left(e^{-K_1 t} - e^{-K_2 t}\right) + D_a e^{-K_2 t} \qquad (9)$$

and Busch's equation for stream assimilation capacity is

$$\frac{dM}{dt} = K_{L(min)}\, D_{max}\, A_i \qquad (13)$$

where $K_L = K_2 x H$.

The coefficient of reaeration (K_2) was calculated by a formula developed by Isaacs, Chulavachana, and Bogart for a simulated stream apparatus at New Mexico State University

$$k_2 = 2.833 \frac{V}{H^{1.5}} \quad \text{(base 10 logarithms)} \qquad (14)$$

This was done for all values of flow in order to determine the minimum K_L which was then used in all calculations using Busch's formulation, and the K_2 corresponding to this $K_L\left(K_2 = \frac{K_L}{H}\right)$ for a given flow was used in all calculations involving the Streeter-Phelps equation. The calculated values for k_2 from the formula developed by Isaacs, et al. were converted to a natural logarithm base by multiplying by 2.303, and then corrected for temperature by use of the formula

$$K_{2(T)} = 1.0241\ K_2^{(T-20^oC)} \tag{15}$$

Analysis of the water quality data available indicated that the highest weekly average temperature condition that might be expected was approximately 29^oC, so this value was used in the correction formula. The value of 29^oC was also used in finding the saturation value of dissolved oxygen for the reach. The effect of chlorides and suspended solids on this saturation concentration was considered to be negligible as discerned from available water quality data, so this saturation value was determined directly from solubility tables of oxygen in distilled water. This value was assumed to be 7.77 mg/l for all calculations for both equations. The maximum allowable deficit was thus 3.77 mg/l (7.77 - 4.00) for Busch's equation.

The initial dissolved oxygen concentration for the Streeter-Phelps equation was assumed to be 5.0 mg/l in all calculations since this is the minimum value allowed for Flint Creek in the State of Arkansas. This value made D_a in the Streeter-Phelps equation 2.77 mg/l (7.77 - 5.00).

Since no data is available on the rate of deoxygenation as might be predicted for possible waste loadings in the future, a constant of deoxygenation was assumed to be 0.23 $days^{-1}$ for all calculations involving the Streeter-Phelps equation. Using other values for K_1 in the calculations would change the values in the results, but not the ideas presented.

The time corresponding to any distance downstream in the Streeter-Phelps equation was found by the relation, distance = V x t, where velocity is as found from the cross-section for a given flow. The computation of the Streeter-Phelps equation was facilitated by a computer program previously developed and is included in Appendix A.

Comparison of Busch's Method to the Streeter-Phelps Equation

Busch's solution for stream assimilative capacity uses the general expression for gas transfer to a liquid,

$$\frac{dM}{dt} = K_{L(min)} D_{(max)} A_i \qquad (13)$$

This equation defines the maximum rate at which oxygen can be uniformly transferred to a reach subject to the worst conditions of reaeration, at the maximum allowable dissolved oxygen deficit. The only kinetics involved in this equation are those used in defining the worst conditions of reaeration for the reach. The kinetics of deoxygenation are not involved, since the rate at which an ultimate biological oxygen demand can be satisfied must be constant and equal to the maximum rate at which oxygen can be transferred. This is if the dissolved oxygen deficit is to remain constant at its maximum allowable value in the reach.

A point discharge of an organic loading into a stream must be defined by some type of kinetics of oxygen uptake if the location and magnitude of the maximum dissolved oxygen deficit is to be found. The Streeter-Phelps equation was developed for such a calculation, and considers that the ultimate biological oxygen demand is not constant, but is decreasing with passage through the reach as biological oxidation

occurs. A series of point discharges can approximate a uniform loading, but for a given length of reach, a certain magnitude of organic loading will cause a greater maximum dissolved oxygen deficit if it is applied at a point than if it is divided and distributed throughout the reach.

This was shown by the Streeter-Phelps equation for the Flint Creek reach by first assuming an initial BOD of 8840 lbs/day at the 7-day low flow of 3.3 cfs for a 20-mile reach. The critical DO value was then calculated. An initial BOD of 4420 lbs/day was next assumed for a 10-mile reach and an artificial waste flow was added containing a biological oxygen demand of 4420 lbs/day at the 10-mile point or half-way through the original 20-mile reach. This artificial waste flow was added at a very high concentration of 15,400 mg/l at 0.1 cfs so as not to alter the flow characteristics of the stream significantly. The maximum DO sag for this case was calculated. In a similar manner, the reach was then divided into four 5-mile increments with 2210 lbs/day of BOD added at the beginning of each increment, then eight 2.5-mile increments with 1105 lbs/day of BOD added at the beginning of each increment. These same calculations were then repeated with the lengths of all reaches halved. The results are summarized in Table VI. These results, although subject to many assumptions, show that when a design waste loading is calculated for a given length of reach, the lower DO concentration will be produced by a single point discharge into the reach.

TABLE VI

MAXIMUM DO DEFICITS FROM THE STREETER-PHELPS EQUATION FOR PROPORTIONAL REACH INCREMENTS AND WASTE LOADINGS

BOD Loadings at Each Reach Increment (lbs/day)	Number of Increments	Length of Increment (miles)	Maximum Critical DO Deficit (mg/l)	Distance Downstream to Max. Critical Deficit (miles)
8840	1	20	5.06	.33
4420	2	10	3.67	10.36
2210	4	5	2.96	15.32
1105	8	2.5	2.46	17.76
		(reach lengths halved)		
8840	1	10	5.06	.33
4420	2	5	4.18	5.34
2210	4	2.5	3.64	7.80
1105	8	1.25	3.15	8.99

Busch's solution for stream assimilation capacity calculates the waste loading that can be uniformly applied to a reach of given length. In his article (3) he states that a shorter length of reach must be used in the calculations for a point discharge, but no quantitative definitions of this shorter length of reach are given. Thus, when a given length of reach is used in calculating the amount of oxygen that can uniformly be transferred over the length, the worst conditions--those of a point source in which the maximum dissolved oxygen deficit is defined by the competing kinetics of reaeration and oxygen uptake--are not considered. This can be illustrated by comparing Busch's method for stream assimilation capacity with the Streeter-Phelps equation for the 12.8-mile Flint Creek reach in

Oklahoma. The comparison is accomplished by determining the length of reach necessary for use in Busch's equation that will yield a BOD loading sufficient to cause the Streeter-Phelps equation to predict a critical dissolved oxygen concentration equal to 4.0 mg/l when the loading is applied at a single point. This analysis was accomplished for the five different flows listed for the Flint Creek cross-section near Kansas. These are listed in Table V. The mass transfer coefficient, K_L, was assumed to be 4.0 $days^{-1}$ for Busch's equation, since this is the minimum K_L calculated for the five different flows. The K_2 used in the Streeter-Phelps equation for any of the given flows was determined by dividing this minimum K_L (4.0) by the depth at that flow. Other assumptions have been defined in the preceeding section.

Busch's equation becomes, considering units

$$\frac{dM}{dt} = K_{L(min)} \times D_{max} \times W \times L \times 6.236 \times 10^{-5} \qquad (16)$$

where $\frac{dM}{dt}$ is in lbs/day, W is in feet, and L is the length of the reach in feet. This can be converted to a waste concentration in the river for a given flow by

$$L_a = \frac{dM}{dt} \; Q = \frac{1.157 \times 10^{-5}}{Q} \; W \; L \; D_{max} K_L(min) \qquad (17)$$

where Q is in cfs, and L_a is in mg/l.

The Streeter-Phelps equation for the critical deficit is

$$D_c = \frac{1}{f} L_a \times e^{-K_1 T_c}$$

where $f = \frac{K_2}{K_1}$. Inserting the L_a calculated from equation (17), and solving for the case when $D_c = D_{max}$, yields

$$e^{K_1 T_c} = \frac{1}{f} \quad 1.157 \times 10^{-5} \quad W \frac{L}{Q} K_{L(min)}$$

$$t_c = \frac{1}{K_1} \quad \ell n \frac{1}{f} \quad 1.157 \times 10^{-5} \quad W \frac{L}{Q} K_{L(min)} \qquad (18)$$

but also from Streeter-Phelps equation, at the critical deficit

$$t_c = \frac{1}{K_1(t-1)} \quad \ell n \quad F \quad 1-(F-1) \frac{D_a}{L_a}$$

but again substituting the L_a calculated from equation (17) yields

$$t_c = \frac{1}{K_1(f-1)} \quad \ell n \quad f \quad 1-(f-1) \frac{D_a Q}{1.157 \times 10^{-5} \; WLD_{max} K_{L(min)}} \qquad (19)$$

Setting equation (18) equal to equation (19) and solving, gives

$$L = \frac{fQ}{(1.157 \times 10^{-5}) W K_{L(min)}} \left[f \left(1-(f-1) \frac{D_a Q}{(1.157 \times 10^{-5}) WLD_{max} K_{L(min)}} \right) \right]^{\frac{1}{f-1}} \qquad (20)$$

Since all of the variables can be determined for a given flow in equation ( ) except L, this equation can be solved by iteration for the value of L in Busch's equation for which the predicted waste loading will cause the critical dissolved oxygen level to equal the minimum allowable value from computation in the Streeter-Phelps equation. A summary of the calculations for the Flint Creek cross-section are given in Table V.

From the equation

$$\frac{dM}{dt} = K_{L(min)} \; D_{max} \; WL \qquad (21)$$

For a given flow and cross-section, the waste loading predicted is directly proportional to the length of the reach. Thus, the design loading calculated by Busch's equation at the 7-day low flow (3.3 cfs) for a 14.6-mile reach proportionately exceeds that predicted for a 14.5-mile reach,

and is proportionately less than that predicted for a 17.0-mile reach. But as shown on Table VII for a point discharge at the beginning of these different reach lengths, the loading predicted for a 14.6-mile reach of 11,365 lbs/day will cause a minimum dissolved oxygen concentration of 4.0 mg/l by the Streeter-Phelps equation, no matter what the length of the reach may actually be. Thus, if the 14.5-mile reach is used in Busch's formulation for stream assimilation capacity, the dissolved oxygen concentration will stay above 4.0 mg/l as predicted by the Streeter-Phelps equation, but if a 17.0-mile reach is used for the calculation in Busch's equation, the Streeter-Phelps equation predicts that the dissolved oxygen concentration will be lowered to 3.12 mg/l at this flow of 3.3 cfs. There is only one reach length which will cause the DO to sag to the minimum allowable value, and this length is independent of the actual length of the reach.

From the calculations, at each flow there is a certain length of reach associated with this flow for which the design loading calculated from Busch's equation will cause the Streeter-Phelps equation to predict a DO concentration of 4.0 mg/l. Since the length of this reach increases with increasing flow, it can be ascertained that the design loadings predicted from Busch's equation become more conservative for increasing values of a design low flow for the given cross-section. For example, if a 14.5-mile reach was actually the length of the reach and the design flow was 67 cfs, Busch's equation calculates a design loading of 11,660 lbs of oxygen demand per day, which the Streeter-Phelps equation predicts would cause no sag in the dissolved oxygen concentration. A BOD loading of 29,925 lbs per day is necessary to cause the dissolved oxygen concentration to drop to 4.0 mg/l, according to the Streeter-Phelps equation. This corresponds to a reach length of

TABLE VII

LOADINGS FROM BUSCH'S EQUATION USED AS A POINT DISCHARGE IN THE STREETER-PHELPS EQUATION

	Reach length, miles									
	14.5 mi		14.6 mi		17.0 mi		37.2 mi		52.3 mi	
Flow (cfs)	lbs BOD/day	DO (mg/l)	lbs BOD/day	DO (mg/l)	lbs BOD/day	DO (mg/l)	lbs BOD/day	DO (mg/l)	lbs BOD/day	DO (mg/l)
1.8	11,300	4.00	11,380	3.95	13,250	3.02	29,000	0	40,535	0
3.3	11,300	4.04	11,380	4.00	13,250	3.12	29,000	0	40,535	0
5.8	11,300	4.19	11,380	4.16	13,250	4.0	29,000	0	40,535	0
67	11,660	5.00	11,740	5.00	13,670	5.0	29,925	4.0	41,825	1.59
133	11,730	5.00	11,810	5.00	13,754	5.0	30,110	4.62	42,085	4.0

lbs BOD/day = calculated from Busch's equation for stream assimilation capacity using length of reach given

DO (mg/l) = calculated from the Streeter-Phelps equation for a point discharge using the loading calculated from Busch's equation, and is the minimum or critical DO concentration for the reach

37.2 miles for the flow of 67 cfs. But if the design flow for this 14.5-mile reach was 1.8 cfs, the loading predicted from Busch's equation would be 11,300 lbs of oxygen demand/day, just 360 lbs less than that predicted for the flow of 67 cfs. For this case, however, the Streeter-Phelps equation predicts that the dissolved oxygen concentration would sag to 4.0 mg/l, the minimum allowable value. The reason for this observation is that for a given length of reach in Busch's equation, the design waste loading is directly proportional to the width of the water surface on the cross-section, since this defines the minimum interfacial surface area available for oxygen transfer. Thus, for the steep bank slopes on Flint Creek, the width varies little with depth, and thus the assimilative capacity as predicted by Busch's formulation varies little for increasing flows. The Streeter-Phelps equation, however, predicts that the assimilative capacity for a point source discharge is much less for lower flows than for increasing flows. The reason for this can be shown from the differential form of the equation

$$\frac{dD}{dt} = K_1 L - K_2 D \qquad (8)$$

From this equation, K_1 and the initial value for D (D_a) are constant at the instant of discharge of flow in Table X, while K_2 is inversely proportional to the depth

$$K_2 = \frac{K_{L(min)}}{H}$$

If it is assumed that at the instant after discharge $\frac{dD}{dt} = 0$, or the DO profile will not sag, the Streeter-Phelps equation becomes

$$0 = K_1 L_a - \frac{K_{L(min)}}{H} D_a$$

but since $L_a = \frac{\text{loading}}{Q}$ where the loading is the rate of BOD application

$$K_1 \frac{\text{loading}}{Q} = \frac{K_{L(min)} D_a}{H}$$

$$\text{loading} = \frac{K_{L(min)} D_a}{K_1} \frac{Q}{H}$$

or the loading rate is proportional to $\frac{Q}{H}$.

Since the flow rate increases much faster than at a linear rate with increasing depths (by the rating tables in Appendix A), the loading can be increased with increasing depths and still not cause the DO concentration to sag. This dilution of pollutants with increased flow rate in the Streeter-Phelps equation has been shown for the specific case $\frac{dD}{dt} = 0$ in order to aid in the explanation of the calculations shown in Table X; or that the total BOD loading can be greatly increased with increasing flow and still maintain a minimum DO concentration greater than 4.0 mg/l by the Streeter-Phelps equation.

Busch's equation does not take into account the fact that dilution is going to have an influence on the rate of change of the dissolved oxygen deficit for different flow regimes, and thus on the maximum dissolved oxygen deficit. The amount of water passing a point per unit time, or the discharge (Q) associated with a given depth, is not considered in Busch's formulation except in the determination of $K_{L(min)}$.

Busch's method gives no information concerning the location of the critical DO deficit, so no comparison can be made with the Streeter-Phelps equation's computation of this location. The critical DO deficit was calculated to occur within a half-mile for most of the data used in the Streeter-Phelps equation. For example, at the 7-day average low flow for a BOD loading at 11,380 lbs/day, the critical DO deficit occurred .30 mi downstream in 2.2 hours. The very shallow depths and high K_2

values used in the equation were the affectors of this calculated quick sag and recovery.

Thus, these results show two points:

1) For a given flow there is a single length of reach which, when used in Busch's equation for stream assimilation capacity, the loading predicted will cause the dissolved oxygen concentration to sag to the minimum allowable value, as predicted for a point source by the Streeter-Phelps equation. This length depends only upon $K_{L(min)}$ and W, so there is no relationship between this reach length and the actual length of the reach.

2) For a given reach length, the BOD loadings predicted by Busch's equation, when applied to a point source, are the least conservative for lower values of flow as compared to the Streeter-Phelps equation, because the velocity of flow or the relation of discharge to depth is not taken into account except for determining $K_{L(min)}$.

The Streeter Phelps equation was not meant to be used as the best possible prediction of the DO profile in these comparisons; its limitations have been previously discussed. It was used for the purpose of

1) showing that for a given length of reach, a point discharge will place the greatest burden upon the oxygen resources of the stream, and

2) showing the anomolies that exist between using a kinetic model to predict the dissolved oxygen profile caused by a point waste discharge and calculating allowable waste loadings for a reach by using a uniform rate of oxygen transfer over the entire reach.

The concept of using only the minimum reaeration capacity of a

stream to predict its assimilative capacity may be a valid line of reasoning. Still, incorporating this idea into the kinetics of competing reaeration and deoxygenation initiated by a point discharge seems to be a more rational way to proceed than in designing for uniform loadings. Uniform loadings usually come under the heading of natural pollution and are nearly impossible to predict. Point discharges are the vandals that have frequently been known to upset natural balances in a stream when a town or industry discharges its wastes into the stream. These wastes are predictable and capable of being controlled. Further defining the applicability of the general aeration formula as presented in Busch's "Five-Minute Solution for Stream Assimilation Capacity," seems necessary if it is to be used in stream pollution problems.

Summary and Conclusions

The distributions of yearly drought flows at the Watts, Tahlequah, and Kansas gaging stations on the Illinois River and Flint Creek were found not to conform to Gumbel's logextremal theory for droughts. These distributions were only slightly skewed and thus were best fit by a straight line on normal probability paper. Logextremal probability paper should not be used to define this type of distribution, as the steeply sloping, concave up curve indicates that the minimum low flow approached is less than zero.

The high degree of variability that was observed in the drought flows at Watts, Tahlequah, and Kansas--the coefficient of variability being greater than 0.60 for the 1-, 7-, and 30-day low flows--and the physical basin characteristics are the reason for the nearly normal distribution. A different distribution was exhibited by the Barren Fork

at Eldon in that the low flows observed at this station approached a minimum low flow.

The 10-year recurrence low flows at these gaging stations are very low, being less than one-fourth of the mean drought flow because of the high variability from year to year of the low flows. The yields of these 10-year recurrence interval drought flows per square mile of drainage area are also very poor, being less than 0.06 cfs/mi^2 at all gaging stations.

To apply a given quantity of organic waste material at a point will cause the dissolved oxygen profile of the stream to sag to a greater extent than if the waste is divided and spread more uniformly throughout the reach. Busch's method for stream assimilative capacity involves calculating the maximum uniform loading rate that a biochemical oxygen demand can be applied to a reach of stream. Applying the loading calculated by Busch's formula as a point discharge to be treated by the Streeter-Phelps equation shows that

1) the actual length of a reach of stream is independent of the length of reach which when used to calculate a BOD loading by Busch's equation, this loading applied at a point will cause the dissolved oxygen concentration to sag to the minimum allowable value, and

2) the dilution capacity of a river or the discharge associated with a given depth is not totally accounted for in Busch's formulation.

There is thus no correlation between the loading that would be predicted by Busch's equation to maintain the dissolved oxygen concentration at acceptable levels, and that predicted by a kinetic model such as the Streeter-Phelps equation when a point discharge is being considered.

STREAMFLOW SIMULATION MODEL

Description of the National Weather Service River Forecast System (NWSRFS)

A streamflow simulation model that is based on observed physical processes occurring in nature has a distinct advantage over correlation models that do not even attempt to relate to known hydrologic processes. But there is a limit to how detailed the hydrologic cycle can be modeled using existing data collection techniques and standards. The ultimate model would perhaps follow each particle of water from the time it ceased to fall in the atmosphere until the time it left the watershed; that would be the ultimate in moisture accounting. But on any real watershed, that would be a task too immense to even contemplate. It would require such a detailed knowledge of the soil structure and characteristics that it probably could not even be done at the current level of technology.

Certain characteristics for a "good" hydrologic simulation model to be used for streamflow simulation are of such importance that they are virtually requirements. First, the model must use for input only those meteorological and hydrological data that are normally observed. It must be capable of continuous simulation for long periods of time, not only for use in calibration in order to fully use all of the data available, but also for generating synthetic streamflow records (for basins or time periods when data is unavailable). As much as possible, parameters should be obtained by measurements, not from the judgement of the person calibrating the model or by iterative procedures. It must be usable on digital computers at a reasonable cost. It must be sufficiently

general that it can be used in all climatic conditions (snow, desert, tropics, etc.) and geographical locations (mountains or plains, etc.). It must be able to output simulated stages and flows on a real-time basis for forecasting as well as continuous records for research. It must be based in the physical processes of the hydrologic cycle, and simulate the entire physical system with sufficient detail and accuracy to sustain confidence in the model. This is essential for use on ungaged watersheds. This also will contribute to a better understanding of the hydrologic processes occurring in the basin, which is valuable as a training tool for the working hydrologist.

Until the physical processes in the hydrologic cycle can be described in much greater detail than at present, as well as measured, and can be used in hydrologic simulation, it will be necessary to be content to use some judgement parameters in order to calibrate or adjust the model simulation by trial and error against a period of continuous historical data. Our present knowledge of the details of the hydrologic cycle is not adequate to rigorously describe each step of the process, and even if it were, the enormous amount of physical data on the watershed as well as the very small computational increments that would be required for computer simulation would probably make such an exact simulation prohibitive in cost. The result is a model that is sufficiently refined to be reliably accurate, but does not contain unnecessary detail. The parameters will thus be basically lumped parameters in that they represent the average of the physical processes over an area, although they will be distributed parameters in the sense that they can be used for small sub-areas of the watersheds.

The model used in this report is the National Weather Service River

Forecast System (NWSRFS) as described in NWS HYDRO 14. This system was assembled by the Hydrologic Research Laboratory (HRL) of the National Weather Service's Office of Hydrology, in Silver Spring, Maryland, and includes programs to process data, compute mean basin precipitation (MBP), optimize parameters, verify model parameters, and simulate streamflow, both in a historical and a future (forecasting) mode. The basis of the NWSRFS is the model of the hydrologic cycle, which is a modified version of the Stanford Watershed Model IV.

Runoff consists of three components which follow different paths to the channel. First is the surface runoff which is flow over the ground surface into the channel as either sheet or overland flow. The second component is water flowing through the upper soil layers to the channel, and is known as interflow. The exact mechanism of interflow is not well known, but its occurrence is enhanced by the presence of a relatively impermeable horizon in the soil. The third component is groundwater flow, which is water flowing from a groundwater aquifer.

Most runoff relations are designed to predict only the direct runoff (the combination of surface runoff and interflow). Since a flood hydrograph is composed mostly of direct runoff, and it is quite difficult as well as arbitrary to separate the two, groundwater flow is frequently assumed to be rather constant and is just added to the direct runoff to give the storm runoff.

The water balance concept involves maintaining a running account of the water in soil moisture storage by adding the amount of each new rainfall less direct runoff and accretion to groundwater, and subtracting evapotranspiration. The amounts of runoff and groundwater accretion are made functions of the prevailing soil moisture storage.

The water balance model is the basis of the NWSRFS model. Soil moisture account is through a two-level moisture storage, which uses a small upper storage zone to simulate surface detention and retention in overland flow and the depression storage and soil moisture in a shallow surface layer, plus a lower storage zone that simulates the storage of soil moisture from the surface down to the capillary fringes. Water is accounted for through all storage categories until it leaves the watershed. Perhaps the best way of describing the NWSRFS model is by discussing the structure of the model. Figure 17 is the flowchart of the land phase of the NWSRFS model, and gives the general sequence of operation.

Input data for the NWSRFS for non-real time applications are mean daily streamflow (cfs) for the basin outflow point, six-hour incremental inflow to the basin (if the basin is not a headwater), mean basin precipitation (inches) in six-hour increments, and daily potential evapotranspiration data. For real time applications input data requirements are streamflow in six-hour increments (both inflow and outflow), precipitation for individual stations in six and 24 hour increments, and daily evapotranspiration data. Hourly and daily precipitation data are readily available on a historical basis from the National Climatic Center (NCC) Environmental Data Service, NOAA, Asheville, North Carolina. However, these data are not readily available on a real time basis, except for a few stations. Except under unusual circumstances, the normal reporting frequency is either every six or twenty-four hours. Potential evapotranspiration is assumed to be equal to the lake evaporation estimated from class A pan records. The actual evapotranspiration is computed by

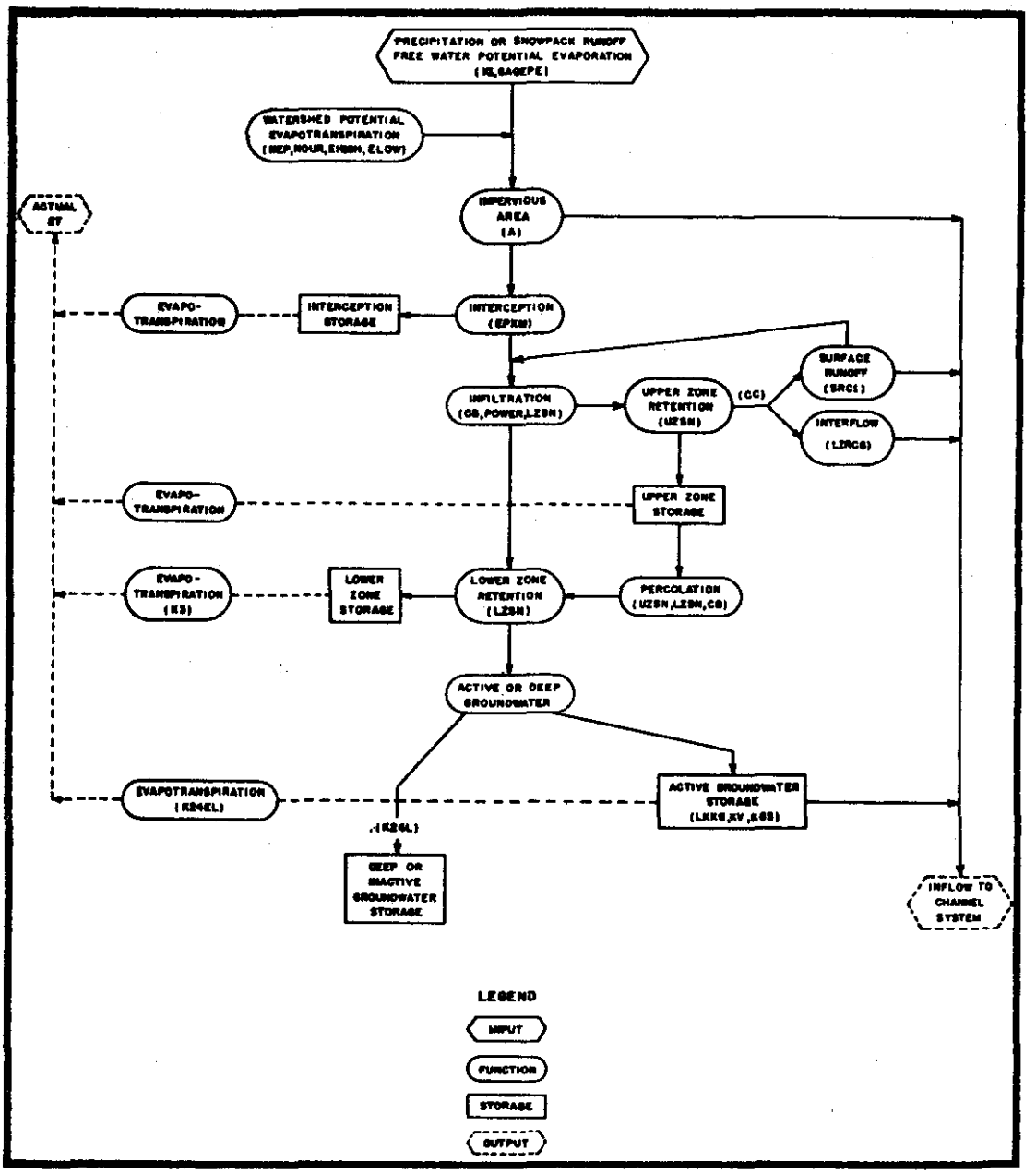

Figure 6. Flowchart of Soil Moisture Accounting Portion of the National Weather Service River Forecasting System

Source: (9), p. 47

the model as a function of the potential evapotranspiration and the current soil moisture conditions.

Interception

Interception is the initial abstraction from the incident precipitation. It is a function of the watershed cover, and is limited by the current volume in interception storage as well as the preset maximum interception storage amount (EPXM). All incident precipitation is directed to EPXM until that preassigned volume is full. Moisture in interception storage is depleted by evaporation at the potential evapotranspiration rate. Thus, interception can continue throughout a storm due to evapotranspiration.

Impervious Area

The impervious areas (A) of a watershed are those areas such as lake or stream surfaces and the adjacent non-permeable surfaces. If rainfall occurs on these areas, it becomes surface runoff immediately. "A" represents a preset percentage of the precipitation that is immediately diverted directly to the channel. It does not include rock outcrops, buildings, or roads that are not immediately adjacent to the streams or which are separated from the stream by previous areas.

Infiltration

Infiltration is a continuously varying function of the soil moisture. First the cumulative watershed infiltration capacity functions determine whether the available moisture infiltrates directly into the soil and into lower zone and groundwater storage or goes to surface

detention storage. What that is directed to surface detention storage is in what is called the upper zone and which is designed to simulate depression storage, soil fissures, and the space around soil particles. The infiltration capacity is divided into two portions (Figure 7); part of the infiltrated water becomes interflow while the rest goes to lower zone and groundwater storage. For a given moisture supply of x inches and a given infiltration capacity, Figure 7 illustrates the division of the available moisture into overland flow, interflow, and lower zone and groundwater storages. Figure 7 also shows the variation of overland flow, interflow, and infiltration as the moisture supply varies.

It is apparent that the variables c and b are extremely important in determining the relative magnitude of each of these flows. c and b are functions of the current lower zone storage ration LZS/LZSN (LZS is the current soil moisture storage in the lower zone, and LZSN is a nominal lower zone storage level that is about equal to the median value of lower zone storage), CB (an infiltration parameter), and CC (the ratio of interflow/overland flow). When LZS/LZSN < 1.0

$$c = CC \cdot 2.0$$

$$b = CB / (LZS/LZSN)$$

The effect of power in shaping the infiltration curve is shown in Figure 8.

Water that does not infiltrate directly, increases the amount in surface detention storage and will either contribute to overland flow or upper zone storage, and then either evapotranspire (at the potential rate) or infiltrate. The rate of filling of upper zone storage decreases as the upper zone becomes full.

b = total direct lower zone and groundwater infiltration capacity
c·b = total infiltration capacity

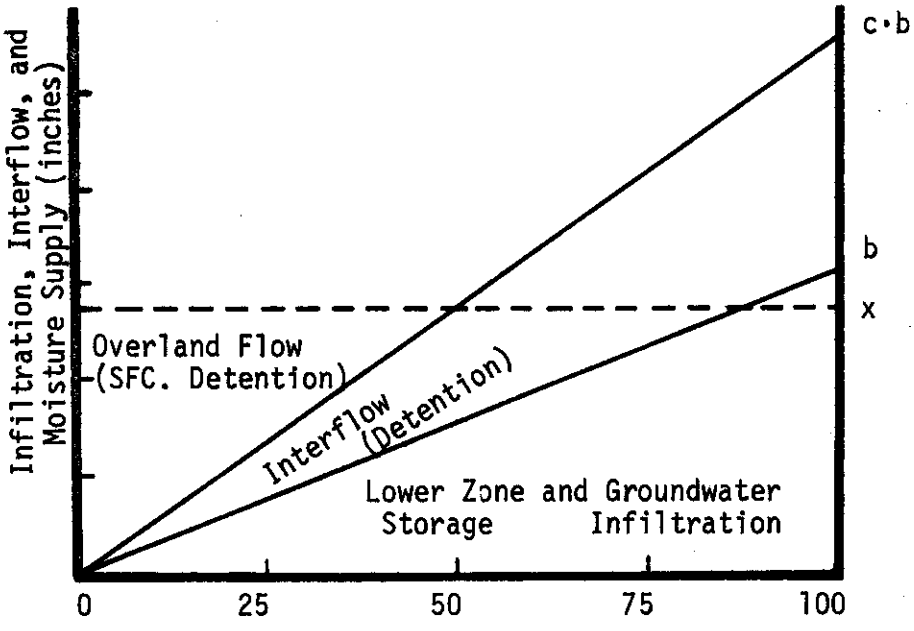

Figure 7. Infiltration Division

Source: (17), p. 33

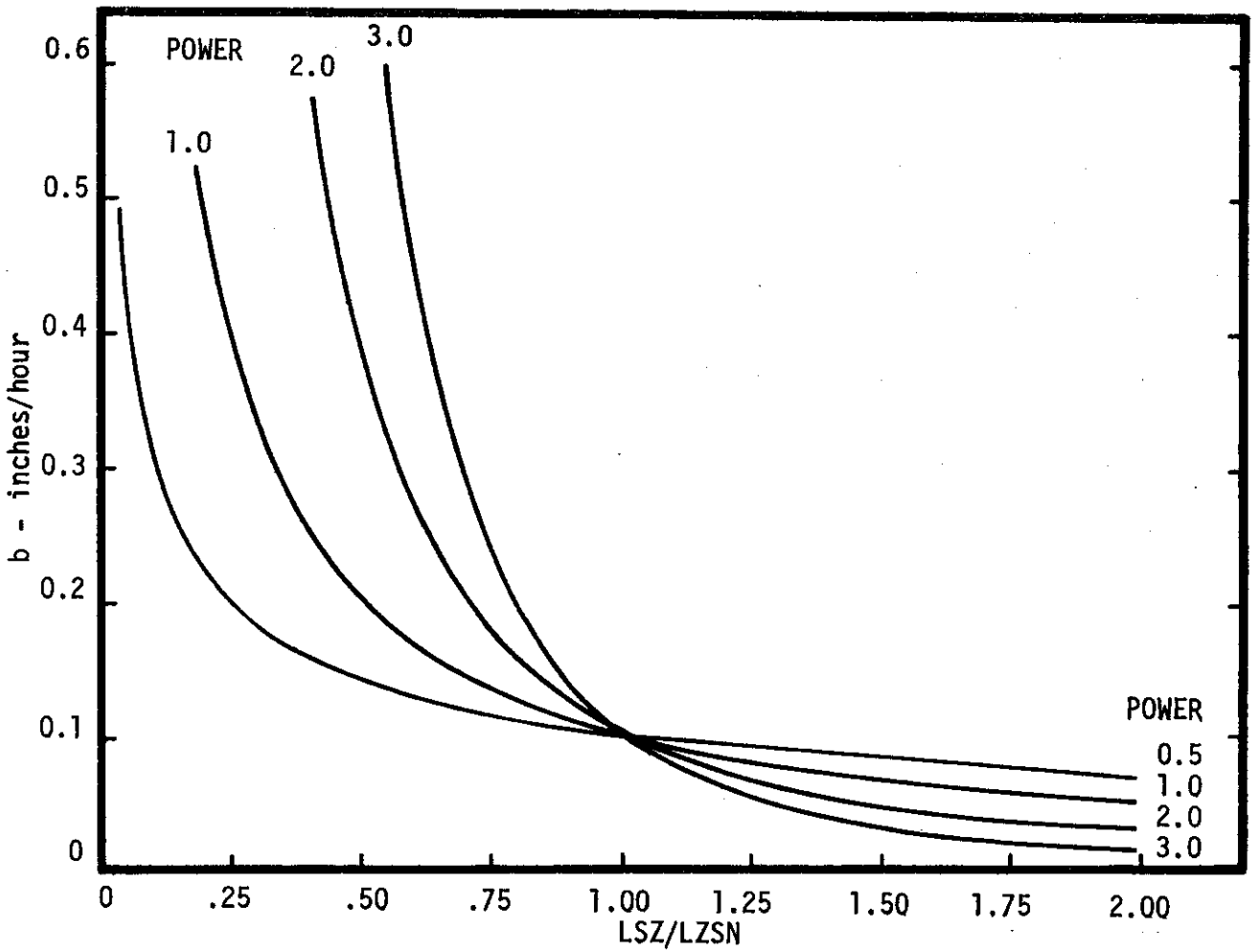

Figure 8. b versus LZS/LZSN for Various Values of POWER for CB = 0.1

Source: (9), p. 4-8

OVERLAND FLOW

Overland flow (fast response runoff) is calculated at one hour intervals. It is a function of the amount of water in surface detention storage, and its rate of flow into the channel. It is computed by the following equation:

$$ROST = SRC1 \cdot RX$$

where

SRC1 = percent of water in RX that reaches the channel each hour
RX = surface detention

Soil Moisture

Briefly, soil moisture is represented by lower zone storage that is filled both by infiltration and percolation from the upper zone, while depleted by evapotranspiration at a rate dependent on the water currently in storage, percolation to deep or inactive groundwater storage and percolation to active groundwater storage (where it either remains or flows to a channel).

Interflow

Interflow storage is principally a function of the infiltration that has occurred, and the infiltration capacity. Its computation is illustrated on Figure 7. Depletion of interflow storage and the movement of interflow is accomplished by a decay or recession function:

$$INTF = LIRC6\text{-}SRGX$$

where

LIRC6 = $1.0 - (IRC)^{1/4}$
LIRC6 = the recession coefficient; percent of interflow detention reaching the channel each 6 hours
INTF = interflow
SRGX = the amount of water in interflow storage
IRC = daily recession or depletion coefficient, the ratio of interflow discharge at any time to the interflow discharge twenty-four hours later

Groundwater

Recharge of groundwater storage is by percolation from the lower zone, and is a function of the amount of water in lower zone storage at that time. The percentage of water that infiltrates (either directly as shown in Figure 7, or as delayed infiltration through upper zone storage) varies as follows:

$$Pg = 100\left(\frac{LZS}{LZSN}\left(\frac{1.0}{1.0 + LZI}\right)^{LZI}\right)$$

where

$\frac{LZS}{LZSN} \leq 1.0$ (if greater, set $\frac{LZS}{LZSN} = 1.0$

Pg = percentage of water entering groundwater storage
LZS = amount of water in lower zone storage
LZSN = lower zone storage level at which fifty percent of all water infiltrated goes to groundwater storage
$LZI = 1.5\left(\frac{LZS}{LZSN} - 1.0\right) + 1.0$

The relationship of Pg and LZS/LZSN is shown in Figure 9. At a LZS/LZSN of zero there is zero groundwater recharge, when LZS/LZSN = 1.0, fifty percent of infiltration is stored in groundwater storage, and as LZS/LZSN approaches 2.5, the percent infiltrated approaches one hundred percent.

Outflow from groundwater storage is to the channel as groundwater flow, by percolation to deep (inactive) groundwater storage, by loss from evapotranspiration. The flow from this aquifer is proportional to the product of the cross-sectional area of flow and the energy gradient of the flow. The energy gradient is composed of a base gradient plus a variable gradient which depends on groundwater accretion. Groundwater flow is computed by the following equation

$$GWF = LKK6 \cdot (1.0 + KV \cdot GWS) \cdot SGW$$

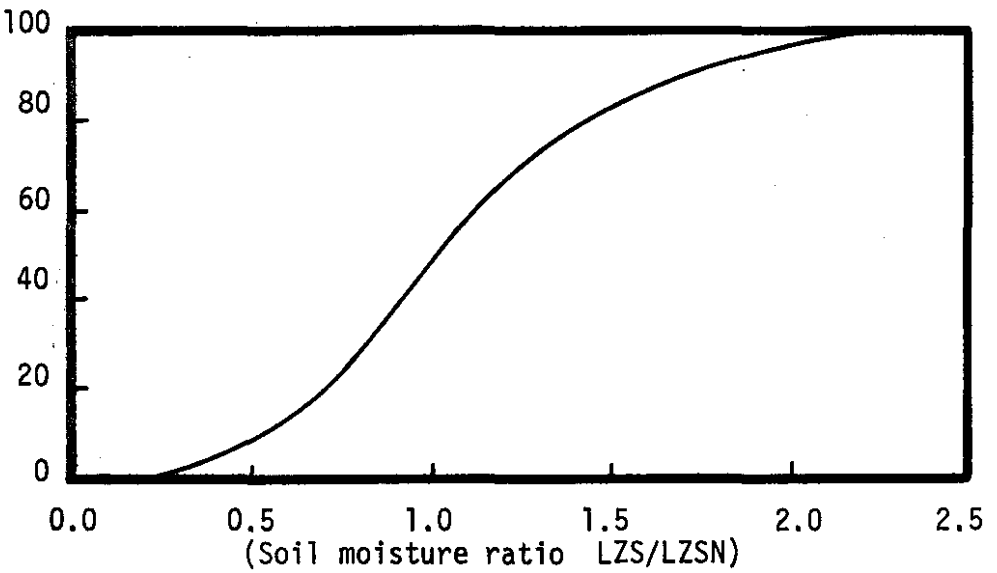

Figure 9. Soil Moisture Ratio (LZS/LZSN) versus Percent of Infiltration Entering Groundwater storage

Source: (17), p. 40

where

GWF = groundwater flow
LKK6 = fair weather groundwater recession coefficient
= $1.0 - (KK24)^{1/4}$
KK24 = ratio of current groundwater discharge to the groundwater discharge twenty-four hours earlier (it is the minimum observed daily recession)
KV = a variable groundwater recession coefficient
GWS = the antecedent groundwater inflow index
= KGS (GWS + inflow to groundwater storage)
SGW = amount of water in groundwater storage
KGS = antecedent index recession factor

Percolation to deep (inactive groundwater storage is simulated by shunting a fixed percentage (K24L) of the inflow to groundwater storage directly to inactive storage.

Evapotranspiration

Evapotranspiration is a function of the potential evapotranspiration and the available moisture supply. It occurs from interception storage, upper zone storage, lower zone storage, and groundwater storage. The SWM IV model also includes evaporation from stream surfaces in this category. Hourly potential evapotranspiration is computed from daily or semi-monthly input data. The program attempts to satisfy potential evapotranspiration first from interception storage, and after that, from upper zone storage. If the potential has not been satisfied at that point, the evapotranspiration opportunity (maximum water available for evapotranspiration in a time interval at a point in the basin) from the lower zone is then computed by use of the following equation

$$E = E_p - \frac{E_p^2}{2r}$$

$$r = K3 \frac{LZS}{LZSN}$$

where

E = evapotranspiration from lower zone (inches per day)
E_p = potential evapotranspiration (inches per day)
$K3$ = variable index to lower zone evapotranspiration

The maximum evapotranspiration for any given lower zone storage level occurs when the potential evapotranspiration equals n/2 inches over the watershed.

Channel System

Storage and flow times in the channel system become large compared to those in overland flow as the size of the watershed increases and the channel system becomes the dominate factor in shaping the outflow hydrograph.

Although Linsley stated that the finite differences method for channel routing is the most general physically based method for simulating unsteady open channel flows, the input requirements and long computing times required led to the adoption of an empirical routing method in the model--the channel time-delay histogram. This is a time versus discharge histogram that represents the response of the channel to an inflow with a duration equal to the time increment (Figure 10). Each element of the histogram represents the fraction of the total watershed that contributes to channel flow for a given travel time. Each element of the histogram is thus associated with a particular travel time zone of the watershed. The main advantages to this method are efficient programming and the avility to provide simultaneous output hydrographs at several points in the watershed.

The outflow hydrograph produced from the time-delay histogram is then routed through a linear reservoir at the basin outflow point. The channel

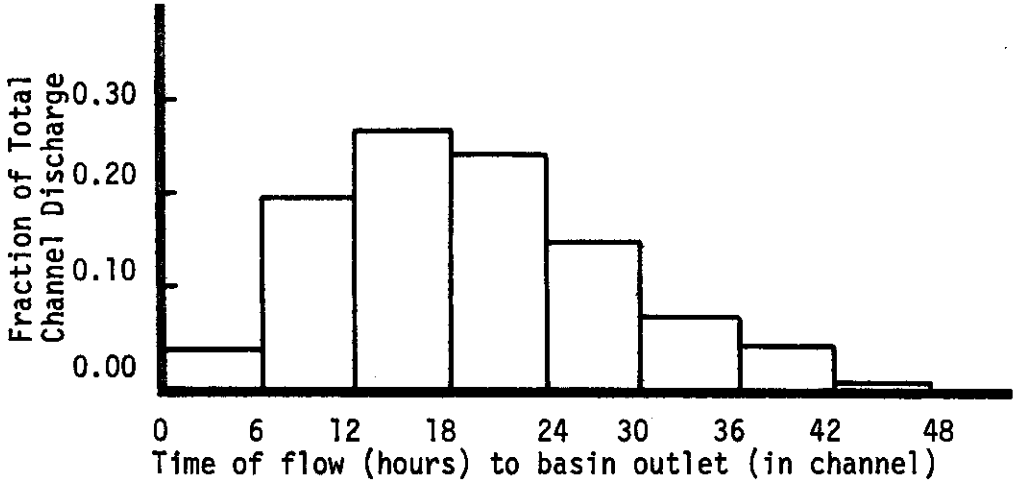

Figure 10. Channel Time-delay Histogram for the Illinois River near Watts, Oklahoma

routing equation is

$$O = I - KSI(I - O_1)$$

where

$KSI = \frac{(1/k - \Delta t/2)}{(1/k + \Delta t/2)}$

O = outflow

I = inflow

KSI = reservoir storage constant

O = hourly recession rate for channel runoff

$O = \frac{\text{discharge in hour (1)}}{\text{discharge in hour (t+1)}}$

If no streamflow data is available, parameters can be estimated from physical basin characteristics or parameters used in nearby and/or hydrologically similar watersheds, and the simulation performed on the basis of those parameters and the available precipitation and potential evapotranspiration (PE) data. The validity of the califration obviously varies with the accuracy of the estimation of the parameters. Nevertheless, done carefully, this can be a useful tool and provides a valuable method of streamflow simulation under difficult circumstances. If this procedure is continued down to the point where stream flow records are available, the accuracy of the calibration can then be determined and parameter adjustments made. This provides a method of forecasting streamflow or developing streamflow records for ungaged streams.

If precipitation (PE) and streamflow data is available, the NWSRFS can be califrated to a given basis. Once a basin has been calibrated, the NWSRFS can be used to extend streamflow records to periods when only meteorological data are available, it can operate in a virtually real-time mode for forecasting use, it can be used with synthetic precipitation data to produce streamflow records for any desired climatological regime, and the parameters in the model can be varied to simulate the effect on the

basin of changes to the watershed. The input data required for the NWSRFS is the mean basin precipitation (MBP) (computed by the MBP portion of the NWSRF using discreet observation), streamflow, and potential evapotranspiration (PE).

Mean Basin Precipitation (MBP)

Since precipitation is measured as point values, and these points are usually few in or near a given basin, it is necessary to be able to estimate the precipitation at other points in the basin and finally arrive at average precipitation amounts over given areas. This frequently (although not necessarily) results in the precipitation being averaged over basin-sized areas. Although the concept of area-wide averaging of the precipitation is not too bad when the precipitation is uniformly distributed over a basin, it leaves much to be desired when the precipitation is not uniformly distributed (such as during air-mass thunderstorm activity). Nevertheless, nothing better has been developed, so the NWSRFS provides for the use of three averaging techniques based upon three weighting methods

1) Grid Point weights

2) Thiessen weights, and

3) predetermined weights.

The Grid Point method is based on a basin covered with a fine grid (Figure 11). The precipitation at each of these grid points is estimated (using the technique described following the description of the weighting methods) and the MBP is simply the arithmetic average of all of these points. The weights for each grid point are calculated by determining the nearest precipitation station to the grid point in each of the four quadrants

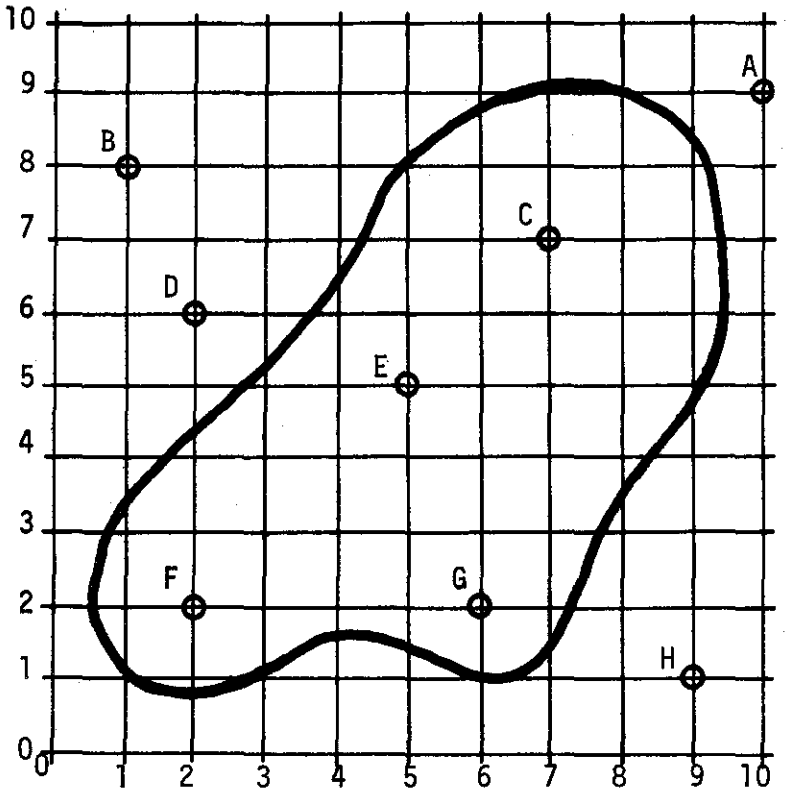

Figure 11. A Grid Superimposed on a Basin

Source: (9), p. 3-5

around the grid point. Each grid point will then have four weights which are equal to the normalized reciprocal of the squared distance ($1/distance^2$) to each of the four precipitation stations (sum of the weights = 1.0). Computation of the weights for each of the 47 grid points within the basin (Figure 11) is summarized in Table VIII. When the grid point coincides with a station, the station is given a weight of 1.000. After this is done for each grid point, the total weight assigned to each station, after being normalized, is its Grid Point weight. Since there are 47 grid points, the sum of the weights is equal to 47.0, which is the total used for normalizing (Table IX). Using the basin (Figure 11) as an example, with point precipitation values of A = 1.0, B = 0.2, C = 4.6, D = 1.0, E = 3.2, F = 1.9, G = 2.1, and H = 1.0, and the Grid Point weights in Table IX,, the MBP was computed to be 2.764 inches. The NWSRFS defines the Thiessen polygon in terms of grid points; the polygon is the boundary of all points which are closer to the subject station than any other station. Table X shows the computed Thiessen weights for this basin. For this example, the Thiessen weights produced an MBP of 3.03 inches, which is close to the 2.764 inches given by the Grid Point method.

Predetermined weights may be entered to compensate for topographical irregularities or unusual aspects such as present in mountains.

The MBP program portion of the NWSRFS has the option of computing and/or using Grid Point weights, Thiessen weights, or predetermined weights, and of producing output MBP for 1, 3, or 6-hour increments. Input to the MBP program consists of hourly (observations each hour) and daily (observations every 24 hours) precipitation for the weighted

TABLE VIII

NORMALIZED WEIGHTS FOR EACH GRID POINT
Source: (9), p. 3-6

		QUAD. I			QUAD. II			QUAD. III			QUAD. IV		
X	Y	Sta	D^2	W	Sta	D^2	W	Sta	D^2	W	Sta	D^2	W
1	2	D	17	.056	-	-	-	-	-	-	F	1	.944
1	3	D	10	.167	-	-	-	-	-	-	F	2	.833
2	1	F	1	.980	B	50	.020	-	-	-	-	-	-
2	2	F	0	1.000	-	-	-	-	-	-	-	-	-
2	3	D	9	.092	B	26	.032	F	1	.828	G	17	.048
2	4	D	4	.411	B	17	.096	F	4	.411	G	20	.082
3	1	G	10	.159	F	2	.797	-	-	-	H	36	.044
3	2	E	13	.065	F	1	.842	-	-	-	G	9	.093
3	3	E	8	.094	D	10	.076	F	1	.755	G	10	.075
3	4	E	5	.295	D	5	.295	F	5	.295	G	13	.115
3	5	C	20	.036	D	1	.714	F	10	.071	E	4	.179
4	2	E	10	.166	F	4	.417	-	-	-	G	4	.417
4	3	E	5	.295	D	13	.115	F	5	.295	G	5	.295
4	4	E	1	.727	D	8	.091	F	8	.091	G	8	.091
4	5	C	13	.057	D	5	.148	F	13	.057	E	1	.738
4	6	C	10	.111	D	4	.278	F	20	.056	E	2	.555
5	2	E	9	.091	F	9	.091	-	-	-	G	1	.818
5	3	E	4	.276	D	18	.061	F	10	.111	G	2	.552
5	4	E	1	.738	D	13	.057	F	13	.057	G	5	.148
5	5	E	0	1.000	-	-	-	-	-	-	-	-	-
5	6	C	5	.146	D	9	.081	E	1	.731	G	17	.042
5	7	A	41	.042	B	17	.101	E	4	.429	C	4	.428
5	8	A	26	.094	B	16	.152	E	9	.269	C	5	.485
6	2	G	0	1.000	-	-	-	-	-	-	-	-	-
6	3	C	17	.044	E	5	.150	G	1	.749	H	13	.057
6	4	C	10	.110	E	2	.552	G	4	.276	H	18	.062
6	5	C	5	.148	E	1	.740	G	9	.082	H	25	.030
6	6	C	2	.458	D	16	.057	E	2	.458	H	34	.027
6	7	A	20	.039	B	26	.030	E	5	.155	C	1	.776
6	8	A	17	.084	B	25	.057	E	10	.143	C	2	.716
7	2	C	25	.032	G	1	.806	-	-	-	H	5	.162
7	3	C	16	.077	E	8	.154	G	2	.615	H	8	.154
7	4	C	9	.189	E	5	.340	G	5	.340	H	13	.131
7	5	C	4	.385	E	4	.385	G	10	.154	H	20	.076
7	6	C	1	.785	D	25	.031	E	5	.157	H	29	.027
7	7	C	0	1.000	-	-	-	-	-	-	-	-	-
7	8	A	10	.088	B	36	.024	C	1	.872	H	53	.016
7	9	-	-	-	-	-	-	C	4	.692	A	9	.308
8	4	A	29	.096	C	10	.278	G	8	.348	H	10	.278
8	5	A	20	.130	C	5	.519	G	13	.199	H	17	.152
8	6	A	13	.107	C	2	.699	E	10	.140	H	26	.054
8	7	A	8	.102	C	1	.814	E	13	.062	H	37	.022
8	8	A	5	.270	B	49	.028	C	2	.675	H	50	.027
8	9	-	-	-	-	-	-	C	5	.444	A	4	.556
9	6	A	10	.279	C	5	.557	E	17	.164	-	-	-
9	7	A	5	.400	C	4	.500	E	20	.100	-	-	-
9	8	A	2	.699	B	64	.022	C	5	.279	-	-	-

TABLE IX

GRID POINT WEIGHTS FOR THE VARIOUS STATIONS
Source: (9), p. 3-7

Station	Sum of Weights	Grid Point Weights
A	3.294	0.0701
B	0.562	0.0119
C	12.312	0.2619
D	2.730	0.0581
E	10.348	0.2202
F	8.931	0.1900
G	7.504	0.1597
H	1.319	0.0281
	47.000	1.0000

TABLE X

GRID POINT WEIGHTS USED TO COMPUTE THIESSEN WEIGHTS
Source: (9), p. 3-8

Station	No. of Points	Thiessen Weight
A	2	0.0426
B	0	-
C	16	0.3404
D	3	0.0638
E	10	0.2128
F	9	0.1915
G	7	0.1489
H	0	-

stations, an 80-by-80 grid map of the basin, and X-Y coordinates of the precipitation stations. More detailed information about the grid map and coordinates is found under calibration of the NWSRFS.

The basic theory behind estimation of precipitation requires determination of the nearest precipitation station in each of the four quadrants around the point to be estimated (Figure 12). Each of these four stations receives a weight equal to 1/distance^2 from the point to that station. The precipitation estimate is then a weighted average of that at the other four points. If there is no precipitation in some of the quadrants, only the quadrants with precipitation are used. A further modification to the operational program as used at the Lower Mississippi River Forecast Center in Slidell, Louisiana, is the option to limit the search for an estimator to a short predetermined distance from the station, when the precipitation is decidedly non-uniform (showers). Stations may be given additional weights if a station gets significantly more precipitation than other stations for a given storm, such as might occur in mountains. This information is called the station's "characteristic."

After the hourly and daily precipitation data have been read into the computer, the MBP program searches the hourly data to estimate missing periods of record and distribute periods for which only an accumulation value is available. It then estimates the missing hourly data by use of the following equation:

$$A_x = \frac{\sum_{i=1}^{i=n} \left[A_i \cdot \frac{N_x}{N_i} \cdot \frac{1}{(d_{i,x})^2} \right]}{\sum_{i=1}^{i-n} \frac{1}{(d_{i,x})^2}}$$

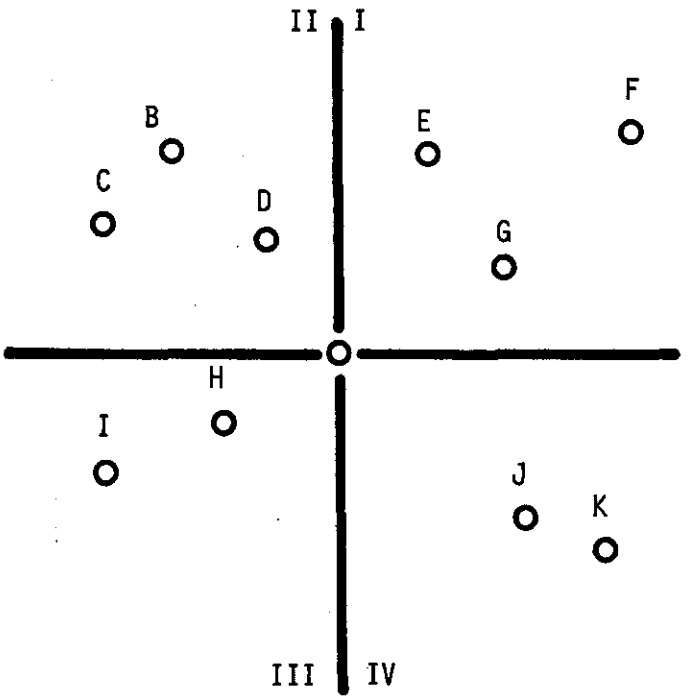

Figure 12. The Four Quadrants Surrounding Precipitation Station A

Source: (9), p. 3-2

where

A_x = the hourly precipitation at the station being estimated
i = station being used as an estimator
n = number of estimators
A_i = hourly precipitation at the estimator station
N_x = monthly characteristic precipitation at the station being estimated (default = 1)
N_i = monthly characteristic precipitation at the estimator station (default = 1)
$d_{i,x}$ = distance from the station being estimated to the estimator station

If only an accumulation value is given, the hourly value is computed by the following equation

$$A_x = \frac{\sum_{i=1}^{i=n} \left[A_i \cdot \frac{T_x}{T_i} \cdot \frac{1}{(d_{i,x})^2} \right]}{\sum_{i=1}^{i=n} \frac{1}{(d_{i,x})^2}}$$

where

T_x = the accumulative amount at the station being distributed

T_i = the total precipitation amount for the period of mixxing time distribution

If no estimator stations are available, that hour is set equal to 0.00, or in the case of an accumulative value, it is left in the last hour. At this point, there is a continuous period of record for all the hourly precipitation stations which is free of accumulative amount indicators.

Next, the daily precipitation amounts are distributed into hourly amounts by use of the hourly data. This is a two-pass operation. On the first pass, the daily observations are put into hourly amounts except that missing data is ignored. The preceding equation is used with

T_x = the daily precipitation amount, and T_i = total precipitation since the last daily observation at the hourly station used to estimate the missing daily amount. The missing periods are then estimated and distributed on the second pass. If there are no estimator stations, the daily amount is set = 0.0. If no stations are available to distribute the precipitation, the undistributed precipitation is left at the time of observation. At this point, the precipitation records are continuous, having no missing data and no accumulative amount indicators.

The MBP is then computed by going through the entire period of record for the area, multiplying the hourly precipitation by the station weight for all stations within the area, and summing these products to give a sequence of MBP values for the period. The MBP values are then written on tape in six-hour increments.

Streamflow

Mean daily flows for the basin outflow point are necessary only as an aid to calibration (so the simulated flow can be compared with the observed flow to assess the accuracy of the simulation and monitor the effect of parameter changes), and as a basis for the generation of six-hour incremental outflows from the basin. For a headwater basin, the NWSRFS can function without streamflow observations. However, for a reach, the NWSRFS requires inflow to the reach in six-hour increments. The mean daily flows must be input to the program from available records; however, the six-hour incremental flows are generated during a simulation (verification) run and can be put on computer mass storage for use in the downstream reach.

Potential Evapotranspiration (PE)

PE is the water loss that would occur if at no time there is a deficiency of water in the soil for the use of vegetation. Due to the probable error associated with computation of free-water evaporation, the Hydrologic Research Laboratory (HRL) assumed the PE was equal to free-water evaporation (although in theory PE is lower than free-water evaporation). PE can be computed from Class A pan evaporation data using the following equation,

$$PE = E_L = 0.70 \left[E_p + 0.00051PN_p \, (0.37 + 0.0041U_p)(T_o - T_a)^{0.88} \right]$$

where

E_L = daily lake evaporation losses (inches/day)
E_p = daily Class A pan evaporation
P = atmospheric pressure
N_p = proportion of advected energy (Class A pan) utilized for evaporation
U_p = daily wind movement at Class A pan height (six inches above surface)(miles/day)
T_o = water surface temperature (F)
T_a = air temperature (F)

If Class A pan data are not available, the PE can be computed from meteorological parameters (air temperature, dew point, daily wind movement, and solar radiation), using the following equation,

$$PE = E_L = \left[e^{(T_a - 212)(0.1024 - 0.01066 \ell nR)} - 0.0001 + 0.0105 \, (E_s - E_a)^{0.88}(0.37 + 0.0041U_p) \right] \cdot \left[0.015 + (T_a + 398.36)^{-2}(6.8554 \times 10^{10})e^{-7.4826/(T_a + 398.36)} \right] - 1$$

where

E_L = daily lake evaporation losses (inches/day)
e = Naperian base
T_a = air temperature (F)
R = solar radiation in Langleys/day
E_s = saturation water vapor pressure at T_a
E_a = atmospheric water vapor pressure at T_a
U_p = wind movement six inches above Class A pan (miles/day)

Since there are only about 40 solar radiation stations in the United States, it is usually necessary to be able to estimate solar radiation from percent sunshine, where the percent sunshine = (1.0-tenths of sky cover)(100). The program will accept solar radiation either in Langleys or as tenths of sky cover.

The daily wind movement reduced from anemometer height to pan height (two ft) follows the equation:

$$\frac{U_1}{U_2} = \left(\frac{Z_1}{Z_2}\right)^{0.3}$$

where

U_1 = wind movement at pan height
U_2 = wind movement at station anemometer height
Z_1 = height of pan anemometer (two ft)
Z_2 = height of station anemometer

The PE data is then placed on tape for use by the NWSRFS. This completes the data requirements for the NWSRFS.

Experience with the NWSRFS at the Lower Mississippi River Forecast Center in Slidell, Louisiana, has shown the NWSRFS is capable of accurate streamflow simulation for normal flood forecasting when the MBP is accurate. However, it has not been tested on low streamflow prior to this study.

Calibration of the NWSRFS

Calibration (fitting) of a model consists of adjusting all of the model's parameters to give the best match of simulated versus observed flow over a given period of record. A parameter optimizing program using the hill climbing technique has been developed to aid in this process (9)(15) and used with care there are situations in which it can be of use. However, it is really useful only for optimizing the parameters once good values have already been determined by trial and error. If the parameter values that go into the optimizing program are not already good values,

the program will proceed to climb the wrong hill and the result will be a worse fit than before. Obtaining good parameter values is also a learning experience for the analyst. As he changes the parameters and sees how the simulation changes, he gains understanding of the hydrologic characteristics of the basin. So the skill and knowledge of the user also can increase through use of the model. Thus, the process of parameter development is essentially a manual process, although the parameter optimizing program can be useful.

With the larger flows, the rainfall is usually more uniform, the errors are smaller (proportionally), and stages change less for a given discharge increment than for low flows. Low flows are mostly the result of groundwater flow with the addition of some runoff produced by small storms, which by their nature are spatially less uniform. Monitoring low flow processes is also more difficult than high flow processes. These indicate that the problem of fitting a model for low flows may be more difficult than for high flows. Total hydrograph reconstitution takes more work than just fitting the rises, and is a real test of the validity of the model as well as the accuracy of the data.

Since low flows have been of no real concern, they have been of little interest in operational model fitting up to this time. As a result, the tendency has been to obtain a good fit for rises--especially the more significant rises--and not worry too much about low flows. Some have even found it difficult to do otherwise. The approach has sometimes been to fit the larger rises well then quit unless the fit at lower flows was unusually bad. It may be that this is backwards. The small rises--the little events--often tell us more about the hydrologic characteristics of a basin than the large events, where much of the

detail is lost. Most simulations have been made using hydrograph plotting scales at which low flow events are hidden, so are not usually noticed. Experience has shown that a basin can be fit with different sets of parameters, many of which are hydrologically unsound, and that can easily happen if low flow events are ignored.

The calibration of the NWSRFS involves a series of steps that are not rigidly ordered, although it will become obvious that certain steps must precede certain other steps. Although the whole procedure will be discussed as it was applied to the two basins on the Illinois River, the procedures will be applicable to other basins. This section will outline the procedures necessary to make simulation (verification) runs using the NWSRFS. This will be accomplished by discussing the data preparation procedures and the initial selection and modification of parameters required to fit the basins.

Raw Data

The raw hourly (observations every hour) and daily (observations once each 24 hours) precipitation data may be obtained on magnetic tape for each state from the National Climatic Center, Asheville, North Carolina, 28801. This data is available in the Office of Hydrology format, which must be reformatted to a standard tape format by use of the program HRTAPE. Ordering information for the data as well as a listing of the program HRTAPE is found in NWS HYDRO 14 in Appendix B. Raw mean daily discharge records, either on tape or cards, are available for each state from the U. S. Geological Survey, Water Resources Division, Washington, D. C. This data must be converted to the standard tape format by use of the program DAILYF.

Mean daily PE data is available in the standard format either on tape or cards for 40 stations in the U. S. from the Research and

Development Laboratory, Office of Hydrology, National Weather Service, Silver Springs, Maryland.

Data that is on standard format cards must be converted to standard format tape by use of program NWSRFS2. NWS HYDRO 14 describes the standard format for cards in Appendix A, and gives a listing of NWSRFS2 in Appendix E.1. By obtaining the data from these sources and processing them, the raw data can be made ready for processing by the MBP program and/or combining onto one data tape (as described in the following sections).

MBP Computation Procedure

The method normally used for computation of the average areal precipitation uses the Grid Point weighting system (the MBP program also computes Thiessen weights). The first step in this procedure is to calculate the Grid Point weights for all of the precipitation stations.

Station Weight Computation

Once the basin to be calibrated has been selected, the next step is to outline the basin on a map such as the U. S. Geological Survey 1:250,000 scale topographical charts. Then overlay the outlined basin with a transparent 80 by 80 grid placed so that the 1-1 point is in the upper left corner (Figure 13). If more than one nearby basin is to be calibrated, time may be saved by overlaying up to ten basins at a time. A map of the basin is then prepared by assigning a "1" to every grid intersection that falls within the basin outline, and inputting this map line by line to the program. Each horizontal line is represented by an 80-column computer card, with the "1"s punched at their proper locations.

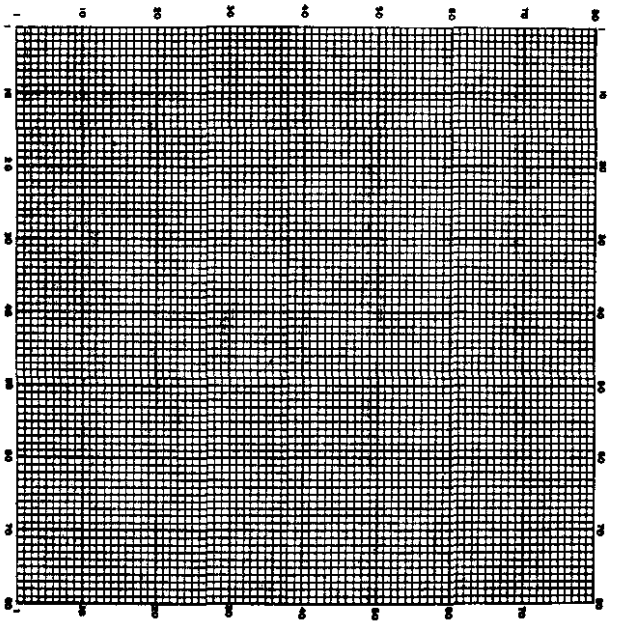

Figure 13. Grid Placement for Basin Gridding

Eighty such cards are required for each basin (some cards may be blank). The same grid overlay should then be rotated 90 degrees so that the 1-1 point is at the lower left corner (Figure 14). Using this grid arrangement, the X-Y coordinates of each precipitation station can then be determined. The basin grid map and the precipitation station X-Y coordinates are then entered into the MBP program and the Grid Point weights are computed for each of the stations used. A listing of input data instructions, sample input deck, and a sample output listing are contained on pages C-2 through C-15 of NWS HYDRO 14, so this information will not be duplicated in this report. The MBP program as well as all of the programs mentioned in this report can be obtained from the Office of Hydrology, National Weather Service, NOAA, Silver Spring, Maryland, 20910.

MBP Computation for Each Basin

Once the station weights were determined, each station (with a weight greater than 0.0) together with its Grid Point weight and the precipitation data (both hourly and daily) for the desired period of record (in this cas, 10/63-9/71) was used as input to the MBP program; then the MBP for the basin was computed and written on magnetic tape in the required format as a continuous record of six-hour incremental MBP.

In order to be able to define the rainfall patterns more precisely, the NWSRFS allows a basin to be divided into sub-areas for MBP computations. According to Morris, this can significantly improve the simulation accuracy for non-uniform precipitation events. The Watts and Tahlequah basins were both divided into two basins each, giving a

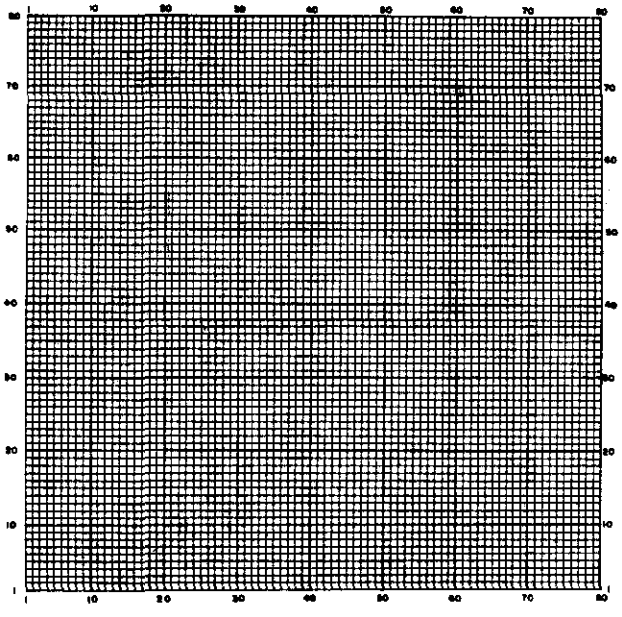

Figure 14. Grid Placement for Precipitation Station Coordinates

total of four MBP areas for the two basins (Figure 15). The weights for each of the four zones are given in Table XI.

TABLE XI

MBP AREA ASSIGNMENTS AND HISTOGRAMS FOR WATTS AND TAHLEQUAH

Illinois River near Watts, Oklahoma								
Histogram Element Number	1	2	3	4	5	6	7	8
Histogram Element (fraction)	.037	.195	.262	.249	.156	.077	.022	.001
MBP Area Assignment	1	1	1	2	2	2	2	2
Illinois River near Tahlequah, Oklahoma								
Histogram Element Number	1	2	3	4	5	6	7	8
Histogram Element (fraction)	.001	.030	.140	.300	.270	.121	.050	.029
MBP Area Assignment	3	3	3	3	4	4	4	4
Histogram Element Number	9	10	11	12	13	14		
Histogram Element (fraction)	.022	.018	.013	.003	.002	.001		
MBP Area Assignment	4	4	4	4	4	4		

Potential Evapotranspiration (PE) Computation

The PE data was obtained on cards from the Fort Worth River Forecast Center in Fort Worth, Texas. The station used was the Class A pan at Fort Gibson Dam, Oklahoma.

Streamflow Computation

The mean daily flows for Watts and Tahlequah were extracted, as discussed under Raw Data, from data tapes obtained from the U. S.

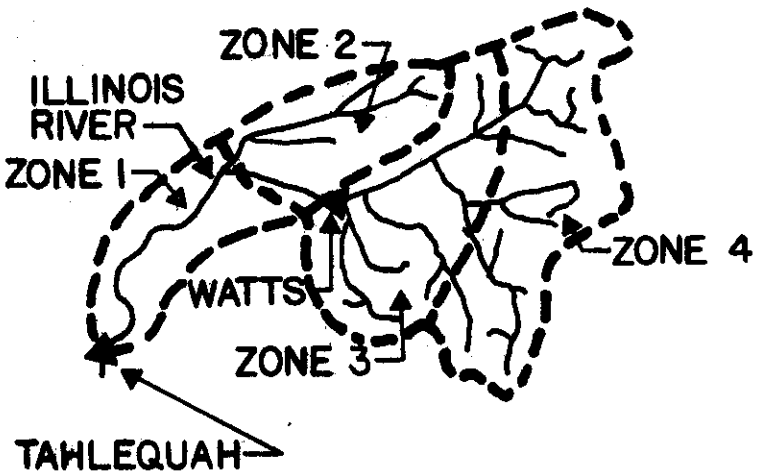

Figure 15. MBP Zones

Geological Survey. The six-hour incremental inflow into the reach below Watts was generated by the simulation run at Watts, placed on temporary disk storage, and used by Tahlequah.

Combined Data Tape

As extracted, the data is on three or four different tapes. In order to reduce the number of tapes, thereby increasing the efficiency of the program, all of the data for the two flow points were put on one data tape by a program called SUPRTP (Appendix E.2 of NWS HYDRO 14 contains a listing of SUPRTP). SUPRTP takes the data on two-four different tapes and combines them on one tape in month-size blocks.

At this point, all of the data required for Watts and Tahlequah, except for the six-hour incremental outflow from Watts, was on one data tape. In this case, both Watts and Tahlequah were simulated sequentially in one computer run, and the six-hour outflow from Watts was generated during each run, placed in temporary storage on disk files, and used when required for the Tahlequah simulation.

Channel Time Delay Histogram

The method used to route flow from the local surface area of a basin to its outflow point is the time delay histogram. This essentially divides the basin into zones of equal travel time (each zone having a different travel time). In Figure 15, the Illinois River basin is divided into four zones, one through four, whose average travel time would be 6-24 hours. The histogram gives the fraction of the flow from each of the four zones. To account for areal variation in runoff, each element of the histogram can have its own separate soil moisture

accounting system (and MBP area). For this study, each of the two basins was divided into two zones (Figure 15). The assignment of the histogram elements for Watts and Tahlequah is given in Table XII. These histogram values were computed by the Tulsa, Oklahoma River Forecast Center staff during initialization of these basins.

The method of developing a histogram is based on the derivation of the unitgraph for that basin. The first step is to derive the unitgraph for the basin [the unitgraph derivation technique is described by Lindsley, Kohler, and Paulhus (2)(3)]. This unitgraph will contain only direct runoff. The histogram ordinates can then be calculated by backrouting the unitgraph by using the following mathematical relationship

$$\bar{I} = \frac{O_{i+1} - \frac{K-3}{K+3}}{1 - \frac{K-3}{K+3}}$$

where

$\bar{I}$ = histogram ordinate

O_i = instantaneous outflow at the time, i

K = six-hour storage constant (the normal range of K is from six to twelve hours, with nine hours being the normal first guess. K must be greater than 3.0)

The histogram elements used in the NWSRFS are simply normalized values of $\bar{I}$. This procedure has been computerized at the Lower Mississippi River Forecast Center, Slidell, Louisiana.

Selection of Initial Parameter and Soil Moisture Values and the Effect of Changes Leading to the Final Values

The initial as well as the final parameters and soil moisture values are found in Table XII. The final 1 parameters were developed mostly by the Tulsa River Forecast Center, while the Final 2 parameters resulted from this study. Both are presented in order to illustrate that different parameter sets can give similar results (both good); however, only the Final 2 values will be discussed. Values for the Illinois River near Watts and Tahlequah, Oklahoma, will be identified by the names Watts and Tahlequah, respectively.

Each of the parameters required for the model will be discussed in alphabetical order. The initial values for each of these parameters were determined by one of four methods:

1) calculation using equations derived from observable watershed hydrologic characteristics

2) parameters transferred from a nearby basin which was already calibrated

3) knowledge of the hydrologic response of the basin, and

4) parameters taken from a set of typical values (Table XIII).

Discussion of initial parameter derivation will be limited to those that can be calculated.

Parameters

A

"A" is the percent of the total watershed area covered by lakes, streams, and impervious areas (excluding areas such as isolated rock

TABLE XII

INITIAL AND FINAL PARAMETER VALUES

	Illinois River near Watts, Oklahoma		Illinois River near Tahlequah, Oklahoma		
Parameter	Initial Value	Initial Value	Initial Value	Final 1 Value	Final 2 Value
K1	1.000	1.000	1.000	1.000	1.000
A	0.000	0.002	0.000	0.000	0.001
EPXM	0.350	0.200	0.840	0.620	0.850
UZSN	0.330	0.380	0.900	0.782	0.800
LZSN	8.500	7.500	10.000	8.398	9.000
CB	0.990	0.120	0.106	0.103	0.150
POWER	1.388	2.500	0.450	1.654	0.450
CC	0.857	1.400	1.200	1.386	1.000
K24L	0.070	0.000	0.100	0.201	0.000
K3	0.473	0.300	0.300	0.317	0.280
GAGEPE	1.000	1.000	1.000	1.000	1.000
E-HIGH	0.930	1.500	1.250	1.005	1.300
E-LOW	0.202	0.080	0.300	0.126	0.150
K24EL	0.000	0.000	0.000	0.014	0.007
SRC1	0.900	0.900	0.900	0.846	0.900
LIRC6	0.060	0.060	0.080	0.051	0.080
LKK6	0.007	0.010	0.014	0.149	0.010
KV	0.439	0.439	2.176	3.015	2.176
KGS	0.993	0.820	0.937	0.9012	0.8370
STHIGH	171	171	171	162	171
NDUR	40	40	40	16	40
STLOW	46	46	46	46	46
NEP	0	0	0	0	0
KS1	9.00	9.00	9.0	0.00	0.00

The histograms and lag curve were unchanged from initial to final run

Histogram - Watts: 0.037, 0.195, 0.262, 0.249, 0.156, 0.077 0.022, 0.001

Histogram - Tahlequah: 0.001, 0.030, 0.140, 0.300, 0.270, 0.121, 0.050, 0.029, 0.022, 0.018, 0.013, 0.002, 0.001

Tahlequah LAG and K:

Variable Lag (hours)	- Final 1:	44.0	33.0	18.0	18.0	
	- Final 2:	56.0	33.0	18.0	18.0	
Flow (cfs)	- Both:	0.0	500.0	1000.0	2000.0	
Variable K (hours)	- Both:	12.0	9.0	9.0	120	12.0
Flow (cfs)	- Both:	0.0	1500.0	7100.0	100000	25000.0

TABLE XIII

TYPICAL INITIAL PARAMETER VALUES AND RANGES

No.	Name	Typical Value	Normal Range	Calculation Procedure
1	A	0.003	0.001 - 0.005	
2	CB	0.150	0.050 - 0.350	
3	CC	1.100	0.500 - 1.500	
4	CSSR	0.350	0.250 - 0.750	From histogram program:CSSR = $\frac{KS1-3}{KS1+3}$
5	EHIGH	1.150	0.900 - 1.500	
6	ELOW	0.400	0.200 - 0.900	See Table XV
7	EPXM	0.170	0.100 - 0.500	See Table XVI
8	GAGEPE (PEADJ)	1.000	1.000 - 1.000	
9	GWSI	0.000	0.000 - 0.000	Start run during dry weather
10	HWARP	N/A	0.400 - 2.000	
11	KGS	0.910	0.820 - 0.990	See Table XIX
12	KS1	9.000	6.000 -12.000	KS1 = 3(1+CSSR)/(1-CSSR)
13	KV	2.500	0.700 -12.000	
14	K1	1.000	1.00 - 1.000	
15	K24EL	0.000	0.001 - 0.010	80% of "A"
16	K24L	0.000	0.000 - 0.250	
17	K3	0.280	0.200 - 0.350	See Table XX
18	L1RC6	0.100	0.050 - 0.150	
19	LKK6	0.010	0.003 - 0.150	LKK6 = 1.0 (daily recession)$^{0.25}$
20	LZSI	COMPUTE	2.000 - 6.000	LZSN = 0.5(LZSN) See Table XXI
21	LZSN	8.500	4.000 -12.000	
22	NEP	0.000	0.0 -60.0	
23	NDUR	40.0	0.0 -60.0	
24	PEADJ (GAGEPE)	1.000	1.000 - 1.000	
25	POWER	2.000	0.500 - 3.000	
26	RESI	0.000	0.000 - 0.000	Start run during dry weather
27	SCEPI	0.000	0.000 - 0.000	Start run during dry weather
28	SGWI	COMPUTE	0.100 - 0.500	SWGI = $\frac{\text{GWF for first day of run}}{(LKK6)(107.7)(\text{basin area}}$
29	SRC1	0.900	0.800 - 0.950	
30	SRGXI	0.000	0.000 - 0.000	Start run during dry weather
31	STHIGH	150.0	100.0 - 200.0	
32	STLOW	46.0	30.0 - 55.0	
33	UZSI	0.000	0.000 - 0.000	Start run during dry weather
34	UZSN	0.250	0.050 - 0.400	
35	VWARP	N/A	0.700 - 2.000	

outcrops, building, or roads). Runoff from this area reaches the stream almost immediately (within one hour). It is a sensitive parameter both in respect to volume as well as hydrograph response, but its effects are primarily on small rises and the initial portions of larger rises (when "A" is increased, the small rises increase). "A" for Watts and Tahlequah was increased from 0.000 to 0.001 and 0.002, respectively, because some impervious area is present in all basins, without exception, and is needed to simulate the amall rises properly. As a minimum, "A" must represent the stream surfaces themselves. Above 0.002, the smaller rises become excessive on the Illinois River, so "A" was finalized at 0.002.

CB

"CB" is the index to infiltration. It is the one-hour infiltration rate (inches/hour) when Lower Zone Storage (LZS) is at its nominal capacity (LZSN). It is a very sensitive parameter; small changes of CB produce large hydrograph changes as well as moderate annual volume changes. Decreasing CB increases the wave amplitude and causes the peaks to occur earlier and higher due to the increased fast response flow. The initial values of CB for Watts (0.99) and Tahlequah (0.106) were increased to 0.120 and 0.150, respectively, in order to reduce excessively high peak flows. Table XIV gives initial CB values based on soil permeability.

TABLE XIV

INITIAL CB VALUES

Soil Permeability	CB(inches/hour
low	0.05
medium	0.10 - 0.20
high	0.25 - 0.50

CC

"CC" is the ratio $\frac{\text{interflow}}{\text{surface runoff}}$. It influences the time distribution of the flow, not the volume. It is only moderately sensitive. If CC is decreased, the proportion of surface runoff increases and the hydrograph peaks become higher, sharper, and slightly earlier; however, only the storm hydrograph is affected, not dry weather flow. The initial value of CC for Watts (0.857) was increased to 1.400 because there was a need for more interflow during the falling limb of the hydrograph, while Tahlequah (1.200) was reduced to 1.000 due to excessive interflow.

EHIGH

"EHIGH" is the maximum value of the annual evapotranspiration (ET) curve (Figure 28). EHIGH is reached after the number of days given by STHIGH, and it remains there for the number of days given by NDUR. As EHIGH is increased, the ET losses increase. Its effect is seasonal, and its reaction is usually only moderately sensitive, although there are times when the ET curve is at EHIGH when the storm simulation becomes markedly sensitive to EHIGH changes. All ET curve parameters should be similar for a given region. All initial values for Watts (0.930) and Tahlequah (1.250) were increased to 1.500 and 1.300, respectively, because the initial ET losses were too low during the summer.

ELOW

"ELOW' is the minimum value of the annual ET curve (Figure 16). ELOW is reached after the number of days given by STLOW, and it remains

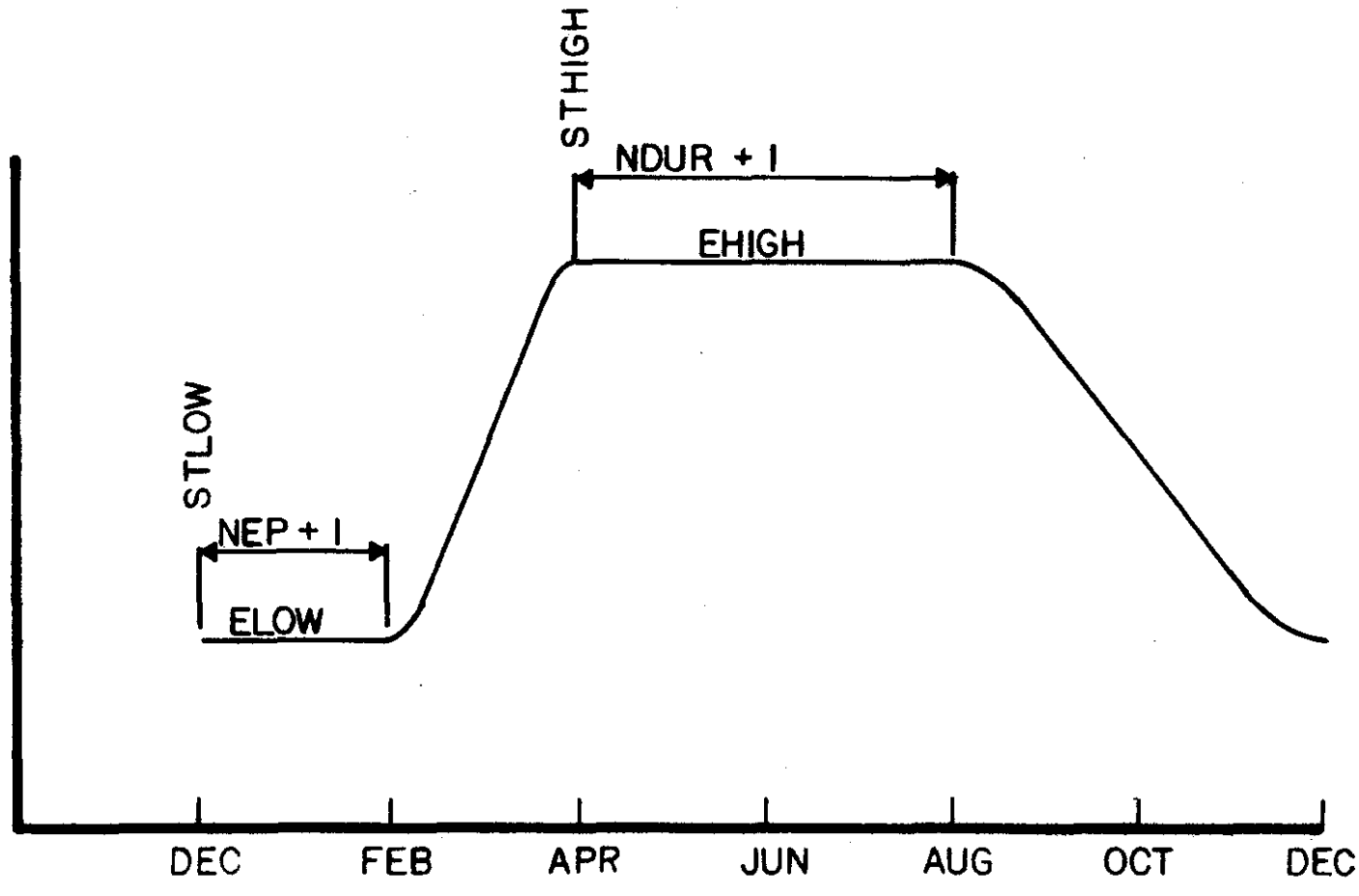

Figure 16. Evapotranspiration Curve

there for the number of days given by NEP. As ELOW is decreased, the ET losses decrease during the period of ELOW, but it is only moderately sensitive. Initial values of ELOW can be taken from Table XV.

TABLE XV

INITIAL ELOW VALUES

Area	ELOW
Southern	0.60
Mid-latitude	0.30
Northern	0.00

The initial values for Watts (0.20 and Tahlequah (0.300) were reduced to 0.080 and 0.150, respectively, because the ET was too high during winter.

EPXM

"EPXM" is the maximum interception storage (inches). It is moderately sensitive for small rises, but has relatively little effect on large rises. Increasing EPXM reduces the small rises. When the small rises are more predominant during one period of the year, EPXM exerts a seasonal effect. It has little effect on the annual flow volume. Table XVI gives initial values for EPXM based on basin characteristics. Table XVI illustrates the greater effect that EPXM has on lower flows than higher flows. Table XVI shows the seasonal effect of EPXM changes. The initial EPXM value for Watts (0.350) was reduced to 0.200 to increase the small rises, while Tahlequah (0.840) was not changed significantly (0.850).

TABLE XVI

INITIAL EPXM VALUES

Vegetation	EXPM (inches)
Grassland	0.10
Moderate Forest	0.020-0.130
Heavy forest	0.15 - 0.20
Exceptions	
Many farm ponds	1.50
Many natural ponds	0.30 or greater

TABLE XVII

EXAMPLE OF CHANGE IN LAYER BIAS DUE TO INCREASE IN EPXM

Flow Interval (cfs)	Percent Bias EXPM = .100	Percent Bias EXPM = .500	Percent Change
29-177	+23.7	-21.3	-45.0
177-645	+16.8	-15.3	-32.1
645-1761	+2.8	-14.4	-17.2
1761-4000	-4.3	-15.6	-14.3
4000-8003	-9.8	-17.3	-7.5
8003-14595	-.3	-5.1	-4.8

TABLE XVIII

EXAMPLE OF CHANGE IN MONTHLY BIAS DUE TO INCREASE IN EPXM

Month	Percent Bias EXPM = .100	Percent Bias EXPM = .500	Percent Change
Oct	+21.2	-30.8	-52.0
Nov	-39.7	-52.2	-12.5
Dec	-15.2	-36.5	21.3
Jan	-.3	-21.2	-20.9
Feb	+.1	-6.7	-6.8
Mar	-.5	-21.3	-20.8
Apr	-2.1	-24.8	-22.7
May	-4.6	-15.7	-11.1
Jun	+39.9	-4.3	-44.2
Jul	+34.8	-5.8	-40.6
Aug	+11.1	-17.7	-28.8
Sep	+18.6	-12.5	-31.1

GAGEPE

"GAGEPE" moves the entire ET curve higher or lower. It should be used only if there is a significant bias in the Potential Evapotranspiration (PE) data. Normally, GAGEPE is left at 1.000, as it was for Watts and Tahlequah. This is an extremely sensitive parameter; small changes produce large hydrograph and annual volume changes. Increasing GAGEPE increased the ET, thereby decreasing the flow.

GWSI

"GWSI" is the initial groundwater slope. It is normally assumed to be 0.000 because the run is normally begun during dry weather (as was done with Watts and Tahlequah).

KGS

"KGS" is the six-hour groundwater carryover. It is one of the parameters allowing variable groundwater recession. It is an index to the time required to reach fair weather recession. Initial KGS values should be set according to Table XIX.

TABLE XIX

INITIAL KGS VALUES

Time to Reach Fair Weather Recession	KGS
1 - 2 months	0.97 - 0.98
1 month	0.94 - 0.96
short	0.90 - 0.93
very short	0.85 - 0.90

The initial value for Watts (0.993) was reduced to 0.820 in order to reduce the rate of groundwater recession. Tahlequah, at 0.837, was not changed.

KS1

"KS1" is the channel storage recession parameter. It represents the

histogram lag, and is normally between 6.0 and 9.0 hours, having a minimum value of 3.0 and a normal maximum of 12.0 (if greater than 12.0, the histogram should be revised). It is computed from the CSSR value (obtained from the histogram computation program) by use of the following equation

$$KS1 = 3(1.0 + CSSR)/(1.0 - CSSR)$$

or a starting value of 9.0 is assumed (as was done for Watts). Watts KS1 was not changed from 9.0 during the run. Tahlequah's KS1 was set and left at 0.0 due to use of variable K for that basin.

KV

"KV" is the major parameter allowing a variable recession for the groundwater flow (other parameters are KGS and LKK6). The larger KV is, the steeper the recession is. KV has little effect on volume, and only a moderate effect on the hydrograph shape. The initial values for Watts (0.439) and Tahlequah (2.176) were not changed.

K1

"K1" is the adjustment factor for MBP that is uniformly too high or too low. Raising K1 increases the amount of MBP along with the annual flow volume. This is a very sensitive parameter that is normally set to 1.00 (as was done for Watts and Tahlequah).

K24EL

"K24EL" is the fraction of the total watershed area from which ET occurs at the potential rate. It is the percent of the watershed with

shallow groundwater that is within reach of vegetation.
Initial values of K24EL are usually set at 0.000, as was done for Watts and Tahlequah. Only Tahlequah was changed (to 0.007 to reduce the groundwater flow in the summer).

K24L

"K24L" is the percent of groundwater inflow that percolates to deep (inactive) groundwater storage. It is the percent of groundwater recharge assigned to deep percolation. An increase of K24L decreases flow, but the annual losses are normally small compared with rainfall. It is a moderately sensitive parameter. It provides a way of reducing the groundwater flow in a relative uniform manner. The initial values for Watts (0.070) and Tahlequah (0.100) were reduced to 0.000 to reduce excessive groundwater losses.

K3

"K3" is the index to the actual ET losses. It is a sensitive parameter that has considerable effect on flow volumes as well as hydrograph shape. Initial values should be either selected from Table XX or set using a similar basin.

TABLE XX

INITIAL K3 VALUES

Watershed Cover	K3
Open Land	0.20
Grassland	0.23
Light Forest	0.28
Heavy Forest	0.30

The initial values for Watts (0.473) and Tahlequah (0.300) produced too high ET losses, so were reduced to 0.300 and 0.280, respectively.

LIRC6

"LIRC6" is the interflow (medium response runoff) routing coefficient; it is the precent of interflow detention storage reaching the channel each six hours. It is normally set at 0.900 and not varied during calibration, its effect being compensated for by other parameters--mainly CC. Other work, however, indicated other values for these basins. Watts and Tahlequah were set to 0.060 and 0.080, respectively, and not changed.

LKK6

"LKK6" is the complement of the six-hour fair weather groundwater recession coefficient. It is the percent of groundwater storage that reaches the channel each six hours when KV = 0.0. The initial value for LKK6 is normally computed by the equation

$$LKK6 = 1.0 - (KK24)^{\frac{1}{4}}$$

where

KK24 is the 24-hour recession coefficient = today's flow/yesterday's flow. If LKK6 is reduced, groundwater flow recession will be slowed, resulting in flatter, higher recession hydrographs. The initial values for Watts (0.007) and Tahlequah (0.014) were both changed to 0.010--Watts because the groundwater recession was too rapid, and Tahlequah because the recession was not rapid enough.

LZSI

"LZSI" is the initial amount (inches) of water held in lower zone storage (LZS). It is normally set equal to 0.5(LZSN) due to beginning the run during dry weather; however, Table XXI gives values for other conditions. Since LZSI simply provides a starting place for LZS, a LZSI of the proper magnitude will suffice. By the end of the first 30-60 days, its effect will be minimal.

TABLE XXI

INITIAL LZSI VALUES

Moisture Supply	
Dry Weather	0.50 (LZSN)
Little Precipitation	0.75 (LZSN)
Normal Precipitation	1.00 (LZSN)
Above Normal Precipitation	1.25 (LZSN)

LZSN

"LZSN" is the nominal lower zone storage capacity (inches). It is about one-half of maximum LZ capacity. It is a sensitive parameter that has a major effect on the volume. If LZSN is decreased, the annual flow volume increases, hydrograph peaks become sharper and higher, recession becomes more rapid, and infiltration is decreased. The initial values for both Watts (8.500) and Tahlequah (10.00) were reduced to 7.500 and 9.000, respectively, in order to obtain more fast response runoff and thereby raise the crests of rises.

NEP

"NEP" is the number of days the ET curve remains at ELOW. It is normally set equal to zero and changed only if an analysis of seasonal bias indicates a need for an adjustment. The initial values of zero for both Watts and Tahlequah were unchanged.

NDUR

"NDUR" is the number of days that the ET curve remains at EHIGH. It represents the average duration of the maximum or near maximum growing activity. It is normally set by use of a nearby basin, and changed after analysis of the simulation for seasonal bias. All ET curve parameters should be similar for adjacent basins. Both Watts and Tahlequah were not changed from their initial value of 46.0.

POWER

"POWER" determines the slope of the infiltration curve; the larger POWER is the faster infiltration. Rates change as the wetness ratio (LZS/LZSN) changes (Figure 18). It is moderately sensitive in respect to hydrograph shape, but has little effect on the annual flow volume. The initial value for Watts (1.388) was increased to 2.500 in order to give more infiltration during dry conditions and less during wet conditions. Tahlequah was not changed from 0.450.

RESI

"RESI" is the initial surface detention storage in inches. It is normally set equal to 0.000 because the run is started during dry

weather. Watts and Tahlequah were both set equal to 0.000.

SCEPI

"SCEPI" is the initial interception storage in inches. Since the fun is normally started during dry weather, SCEPI is normally set equal to 0.000, as was done for Watts and Tahlequah.

SGWI

"SWGI" is the initial groundwater storage in inches. It is computed from the following equation:

$$SWGI = \frac{\text{groundwater flow for the first day of the run}}{(LKK6)(107.7)(\text{Basin Area})}$$

SRC1

"SRC1" is the fast response (surface detention) flow routing coefficient; it is the percent of calculated potential fast response (surface detention) flow that reaches the channel each hour. It was set at 0.900 for both Watts and Tahlequah and not changed.

SRGXI

"SRGXI" is the initial interflow detention storage in inches. It is normally set equal to 0.000, because the run starts during dry weather, as was done for Watts and Tahlequah.

STHIGH

"STHIGH" is the Julian date on which the ET curve reaches EHIGH, which is the date when the watershed vegetation reaches its maximum

growing activity (about April 1 for southern basins, and about May 15 for northern basins). It is usually set according to nearby basins and changed after analysis of the simulation run for seasonal bias. The initial and final values for Watts and Tahlequah were 171 days.

STLOW

"STLOW" is the Julian date on which the ET curve reaches ELOW. It is normally set according to nearly basins (the most common date is 46), and changed after analysis of the data for seasonal bias. The initial and final dates for Watts and Tahlequah were 46 days.

UZSI

"UZSI" is the initial upper zone storage in inches. It is normally set equal to 0.000, since the run usually starts during dry weather. Watts and Tahlequah were both set to 0.000.

UZSN

"UZSN" is the nominal upper zone storage capacity; it is about equal to 1/3 of the maximum storage capacity. It includes both surface depression storage as well as storage in the soil profile near the soil surface. It is a very sensitive parameter that has a major effect on the annual flow volume, as well as small rises. Decreasing UZSN increases smaller rises and the beginning of larger rises. UZSN is normally larger than EPXM. If there is a deep litter layer, UZSN varies from 0.75-1.00. If the soil is permeable, UZSN varies from 0.10-0.25. The initial value for Watts (0.330) was increased slightly to 0.380 to decrease the amplitude of small rises, while Tahlequah (.900)

was decreased to .800 to increase the magnitude of the small rises.

LAG

"LAG" is the amount of constant lag for the reach from Watts to Tahlequah. It was set to 0.00 because all of the lag was accounted for by the variable lag (Table XII).

The NWSRFS was calibrated for Watts and Tahlequah using an eight-year period of record--Water Years (October through September) 1964-1971. This period of record includes dry, wet, as well as average years. In the Appendix will be found a one-year sample of the output hydrographs, the actual computed (simulated) and observed mean daily flows (cfs), and the mean basin precipitation for each day. The period of record displayed was chosen to include a period with low flow values; these are not necessarily the years in which the fit was optimum. In fact, the simulation for Watts for that period is not extremely good but it does illustrate problems such as non-representative mean basin precipitation and streamflow measurements, as well as the fact that there is some degree of regulation of low flows resulting from the dam and waterfall upstream at Lake Francis. Data for the whole period of record, however, does show that the overall fit for Watts is reasonably good. Seasonal bias is also quite in evidence for that year, which suggests that a more flexible method of defining the seasonal potential evapotranspiration would be useful in obtaining a better fit. More work would enable a better fit at Watts. The simulation for Tahlequah, however, is noticeably better than for Watts. Low flow simulation inadequacies for Tahlequah are due primarily to inadequate mean basin precipitation. Peak flows are not optimum for Tahlequah for this year, but

they are better during years with higher flows. The need for better seasonal potential evapotranspiration definition is also apparent for Tahlequah. The output for Tahlequah begins in November rather than in October, because Water Year 1964 was the first year of the run, and the soil moisture balance had not yet stabilized during October.

With the model calibrated for both Watts and Tahlequah, the NWSRFS may now be used for predicting streamflow, for developing additional periods of records, and for examining the hydrologic effects of changes to the watersheds. As there is much interest in developing records of extreme values of streamflow for these basins, it should be noted that this can now be done by simply running the model using synthetic data. For a synthetic record of low flows, mean basin precipitation and potential evapotranspiration data which reflect drought conditions can be generated for as long a period as desired and then used with the NWSRFS to synthesize the desired low flow records. In fact, synthetic streamflow records of any desired length for any desired climatic conditions can be generated simply by using the appropriate mean basin precipitation and potential evapotranspiration data. Watershed changes can also now be examined by changing some of the parameters and running the model. For example, extensive deforestation could be simulated by reducing EPXM, and extensive creation of impervious areas could be simulated by increasing A. Various combinations can be created by thoughtful variation of the parameters which will cover most changes possible to a watershed, both for past periods of record as well as for generated future records.

Discussion of the Calibration

The process of calibrating a model to a basin can be a long, tedious process that has no clear-out ending point. Normally, the analyst must establish criteria that will tell him when to stop. The criteria are usually time, money, or goodness-of-fit. The limiting resource for this study was time. The results are given in Tables XXII and XXIII.

TABLE XXII

MODEL FIT BY FLOW INTERVALS FOR TAHLEQUAH
WATER YEARS 1964-1971

Flow Interval (cfs)	Number of Observed Cases	Observed Mean Flow (cfs)	Simulated Mean Flow (cfs) (1)	(2)	Percent Bias (1)	(2)
0-33	6	32	35	35	9.4	9.4
33-88	199	69	72	70	4.3	1.4
88-200	891	136	130	125	4.4	8.1
200-399	573	287	287	278	0.0	3.1
399-727	487	552	549	536	0.5	2.9
727-1234	370	943	885	873	6.2	7.4
1234-1983	201	1518	1473	1955	3.0	3.0
Above 1983	195	4287	4205	4116	1.9	4.0

TABLE XXIII

MODEL FIT BY FLOW INTERVAL FOR WATTS
WATER YEARS 1964-1971

Flow Interval (cfs)	Number of Observed Cases	Observed Mean Flow (cfs)	Simulated Mean Flow (cfs)	Percent Bias
0-88	522	67	66	-1.4
88-200	911	135	144	6.3
200-399	545	286	336	14.9
399-727	508	535	552	3.2
727-1234	226	921	855	-7.2
1234-1983	105	1528	1419	-7.1
Above 1983	105	4206	2990	-28.1

The U. S. Geological Survey rates the accuracy of measurements taken at the two stations as "good," which represents an accuracy within ten percent. Accordingly, it was decided that a fit that yielded biases less than ten percent would be acceptable. Inspection of Tables XXII and XXIII shows that the fit obtained for Tahlequah is thus acceptable, while the fit for Watts is outside the limits for flows from 200-399 cu ft per second (cfs) and above 1983 cfs. The reasons that better results were not obtained at Watts are inaccurate data, insufficient data, and deficiencies in the model itself. Experience with other basins has shown it is common to have difficulties fitting a headwater basin accurately. Inspection of the data disclosed numerous occasions where the

river stage at Watts rose, although no precipitation had been recorded in the basin. Obviously, rain had fallen in places other than in the rain gages. With thunderstorm activity especially, it is not surprising that the rain often misses the eight-inch rain gages, although it may fall nearby. With most of the precipitation stations reporting on a daily basis and the others every six hours, there is ample room for error also in the precipitation timing. Averaging the precipitation over the basin can sometimes erroneously spread precipitation over areas where it did not fall, as well as reduce the intensity over the area where it did fall. The rating of a gage can also change due to channel configuration changes as well as vegetative growth and accumulation of debris. The rating at Watts is known to occasionally vary seasonally due to aquatic growth. In basins such as these, where most of the trees are deciduous, the surface area available for interception storage varies widely both during the course of a year as well as from year to year, depending on meteorological conditions. However, the model cannot account for year to year changes except by parameter changes to give some sort of average fit for each year, and the only way of controlling seasonal changes is through changes in the evapotranspiration curve, which is only an indirect method, and not really satisfactory for an area in which interception is as important as it is in these basins.

The model fit for Tahlequah is obviously much better than the fit for Watts. Experience with numerous other basins has shown that this is normal; reaches are usually fit more accurately and easily than headwater basins. The reason for this is that a reach has a known inflow, while a headwater or even the local area of a reach does not.

The implication here is that the model does a better job of routing flow than it does of hydrologic simulation. Although this implication is probably true, it is also probably true that this is a result of the model being data bound, and as Linsley stated, there is no point in trying to make a simulation model with greater accuracy than the stream gaging. His comment is just as applicable to precipitation measurements as to streamflow measurements. Still, it is apparent that the model needs to be refined still further to enable it to more closely match watershed responses. Further refinement, however, may lead to an increase in the number of parameters the analyst has to be concerned with, which would not be good. In its present state, there are more than enough parameters available to make the task of fitting a basin a complex matter. There is also a great degree of interaction among the various parameters. A given hydrograph can be reconstituted using many different parameter value sets--a good fit does not imply a unique set of parameters. These factors require considerable experience and ability on the part of the analyst to achieve a good fit.

Since both engineering and forecasting activities are primarily interested in results, the most desirable solution for the model fitting problem is a computer based parameter optimizing model. HYDRO 14 describes such a currently available model, but it is only a step in the right direction. It requires a good fit prior to using it, and is not controllable as to how the model is fit (low flows, high flows, or seasons). The ideal parameter optimizing model would accept rough parameter values and would have adjustable fitting criteria, so that the analyst can emphasize that segment of the hydrograph or time of year

that needs to be refined. Since fitting errors are frequently systematic, and can be located in terms of flow intervals and/or time of year, the ability to work only on specific problems would be helpful. This approach would also cut down on the costs of using such a program.

CONCLUSIONS

Based on the results of this study of using a digital conceptual hydrologic model for simulating streamflow, the following conclusions can be drawn:

1) The NWSRFS can be used to simulate accurately low flows in addition to high flows, using as data only mean basin precipitation, potential evapotranspiration and, if the basin is a reach, the inflow to the reach.

2) It is more difficult to fit a headwater basin than a reach.

3) The limiting factors in model calibration are data and parametric complexities.

4) There are variations in a basin from one year to another, such as amount of vegetation and moisture conditions that cannot be accounted for by the model.

5) Once the NWSRFS has been calibrated for a given basin, it may be used to predict future streamflow, with the sunthetic use of data (mean basin precipitation, potential evapotranspiration and, if the basin is a reach, inflow to the reach).

Water Quality Studies

In the environmental assessment of a river basin, the water quality of the river is very important. Therefore, a search of all existing water quality records for the Illinois River and Flint Creek was conducted. The search produced very little water quality data. Data was found for three sites on the Illinois River. These being Siloam Springs, Watts and Gore. No water quality data was found for Flint Creek. Existing water quality data for the Illinois River are shown in Figures 17 to 36. It can be seen that in most cases water quality data is available for only a few years.

The water quality of the Illinois River is very good. The dissolved oxygen concentration at Siloam Springs varied from about 5.8 mg/l to 12.0 mg/l. at Watts the D.O. concentration varied from about 7.0 mg/l. to 12.0 mg/l at Watts this variation is primarily due to the temperature variation since the D.O. as % saturation is fairly constant at 100% throughout the year. However, at Siloam Springs the D.O. as % saturation is not constant throughout the year. The D.O. varies from a low of 65% saturation during the summer to about 100% during the winter. This indicates that some environmental factor was causing an oxygen demand.

Water quality parameters such as BOD_5, turbidity, iron, orthophosphate, coliform bacteria, alkalinity, nitrate-nitrogen, ammonia-nitrogen, hardness, and chlorides were all quite low.

Water quality analysis were also conducted by the project personnel during March and April, 1975. All analysis were conducted in the field using a Hach Water Quality kit. Samples were taken at three sites on the Illinois River and one site on Flint Creek. The results are shown in Tables XXIV and XXV.

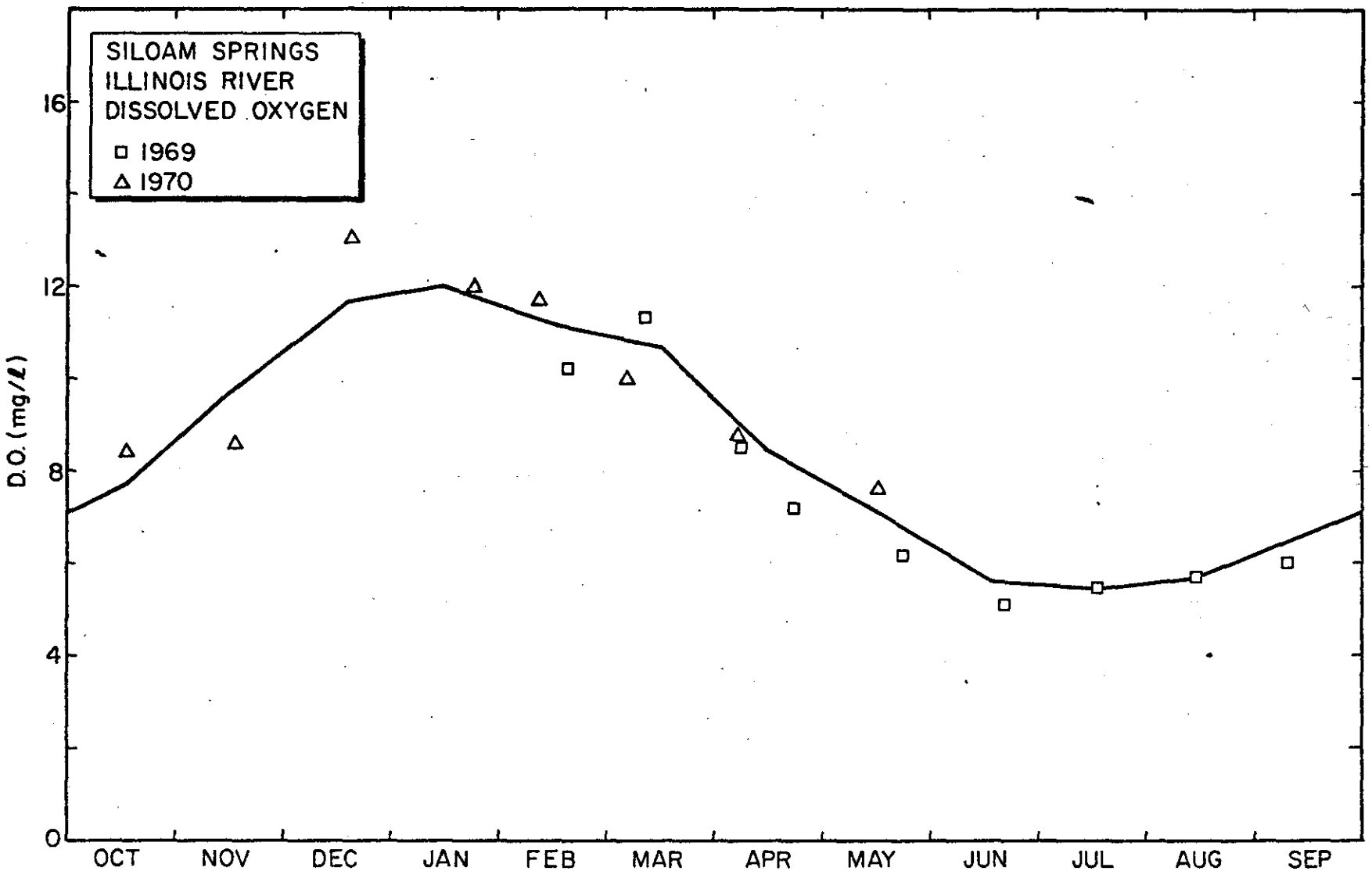
SILOAM SPRINGS
ILLINOIS RIVER
DISSOLVED OXYGEN
□ 1969
△ 1970
D.O. (mg/ℓ)
16
12
8
4
0
OCT
NOV
DEC
JAN
FEB
MAR
APR
MAY
JUN
JUL
AUG
SEP

Figure 17.

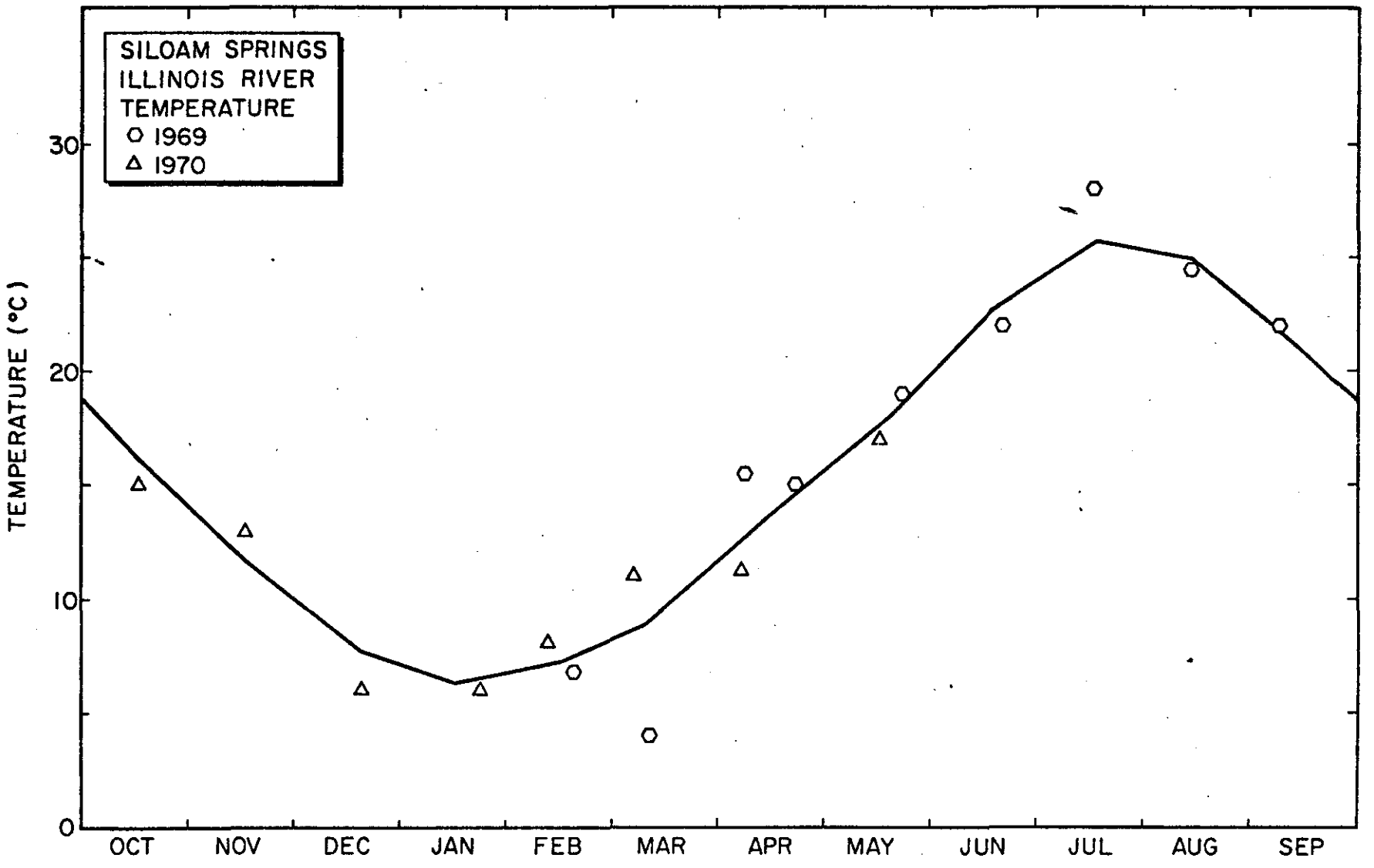
SILOAM SPRINGS
ILLINOIS RIVER
TEMPERATURE
1969
1970
TEMPERATURE (°C)
30
20
10
0
OCT
NOV
DEC
JAN
FEB
MAR
APR
MAY
JUN
JUL
AUG
SEP

Figure 18

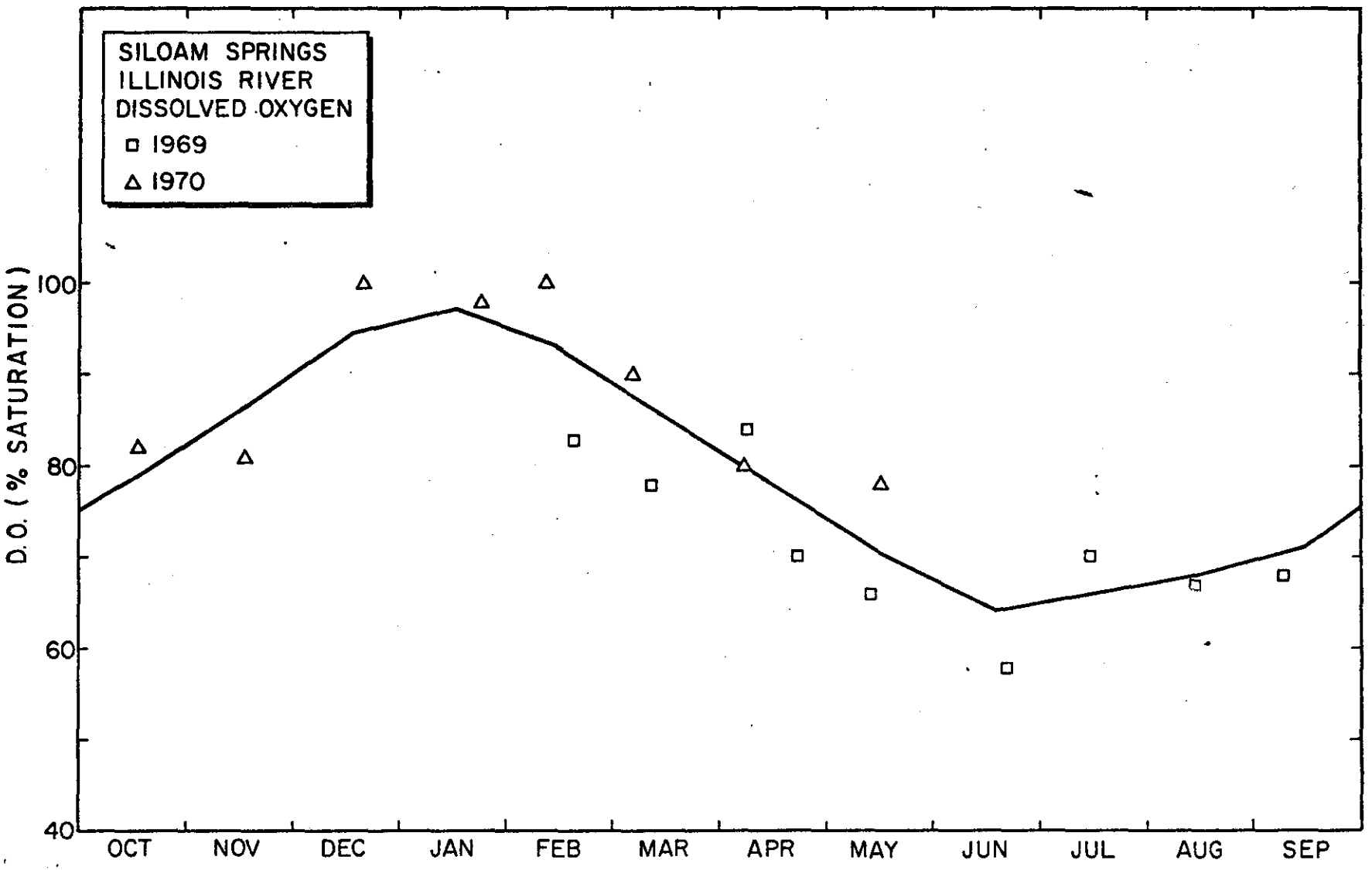
SILOAM SPRINGS
ILLINOIS RIVER
DISSOLVED OXYGEN
□ 1969
△ 1970
D.O. (% SATURATION)
100
80
60
40
OCT
NOV
DEC
JAN
FEB
MAR
APR
MAY
JUN
JUL
AUG
SEP

Figure 19

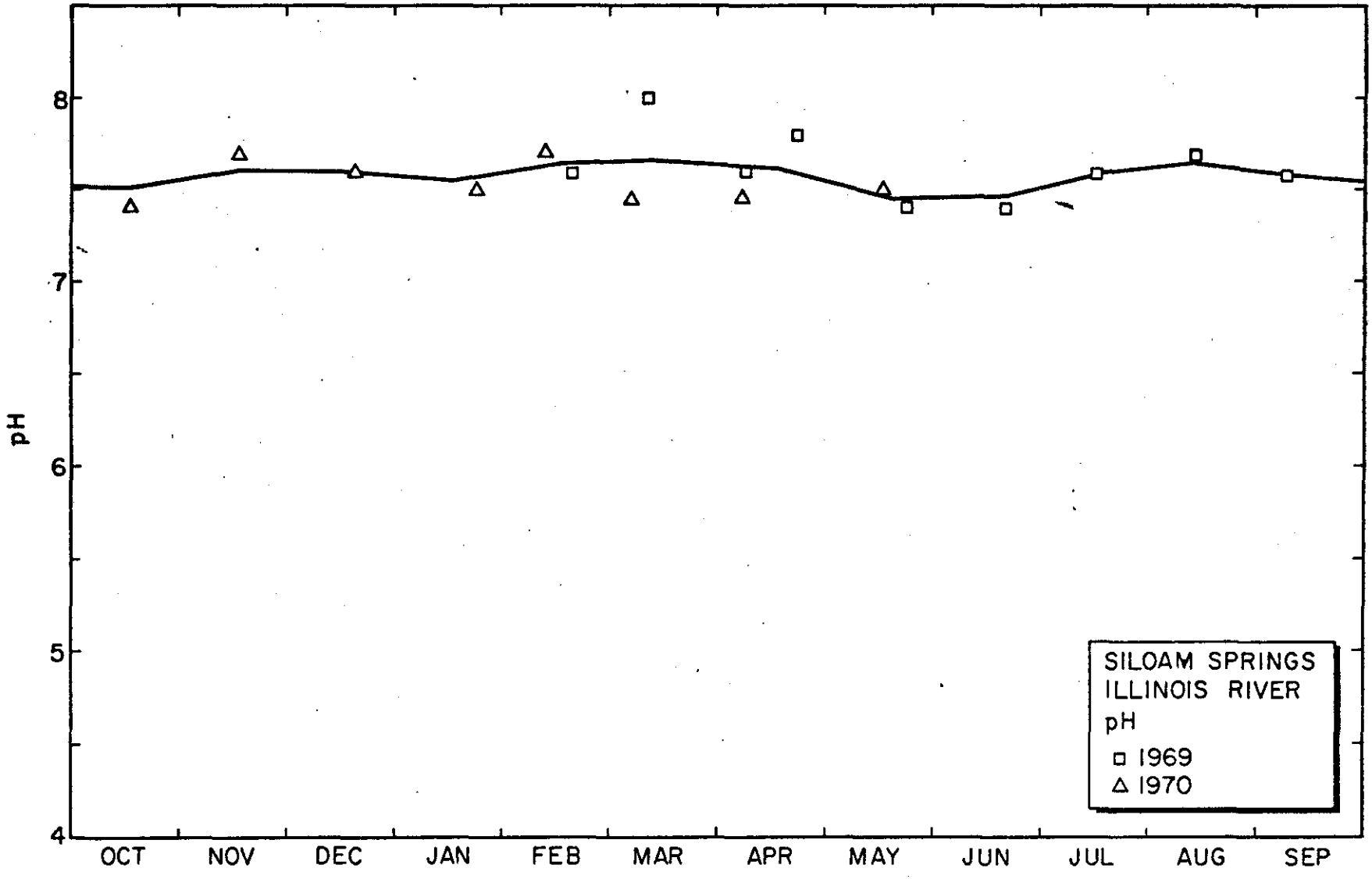
8
7
6
5
4
pH
OCT
NOV
DEC
JAN
FEB
MAR
APR
MAY
JUN
JUL
AUG
SEP
SILOAM SPRINGS
ILLINOIS RIVER
pH
□ 1969
△ 1970

Figure 20

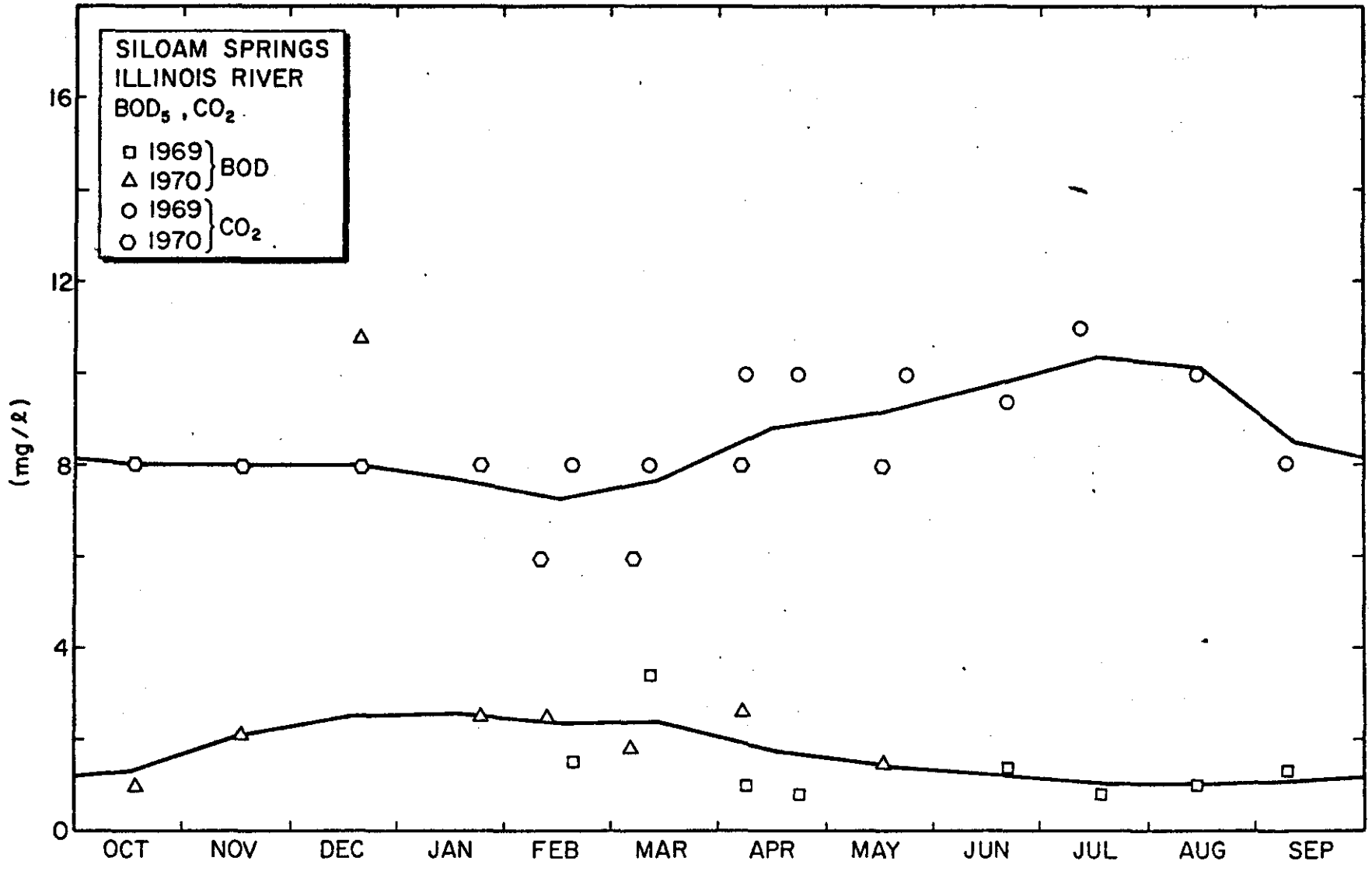
SILOAM SPRINGS
ILLINOIS RIVER
BOD5 , CO2
1969 } BOD
1970 }
1969 } CO2
1970 }
16
12
8
4
0
(mg/ℓ)
OCT
NOV
DEC
JAN
FEB
MAR
APR
MAY
JUN
JUL
AUG
SEP

Figure 21

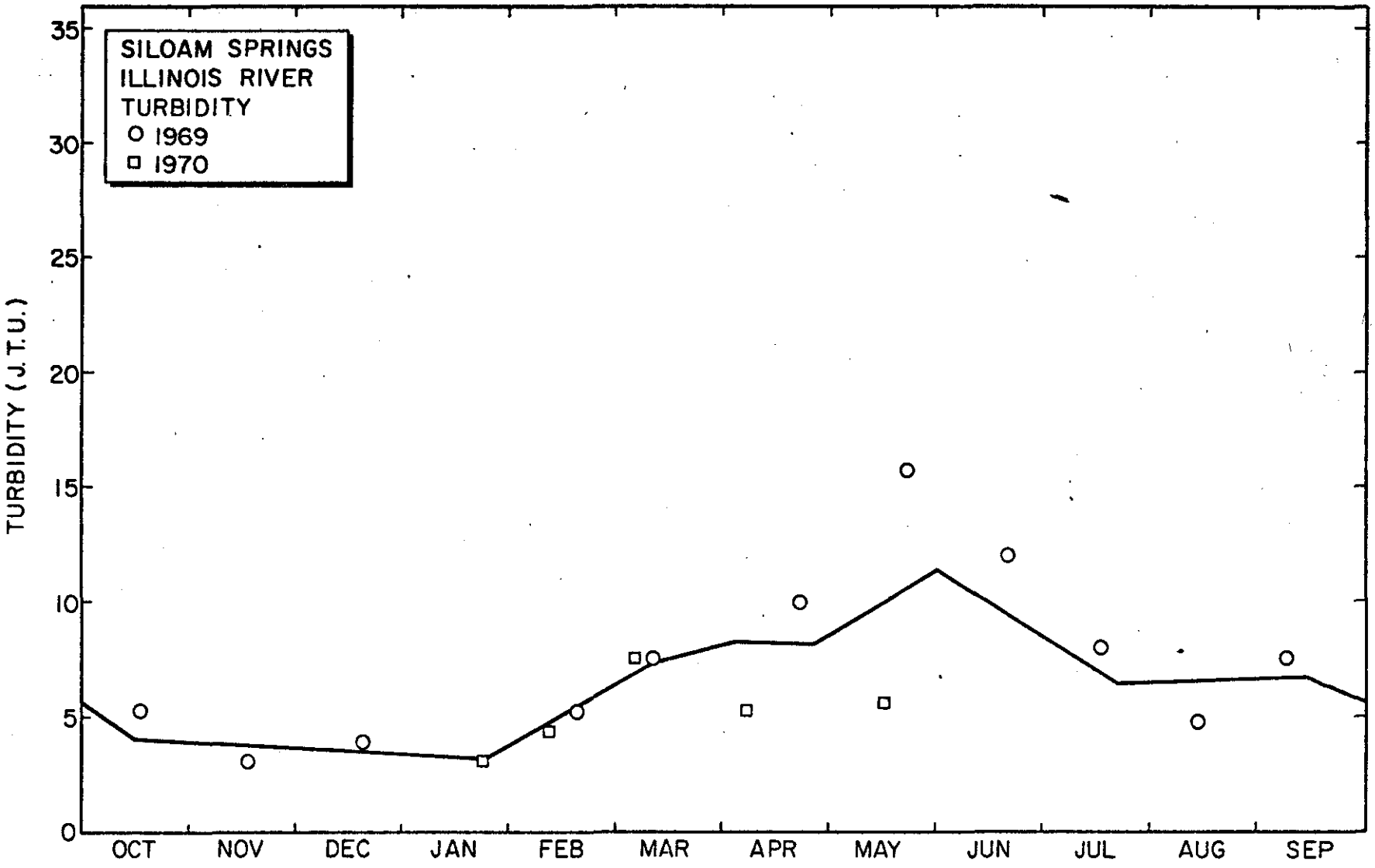
SILOAM SPRINGS
ILLINOIS RIVER
TURBIDITY
O 1969
□ 1970
TURBIDITY (J.T.U.)
35
30
25
20
15
10
5
0
OCT
NOV
DEC
JAN
FEB
MAR
APR
MAY
JUN
JUL
AUG
SEP

Figure 22

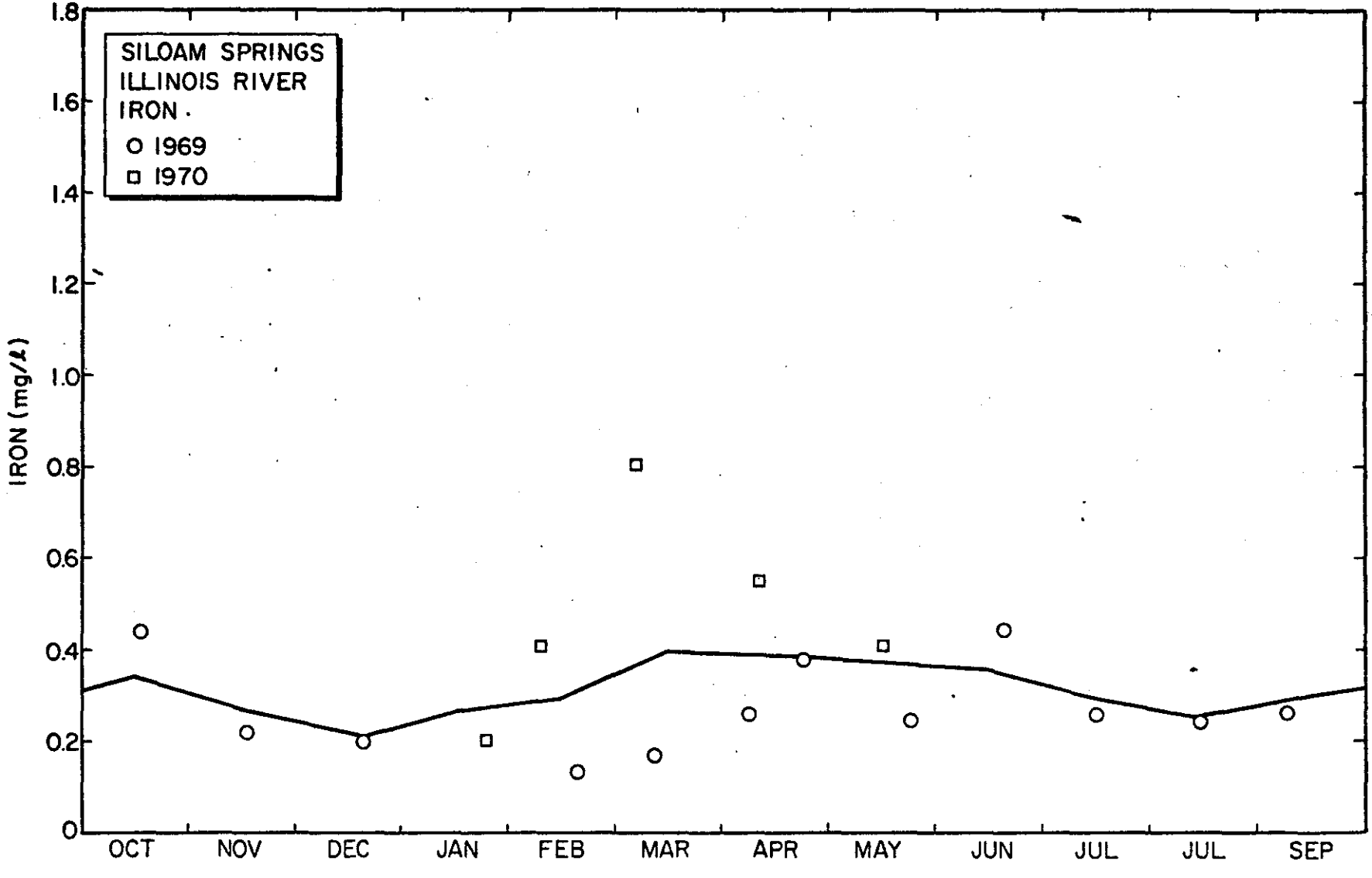
SILOAM SPRINGS
ILLINOIS RIVER
IRON .
O 1969
□ 1970
IRON (mg/ℓ)
1.8
1.6
1.4
1.2
1.0
0.8
0.6
0.4
0.2
0
OCT
NOV
DEC
JAN
FEB
MAR
APR
MAY
JUN
JUL
JUL
SEP

Figure 23

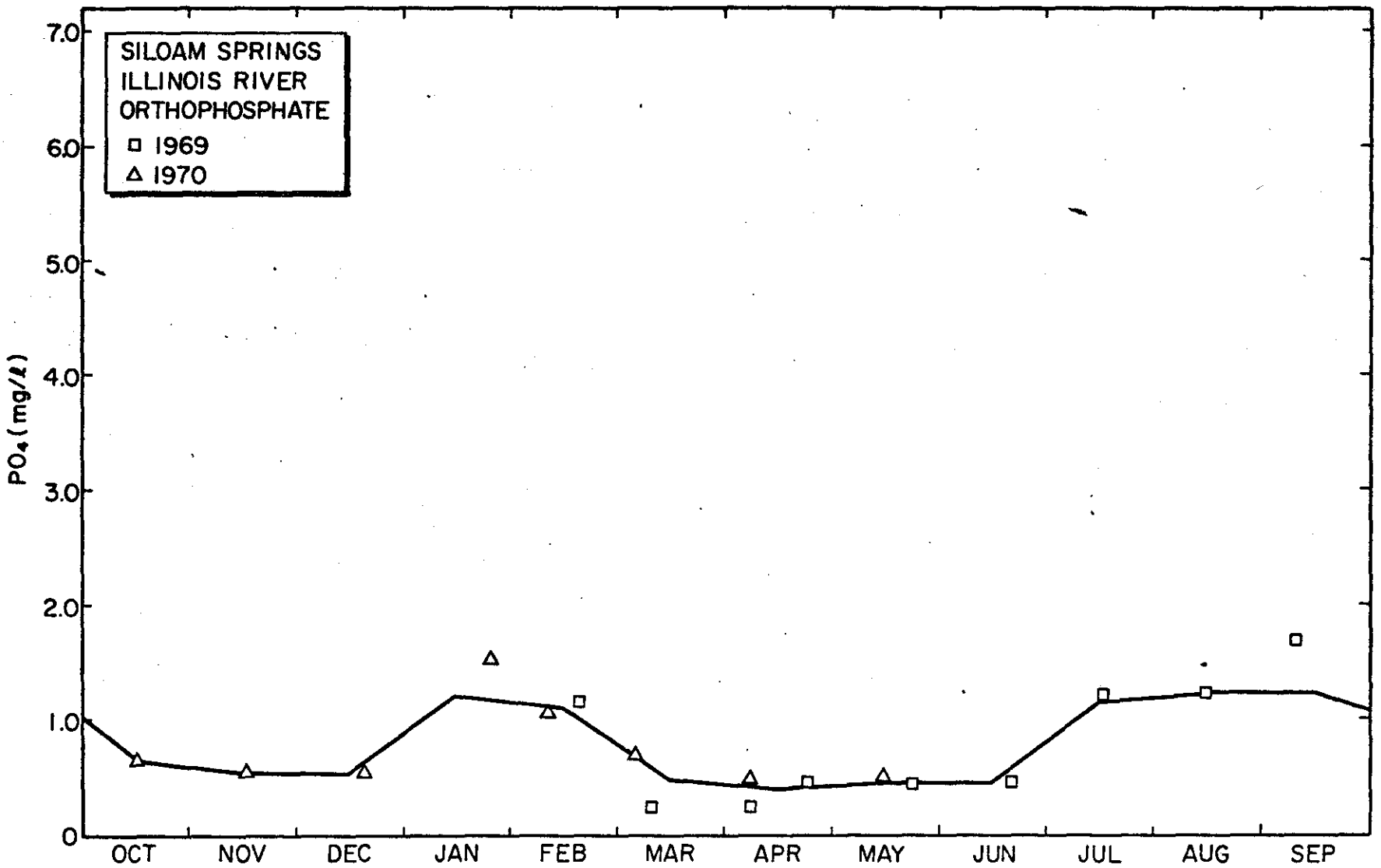
SILOAM SPRINGS
ILLINOIS RIVER
ORTHOPHOSPHATE
1969
1970
PO4 (mg/l)
7.0
6.0
5.0
4.0
3.0
2.0
1.0
0
OCT
NOV
DEC
JAN
FEB
MAR
APR
MAY
JUN
JUL
AUG
SEP

Figure 24

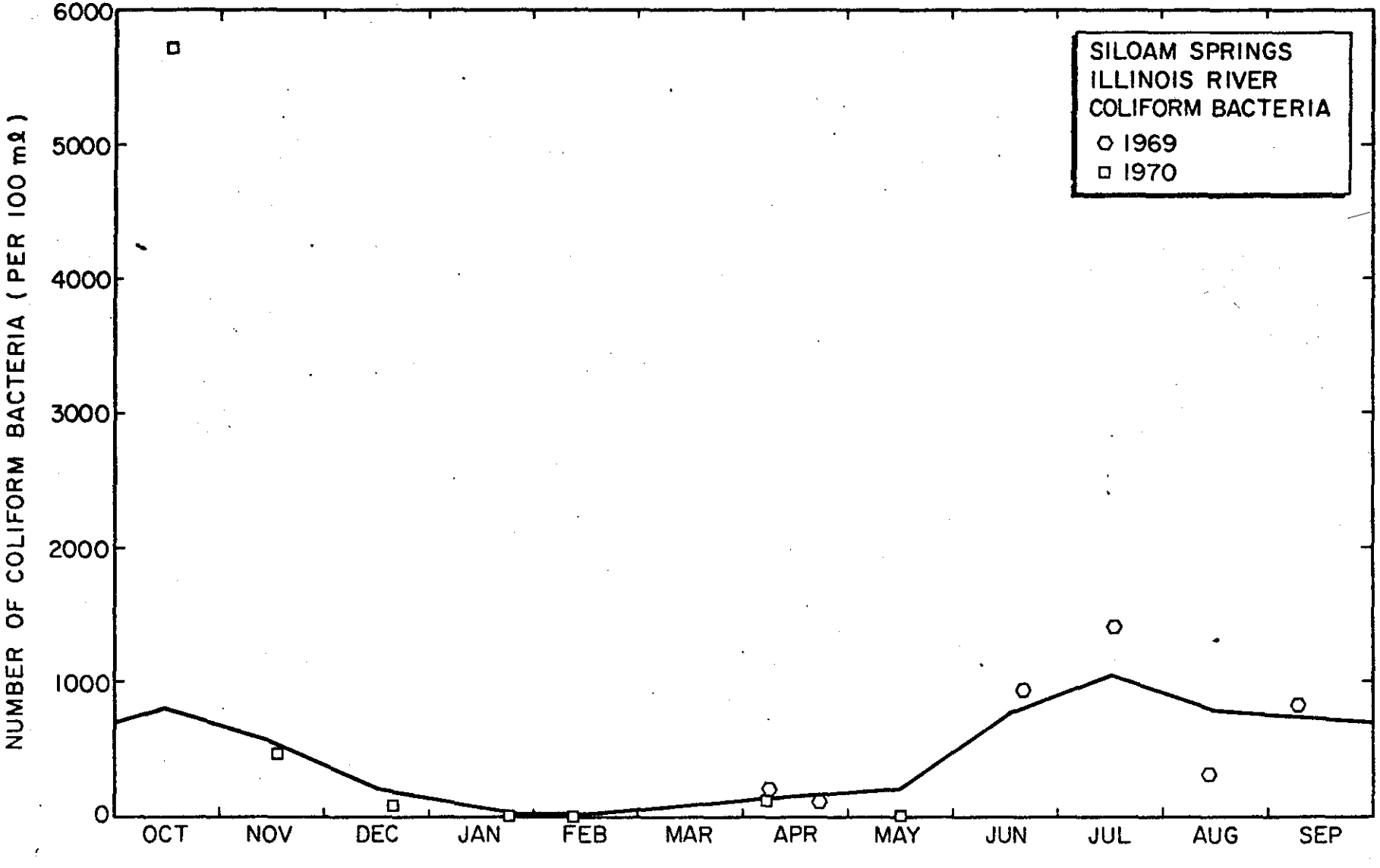
SILOAM SPRINGS
ILLINOIS RIVER
COLIFORM BACTERIA
1969
1970
NUMBER OF COLIFORM BACTERIA (PER 100 ml)
6000
5000
4000
3000
2000
1000
0
OCT
NOV
DEC
JAN
FEB
MAR
APR
MAY
JUN
JUL
AUG
SEP

Figure 25

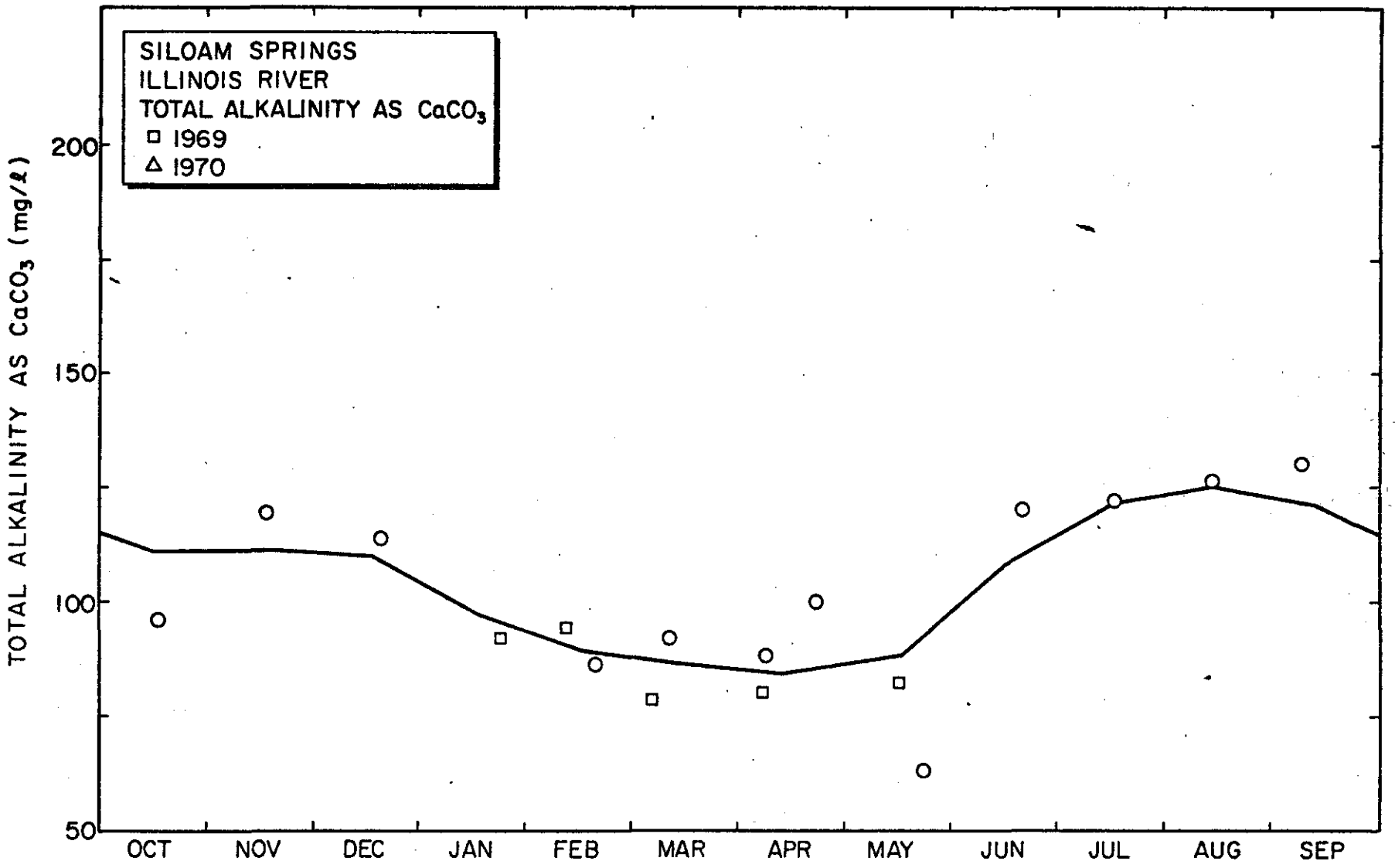
SILOAM SPRINGS
ILLINOIS RIVER
TOTAL ALKALINITY AS CaCO3
1969
1970
TOTAL ALKALINITY AS CaCO3 (mg/l)
200
150
100
50
OCT
NOV
DEC
JAN
FEB
MAR
APR
MAY
JUN
JUL
AUG
SEP

Figure 26

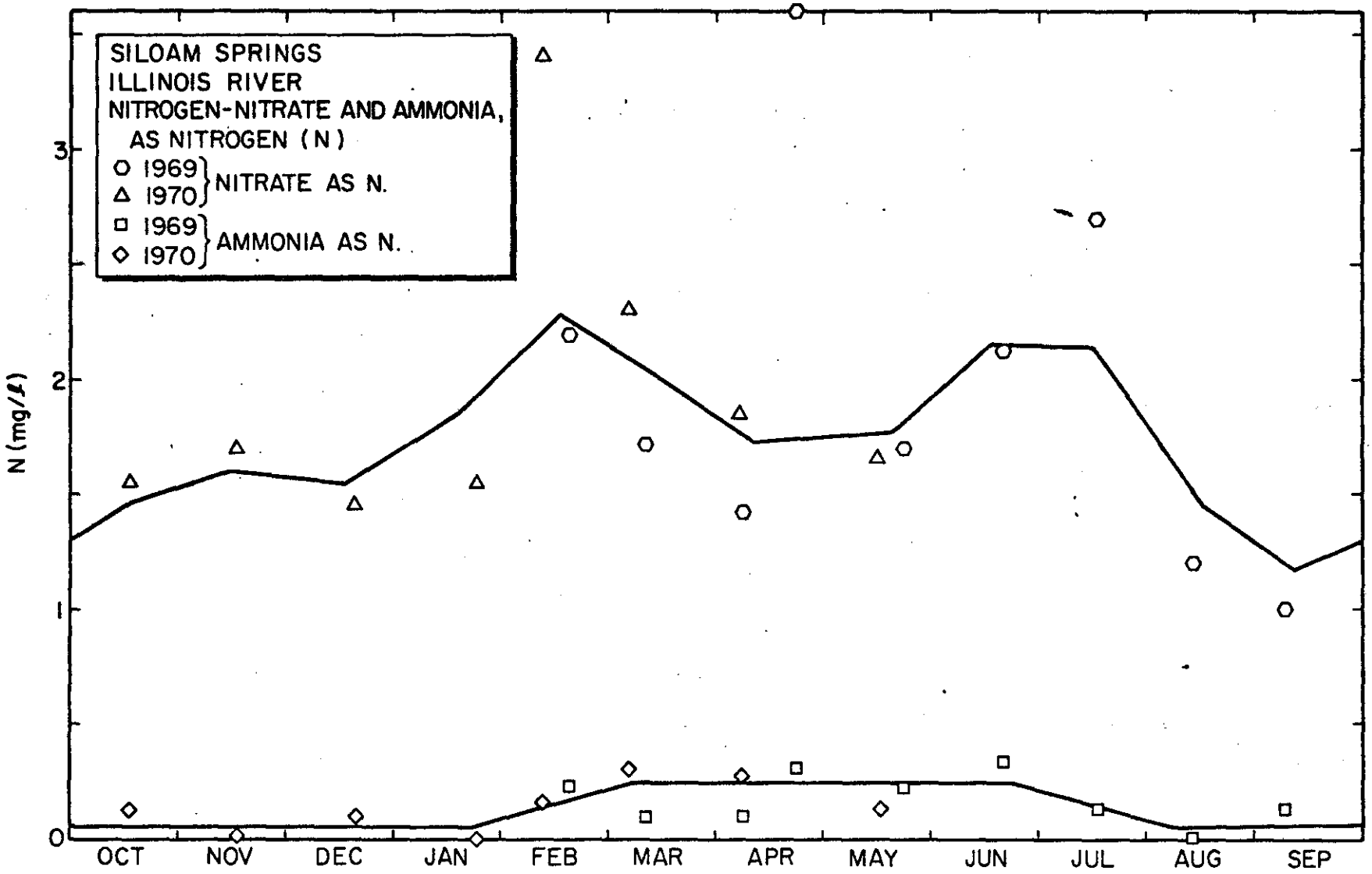
SILOAM SPRINGS
ILLINOIS RIVER
NITROGEN-NITRATE AND AMMONIA,
AS NITROGEN (N)
1969
1970
NITRATE AS N.
1969
1970
AMMONIA AS N.
N (mg/l)
3
2
1
0
OCT
NOV
DEC
JAN
FEB
MAR
APR
MAY
JUN
JUL
AUG
SEP

Figure 27

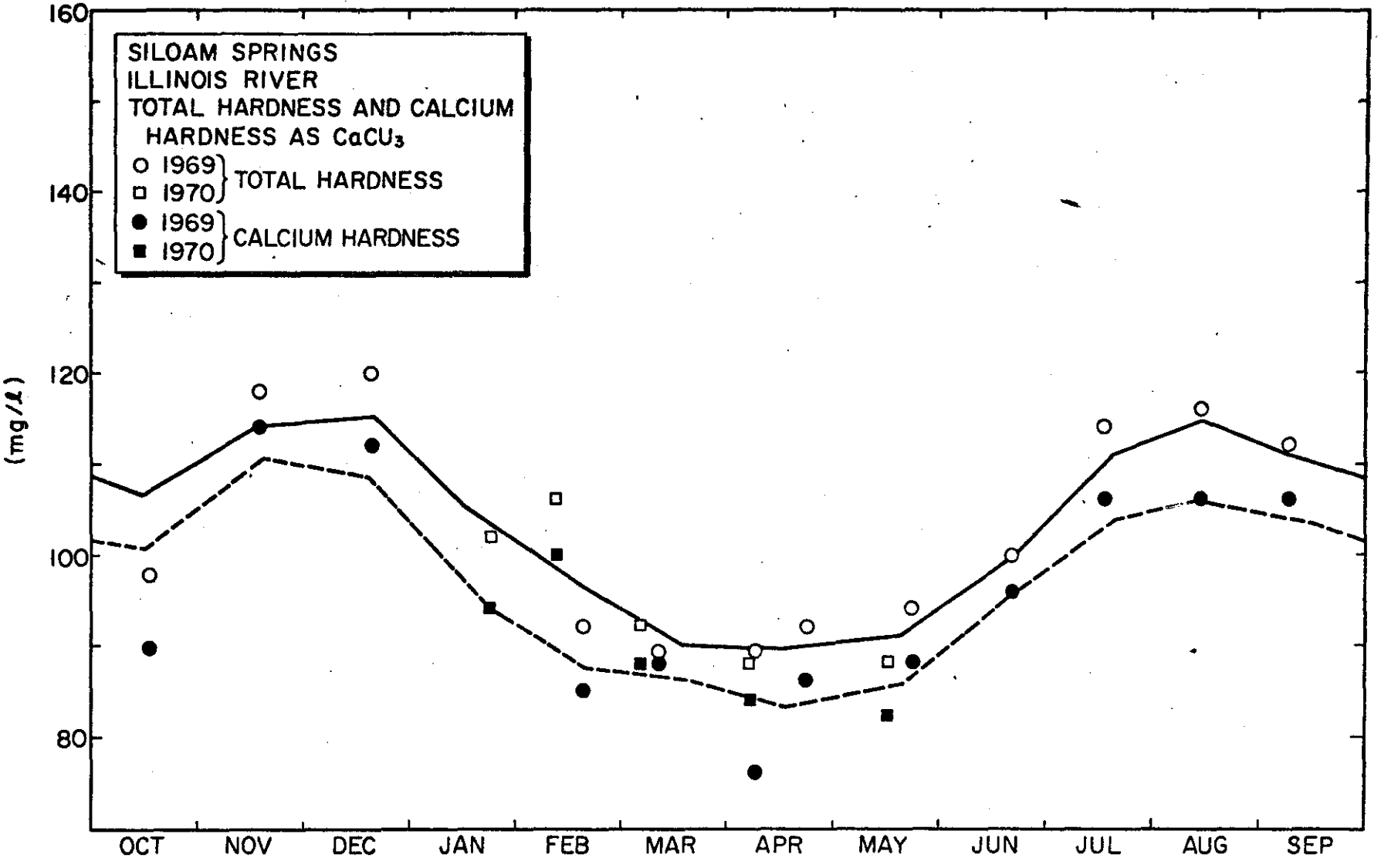
SILOAM SPRINGS
ILLINOIS RIVER
TOTAL HARDNESS AND CALCIUM HARDNESS AS CaCU3
1969
1970
TOTAL HARDNESS
1969
1970
CALCIUM HARDNESS
160
140
120
100
80
(mg/l)
OCT
NOV
DEC
JAN
FEB
MAR
APR
MAY
JUN
JUL
AUG
SEP

Figure 28

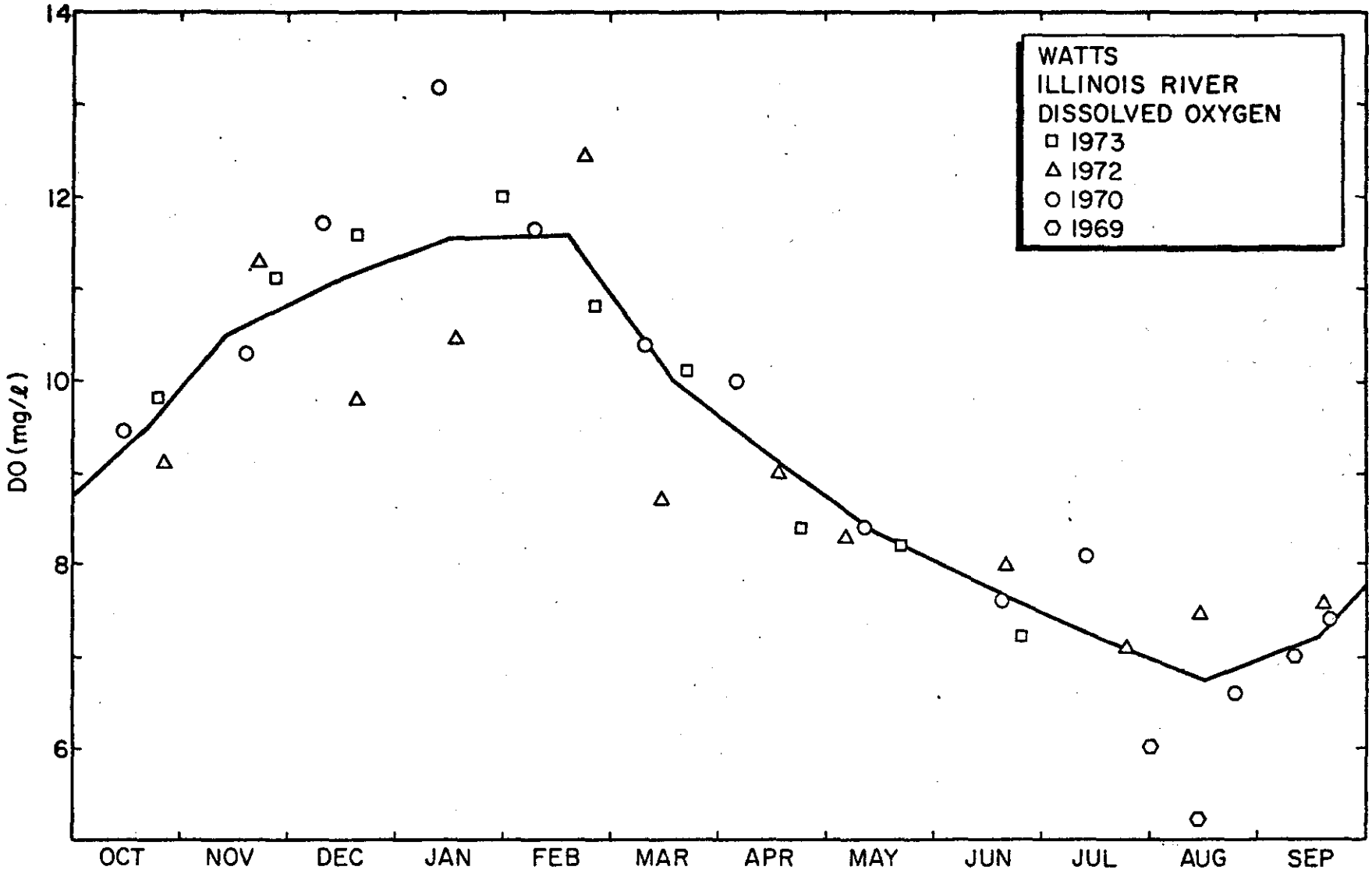
WATTS
ILLINOIS RIVER
DISSOLVED OXYGEN
1973
1972
1970
1969
DO (mg/ℓ)
14
12
10
8
6
OCT
NOV
DEC
JAN
FEB
MAR
APR
MAY
JUN
JUL
AUG
SEP

Figure 29

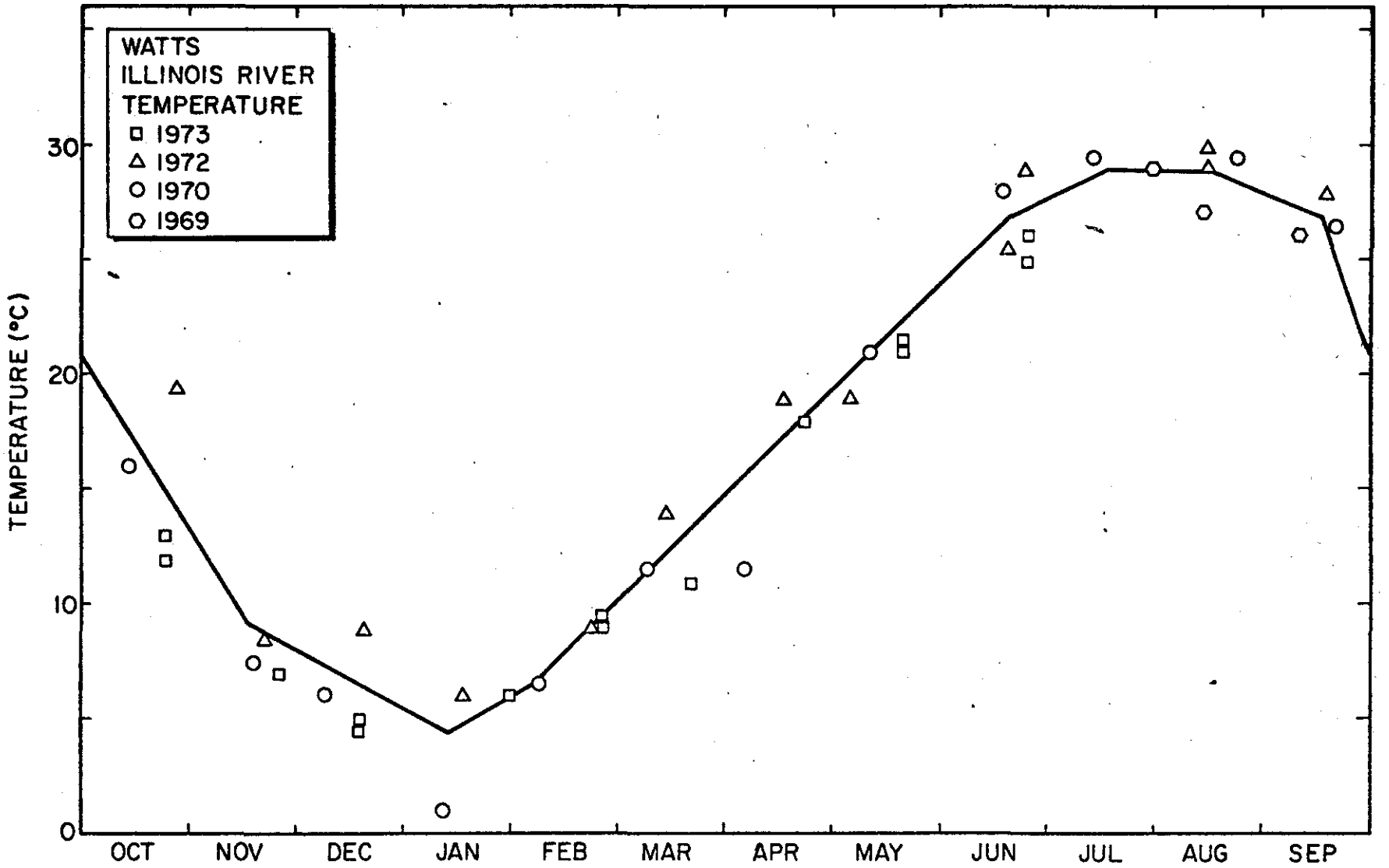
WATTS
ILLINOIS RIVER
TEMPERATURE
1973
1972
1970
1969
TEMPERATURE (°C)
0
10
20
30
OCT
NOV
DEC
JAN
FEB
MAR
APR
MAY
JUN
JUL
AUG
SEP

Figure 30

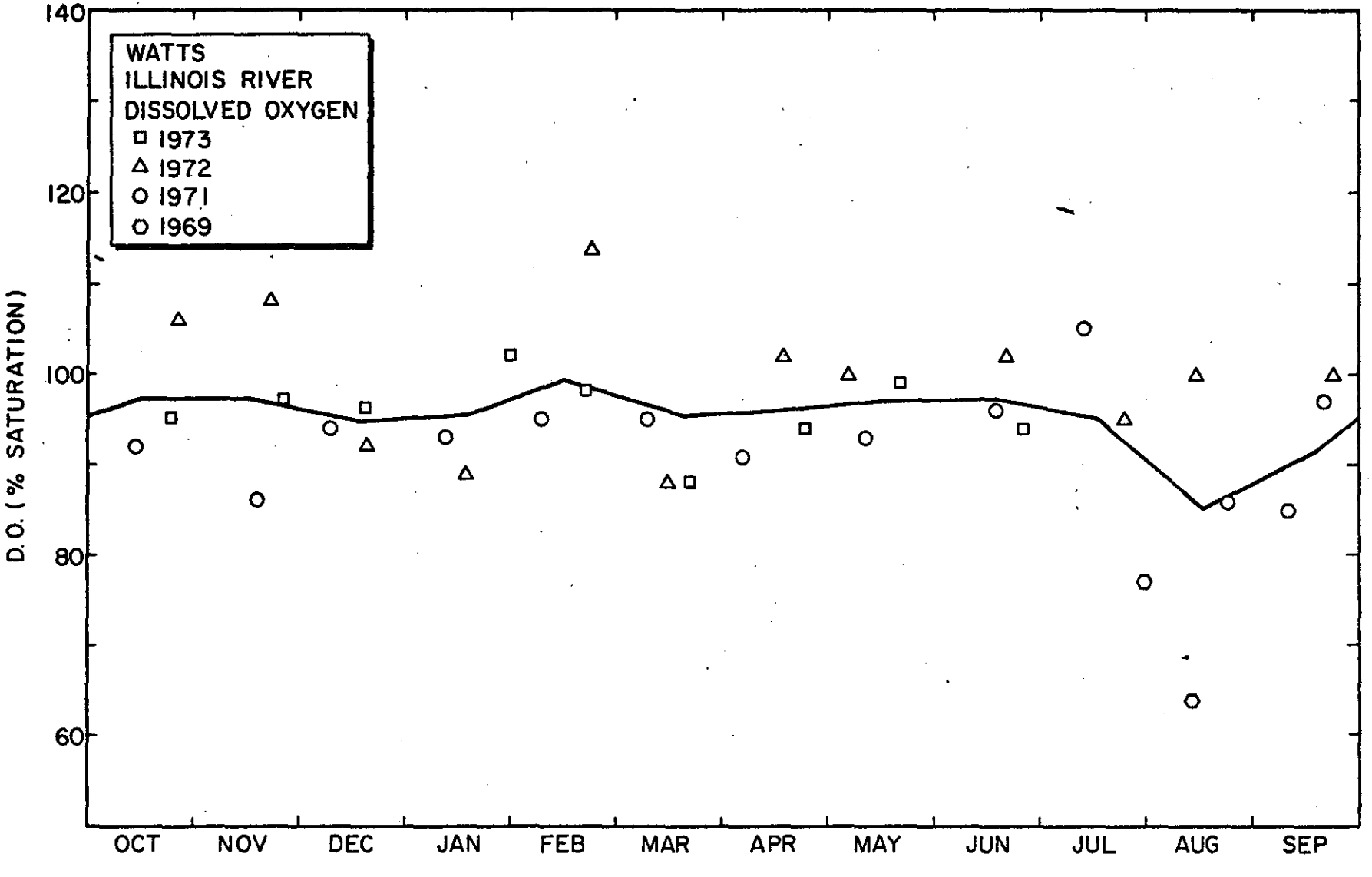
WATTS
ILLINOIS RIVER
DISSOLVED OXYGEN
1973
1972
1971
1969
D.O. (% SATURATION)
140
120
100
80
60
OCT
NOV
DEC
JAN
FEB
MAR
APR
MAY
JUN
JUL
AUG
SEP

Figure 31

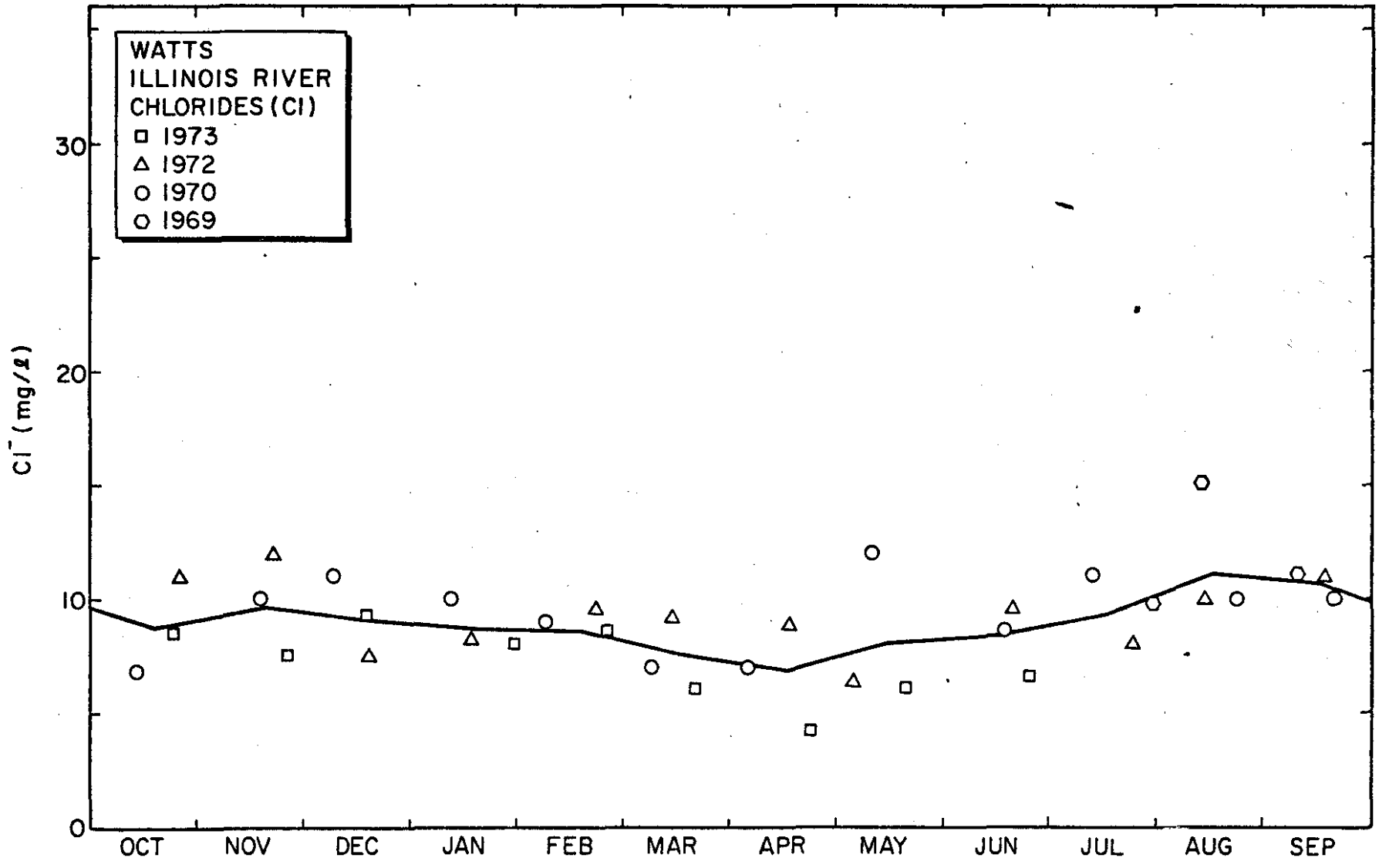
WATTS
ILLINOIS RIVER
CHLORIDES (Cl)
1973
1972
1970
1969
Cl⁻ (mg/ℓ)
0
10
20
30
OCT
NOV
DEC
JAN
FEB
MAR
APR
MAY
JUN
JUL
AUG
SEP

Figure 32

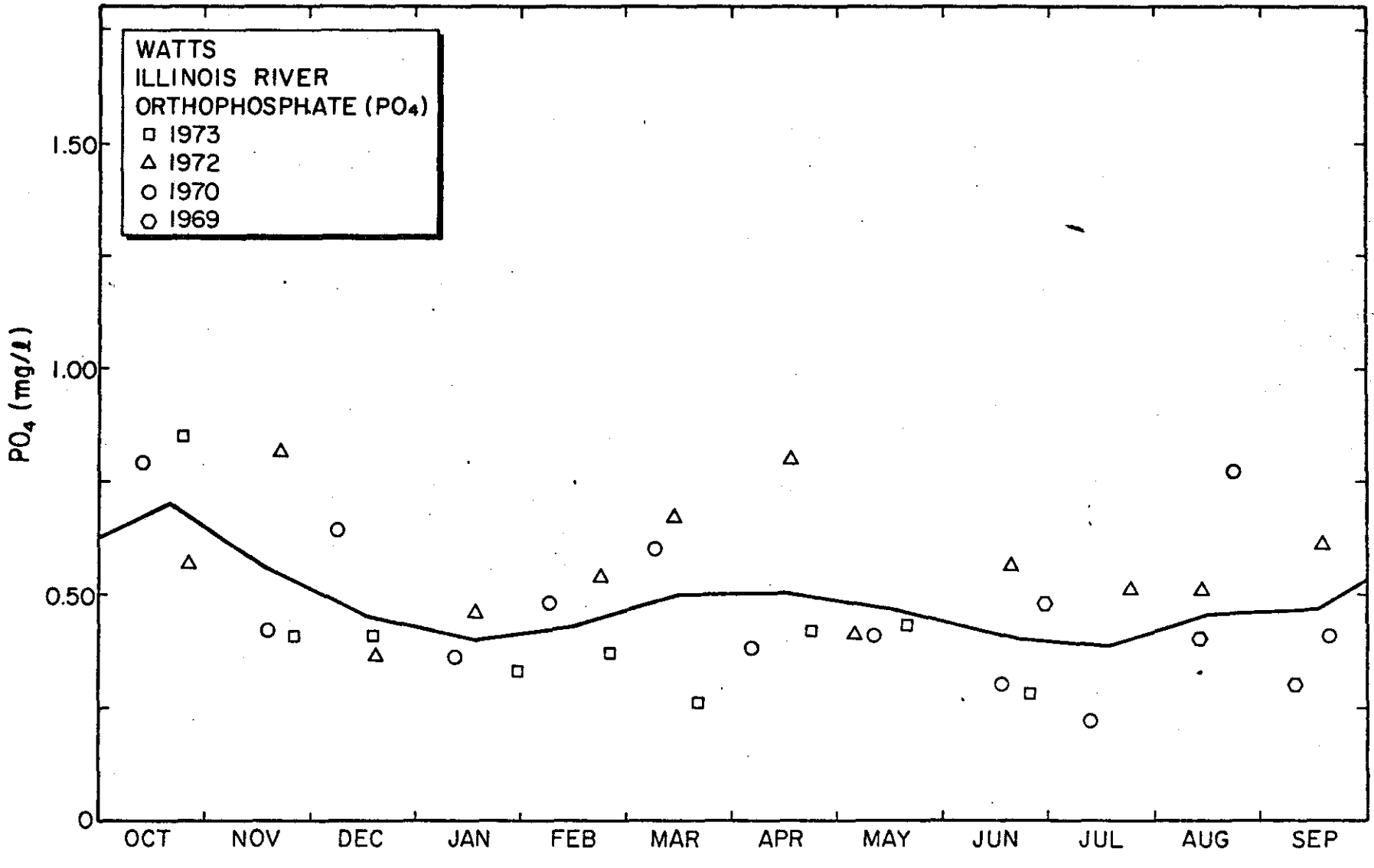
WATTS
ILLINOIS RIVER
ORTHOPHOSPHATE (PO4)
1973
1972
1970
1969
PO4 (mg/l)
1.50
1.00
0.50
0
OCT
NOV
DEC
JAN
FEB
MAR
APR
MAY
JUN
JUL
AUG
SEP

Figure 33

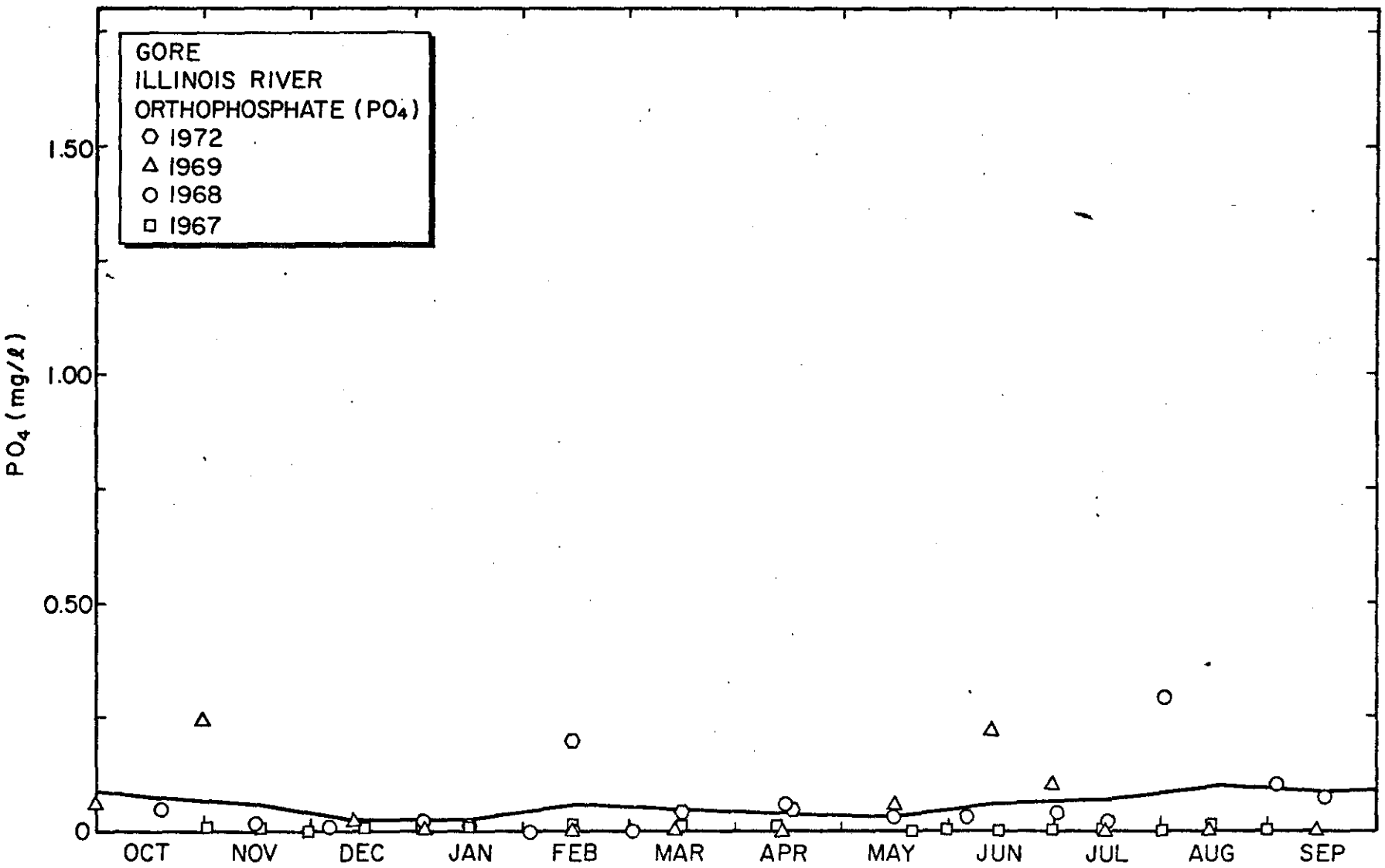
GORE
ILLINOIS RIVER
ORTHOPHOSPHATE (PO4)
1972
1969
1968
1967
1.50
1.00
0.50
0
PO4 (mg/ℓ)
OCT
NOV
DEC
JAN
FEB
MAR
APR
MAY
JUN
JUL
AUG
SEP

Figure 34

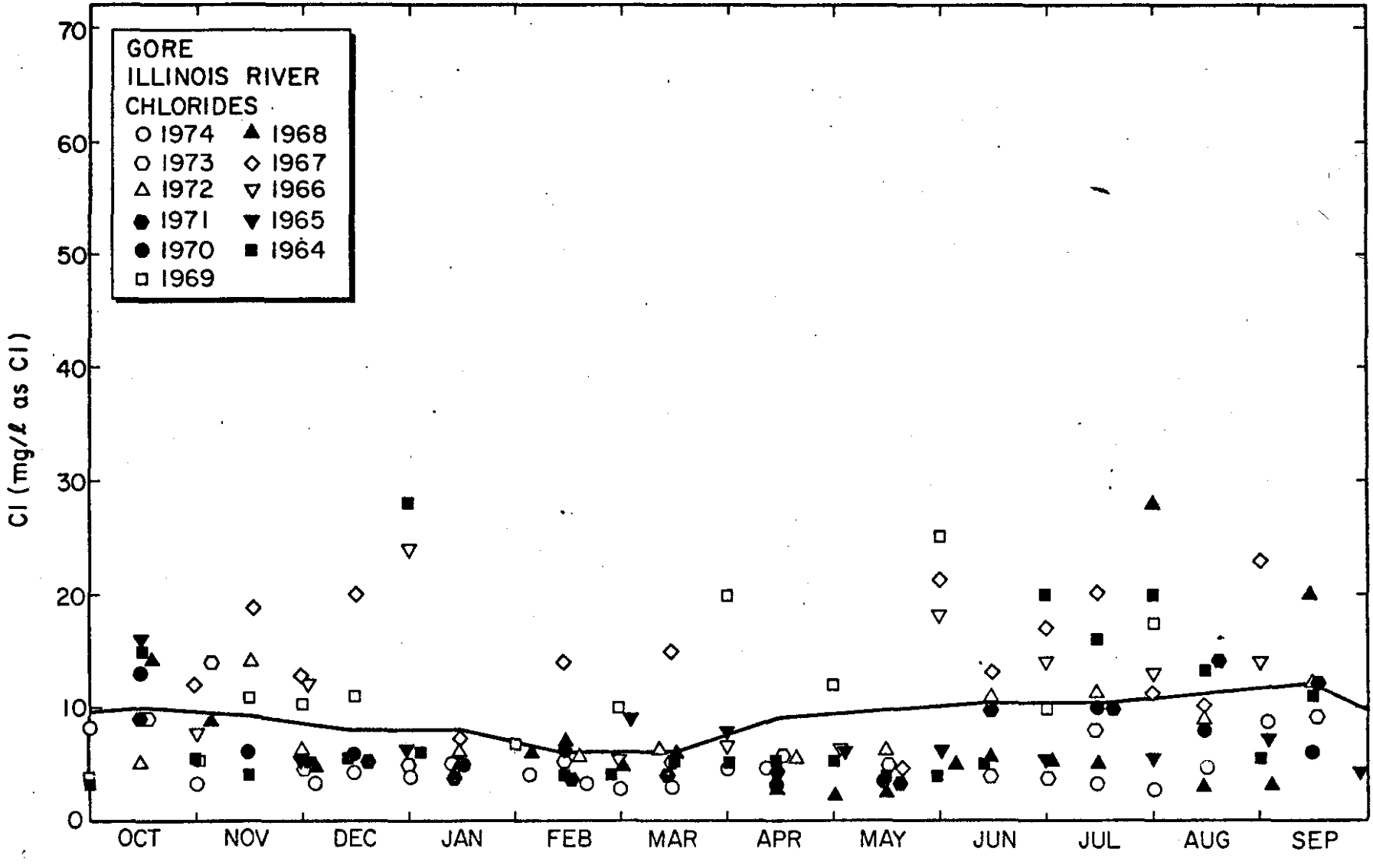
GORE
ILLINOIS RIVER
CHLORIDES
1974
1973
1972
1971
1970
1969
1968
1967
1966
1965
1964
Cl (mg/ℓ as Cl)
0
10
20
30
40
50
60
70
OCT
NOV
DEC
JAN
FEB
MAR
APR
MAY
JUN
JUL
AUG
SEP

Figure 35

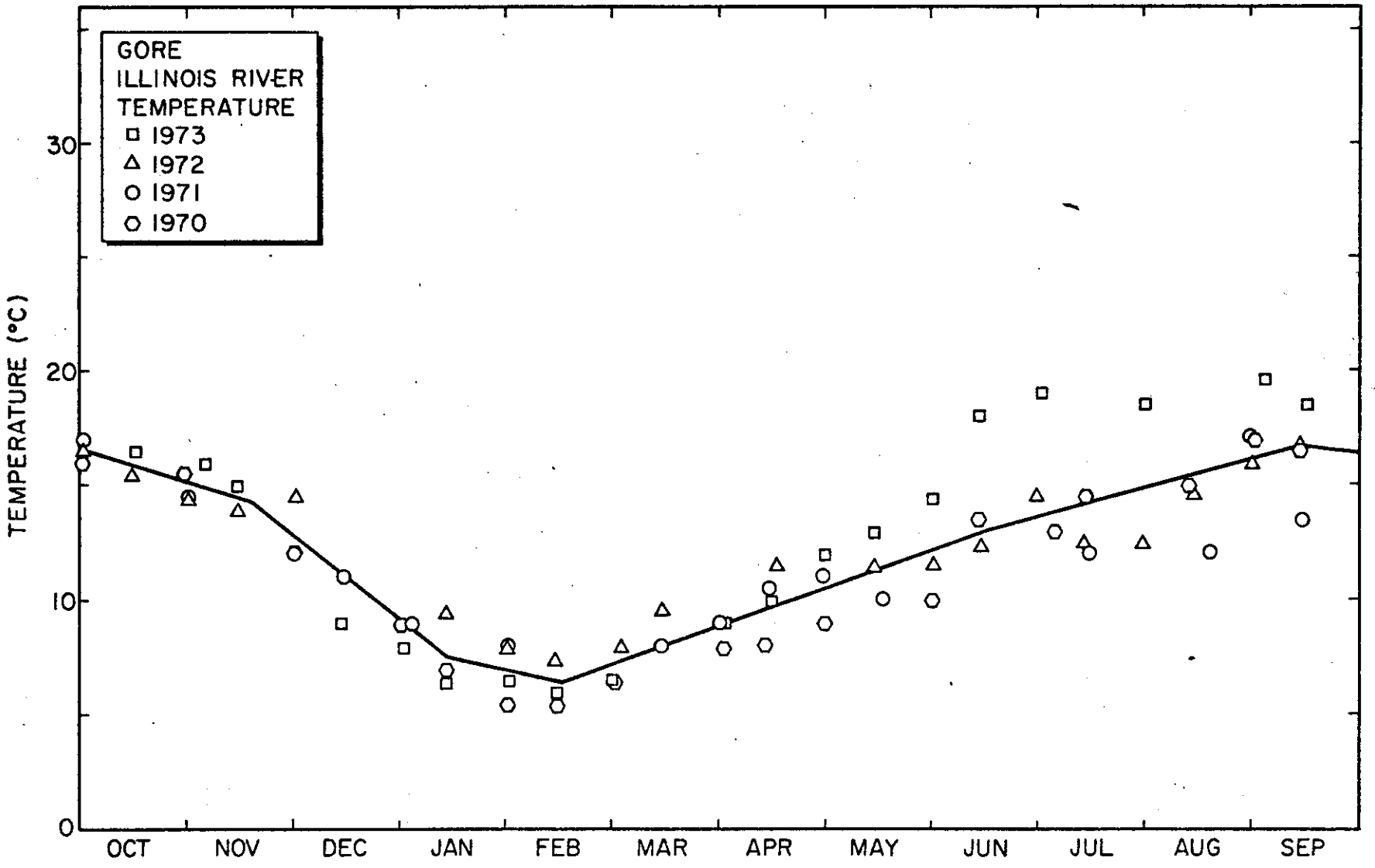
GORE
ILLINOIS RIVER
TEMPERATURE
1973
1972
1971
1970
TEMPERATURE (°C)
0
10
20
30
OCT
NOV
DEC
JAN
FEB
MAR
APR
MAY
JUN
JUL
AUG
SEP

Figure 36

TABLE XXIV

WATER QUALITY DATA

March 12, 1975

Water Quality Parameter	Flint Creek at Kansas Hwy 33 bridge	Illinois River at Watts Hwy 59 bridge	Illinois River at Hampton bridge	Illinois River at Tahlequah Hwy 51 bridge
Temperature ^{o}C	2^{o}	1^{o}	2.5^{o}	--
D.O. mg/l	12	14	12	10
Nitrate -N mg/l	1.4	1.6	1.0	1.5
Nitrite -N mg/l	--	0.005	--	0.005
Orthophosphate mg/l	0.3	0.45	0.28	0.18
pH	8.4	8.1	8.0	7.8
Turbidity	0	50	--	--
Chloride mg/l	10	7.5	10	15
Alkalinity mg/l	65	75	90	80
Iron mg/l	0.25	0.40	0.25	0.20
Manganese mg/l	--	0	0	--
Hardness mg/l	70	--	80	80
Sulfate mg/l	--	--	14	--

TABLE XXV

WATER QUALITY DATA

April 26, 1975

Water Quality Parameter	Flint Creek at Kansas Hwy 33 bridge	Flint Creek at Watts Hwy 59	Illinois River at Hampton bridge	Illinois River at Tahlequah Hwy 51
Temperature ^{o}C	9.5	12	10.5	10.2
D.O. mg/l	9	9	10	11
Nitrate -N	1.5	1.7	1.2	0.8
Nitrite -N	0.018	0.01	0.014	0.005
Orthophosphate	0.35	0.3	0.2	0.3
pH	8.6	8.5	8.6	8.6
Turbidity	0	20	-	-
Chloride	10	10	10	10
Alkalinity	75	100	86	90
Iron	0.05	0.22	0.12	0.02
Manganese	0.2	0.1	0.6	0.6
Hardness	90	100	100	90
Sulfate	5.0	10.1	10.0	8.0

LAND USE

Land use in the Illinois River basin was studied with the aid of NASA ERTS satellite photographs. Forest areas, agricultural areas, and urban areas are discernible on the photos. Figure 37 shows the major forest regions, as well as the larger cities.

Forests occupy approximately 45% of the Illinois River basin. Forests are found primarily in the hilly regions. The slopes may be quite steep up to the closely packed sandstone ridges. Valley's may be wide, with cleared areas used for grazing. Population density is low in the hills, and wildlife is abundant.

Agricultural areas exist in the flatter parts of the basin. Both farming and ranching are practiced. Cattle are raised in cleared pastures. Vegetable production supports a cannery in Siloam Springs, Arkansas. Feed crops are also grown. Approximately 54% of the land in the basin is used for agriculture.

Urban areas occupy less than 1% of the Illinois River basin. Tahlequah is the only major Oklahoma city lying in the basin. But Rogers, Springdale, Siloam Springs, Prairie Grove and Fayetteville, Arkansas are all at least partly within the basin. Thus the quality of water in the Illinois River is highly dependent upon the policies of these Arkansas cities.

The Oklahoma portion of the Illinois River basin is primarily a forested area supporting cattle. It supports trees and wildlife, and is considered by many to be one of the more scenic areas in Oklahoma.

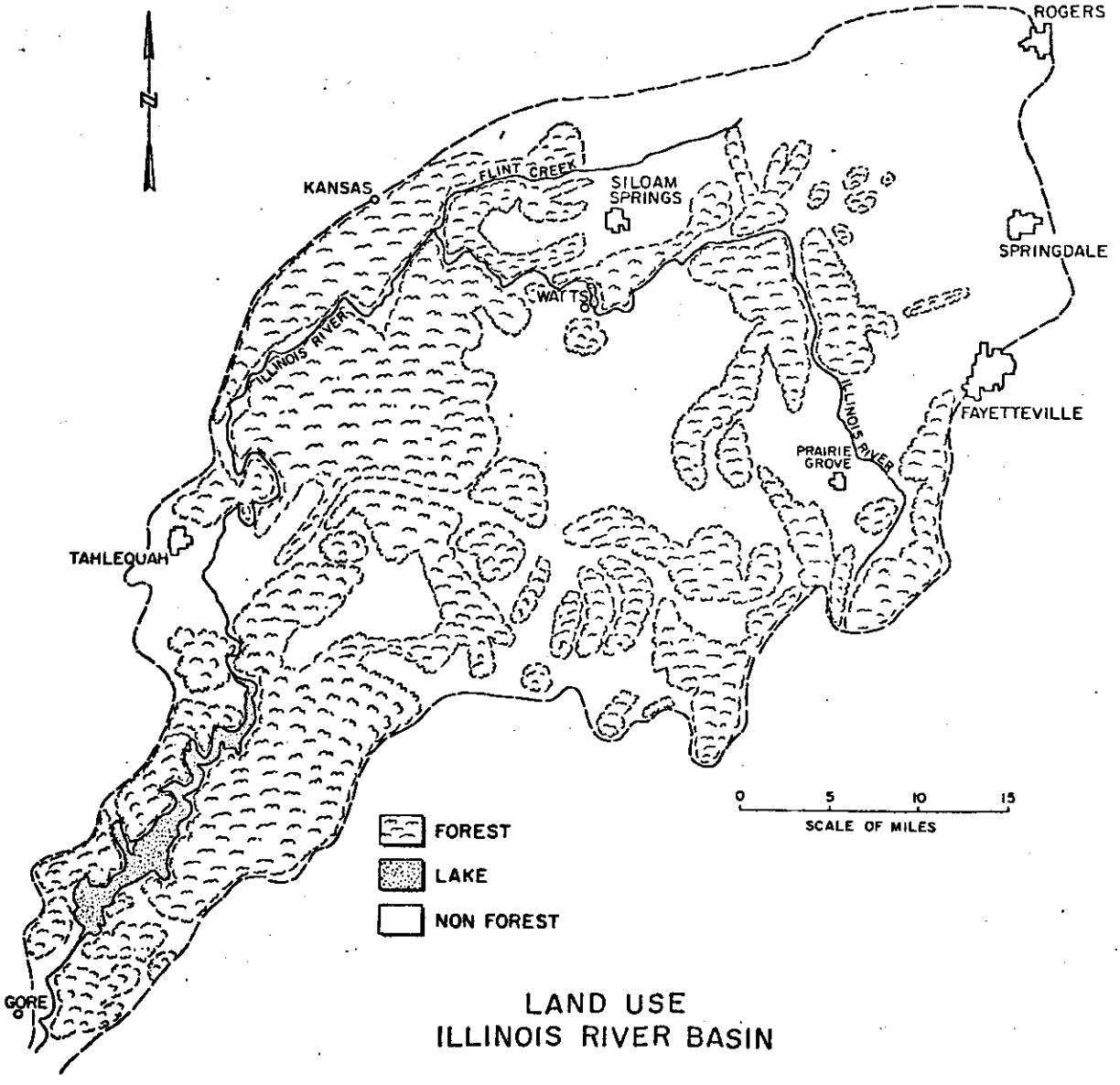
N
ROGERS
KANSAS
FLINT CREEK
SILOAM SPRINGS
SPRINGDALE
WATTS
ILLINOIS RIVER
FAYETTEVILLE
PRAIRIE GROVE
ILLINOIS RIVER
TAHLEQUAH
GORE
0 5 10 15
SCALE OF MILES
FOREST
LAKE
NON FOREST
LAND USE
ILLINOIS RIVER BASIN

Figure 37

SUMMARY AND CONCLUSIONS

Summary

The objectives of this study were to determine the hydrologic characteristics of the Illinois River, to determine what field measurements are required, to determine what water quality data are presently available and to determine the present land use of the basin. All of these objectives were accomplished and are briefly summarized below.

1. The hydrologic characteristics of the basin are quite variable. Of primary concern where the low flow and these where found to approach zero for the gaging stations in the basin.

2. The present quality and quantity of the water in the Illinois River basin needs to be better defined. Routine sampling and gaging, such as monthly data taken at five or six locations along Flint Creek and the Illinois River, could provide adequate background. Emphasis should be given to the months of August, September, and October, when nearly all of the historic low flows have occurred.

The above data would allow for better correlation of water quality data to the hydrology of the basin.

The flows in basin can be simulated quite well using the National Weather Service River Forecast Hydrology Model. Through application of this model and with additional water quality data, any environmental stress on the river's waters can be analyzed. The Hydrology model along with a model for stream assimulation capacity such as the Streeter-Phelps model can be used effectively to predict the effects of these environmental stresses.

3. The water quality of basin is extremely good. The quality data presently available is inadequate for correlation with the hydrology, but

does indicate the general excellent quality within the basin. This quality should be maintained.

4. The present land use of the basin is in primarily forest, and agriculture. However, demands are present to convert the forest areas to recreational type housing. If this conversion continues then the total environmental quality of the basin will be degraded.

Conclusions

The Illinois River basin is one of the few remaining basins in the United States that is relatively unpolluted. However, because of its environmental quality it is being subjected to many stresses. In order for the basin to remain environmental attractive, it is imperative that some restraints be legislated. However, before the magnitude of these restraints can be determined additional data must be gathered on the basin's environmental factors.

This report is but a start at trying to determine what, and how much any of the environmental elements can be stressed without harmful consequences.

PROJECT RELATED PUBLICATIONS

Martin, Ronald Creighton, "Low Flow Simulation Of The Illinois River Using A Conceptual Hydrologic Model." Unpublished Master's Thesis, Oklahoma State University, Stillwater, Oklahoma, May 1975

Reusser, Steven Roy, "Analysis Of Drought Flows And Of Methods For Determining The Self-Purification Capacity Of The Illinois River." Unpublished Master's Thesis, Oklahoma State University, Stillwater, Oklahoma, May 1975

PROJECT PERSONNEL

The following personnel received financial support from this Project:

1. R. N. DeVries, Professor of Civil Engineering, Co-Principal Investigator.
2. D. F. Kincannon, Professor of Civil Engineering, Co-Principal Investigator.
3. N. N. Azar, Graduate Student
4. H. M. Chen, Graduate Student
5. K. C. Kepler, Graduate Student
6. R. C. Martin, Graduate Student
7. S. R. Reusser, Graduate Student
8. G. L. Weaver, Graduate Student

SELECTED BIBLIOGRAPHY

1. Ali, H., and Bewtra, J. K., "Influence of Turbulence on BOD Progression." J. Water Pollution Control Federation, 44, 1798-1807 (1972).

2. Bhatla, M. N., and Gaudy, A. F. Jr., "Role of Protozoa in the Diphasic Exertion of BOD." J. San. Engr. Div., ASCE, 91, 63-87 (1965).

3. Burnash, R. J. C., Ferral, R. L., and McGuire, R. A., "A Generalized Streamflow Simulation System." U. S. Dept. of Commerce and State of California Dept. of Water Resources (1973).

4. Busch, A. W., "A Five Minute Solution for Stream Assimilative Capacities." Proceedings, 26th Industrial Waste Conference, Purdue University, Lafayette, Indiana, 151-155 (1971).

5. Camp, T. R., Water and Its Impurities. Reinhold Publishing Corporation, New York (1963).

6. Chow, Ven Te, Handbook of Applied Hydrology. McGray-Hill, New York (1964).

7. Churchill, M. A., and Buckingham, R. A., "Statistical Method for Analysis of Stream Purification Capacity." Sewage and Industrial Wastes, 28, 517-537 (1956).

8. Churchill, M. A., Elmore, H. L., and Buckingham, R. A., "The Prediction of Stream Reaeration Rates." J. San. Engr. Div., ASCE, 88, SA4, 1-46 (1962).

9. Crawford, N. H., and Linsley, R. K., "Digital Simulation in Hydrology: Stanford Watershed Model IV." Technical Report No. 39, Stanford University (1966).

10. Di Toro, D. M., and O'Connor, D. J., "The Distribution of Dissolved Oxygen in a Stream With Time Varying Velocity." Water Resources Research, 4, 639-646 (1968).

11. "Environmental Groups Praise Court Decision." Daily Oklahoman, August 3 (1974).

12. Gumbel, E. J., "Statistical Theory of Droughts." Proceedings, American Society of Civil Engineers, 80 (Separate No. 439), 1-19 (1954).

13. Hall, C. H., Report No. III of the Low Flow Augmentation Project. Johns Hopkins University, Baltimore, Md., April (1960).

14. Hardison, C. H., and Martin, P. O. R., "Low Flow Frequency Curves for Selected Long-Term Stream Gaging Stations in Eastern United States." U. S. Geological Survey Water Supply Paper No. 1669-G (1963).

15. Harper, M. E., "Assessment of Mathematical Models Used in Analysis of Water Quality in the Streams and Estuaries." Washington State Research Center, June (1971).

16. Hileman, Leslie H., "Pollution Factors Associate With Excessive Poultry Litter (Manure) in Arkansas." Relationship of Agriculture to Soil and Water Pollution, Cornell University Conference of Agricultural Waste Management Proceedings, 41-77 (1970).

17. "Illinois River Menaced by Man." Tulsa Tribune, June 26 (1974).

18. "Illinois River Sub-basin." Report of the Engineering Advisory Committee to the Arkansas-Oklahoma Arkansas River Compact Committee, January (1969).

19. Isaacs, W. P., Chulavachana, P., and Bogart, R., "An Experimental Study of the Effect of Channel Surface Roughness on the Reaeration Rate Coefficient." Proceedings, 24th Industrial Waste Conference, Purdue University, Lafayette, Indiana, 1464-1476 (1969).

20. Isaacs, W. P., and Gaudy, A. F. Jr., "Atmospheric Oxygenation in a Simulated Stream." J. San. Engr. Div., ASCE, 94, SA2, 319-344 (1968). Closure, J. San. Engr. Div., ASCE, SA1, 171-178 (1970).

21. Jennelle, E. M., and Gaudy, A. F. Jr., "Studies on Kinetics and Mechanism of BOD Exertion in Dilute Systems." Biotechnology and Bioengineering, XII, 519-539 (1970).

22. Kao, Wen-hsiung, "Studies on Drought Flow Distribution and Use of Zone-Treatment Principle in Water Quality Management." PhD Thesis, Oklahoma State University (1972).

23. Kincannon, D. F., Gaudy, A. F. Jr., Bechir, M. H., Graves, Q. B., and Rice, C. A., Final Report, OWR-006 Oklahoma Water Resources Planning Studies Oklahoma-Arkansas, June (1969).

24. Kincannon, D. F., Final Report, Water Resources Planning Studies Oklahoma and Arkansas, Phase II (Quality), August (1971).

25. Ligon, J. T., Law, A. G., and Higgins, D. H., "Evaluation and Application of a Digital Hydrologic Simulation Model." WRRI, Clemson University (1969).

26. Lindsley, R. K., Kohler, M. A., and Paulhus, J. L. H., Applied Hydrology. New York: McGraw-Hill (1949).

27. Lindsley, R. K., Kohler, M. A., and Paulhus, J. L. H., Hydrology for Engineers. New York: McGraw-Hill (1974).

28. Linsley, R. L., "A Critical Review of Currently Available Hydrologic Models for Analysis of Urban Stormwater Runoff." Hydrocomp International (1972).

29. "Little Danger of Tenkiller Pollution." Sequoyah County Times, July 25 (1974).

30. Matalas, N. C., "Probability Distribution of Low Flows." United States Geological Survey Professional Paper 434-A (1963).

31. Mitchell, D., "Northwest Arkansas Regional Water Quality Management Plan." Unpublished Report prepared for the Northwest Arkansas Regional Planning Commission, March (1974).

32. Morris, David G., "The Use of a Multi-Zone Hydrologic Model With Distributed Rainfall and Distributed Parameters in the National Weather Service River Forecast System." Unpublished Manuscript (1974).

33. "National Weather Service River Forecast System Forecast Procedures." NOAA Technical Memorandum NWS HYDRO 14. Dept. of Commerce (1972).

34. Nemerow, Nelson L., Scientific Stream Pollution Analysis. Scripta Book Company, Washington, D. C. (1974).

35. O'Connor, D., and Dobbins, W., "The Mechanism of Reaeration in Natural Streams." J. San. Engr. Div., ASCE, 82, SA6, Paper 1115, 1-30 (1956).

36. O'Connor, D. J., "A Comparison of Probability Distribution in the Analysis of Drought Flows." Water and Sewage Works, 111, 180-185 (1964).

37. Oklahoma Water Resources Board, "Hydrographic Survey Illinois River Basin, Oklahoma," June 30 (1959).

38. Peil, K. M., and Gaudy, A. F. Jr., "A Rational Approach for Predicting the DO Profile in Receiving Waters." Biotechnology and Bioengineering, XVII, 69-84 (1975).

39. Public Law 92-500, 92nd Congress of the United States of America, S. 2770, 1 (1972).

40. Riggs, H. C., "Estimating Probability Distributions of Drought Flows." Water and Sewage Works, 112, 153-157 (1965).

55. "Water Quality Standards for the State of Oklahoma." Oklahoma Water Resources Board (1968).

56. Young, J. C., and Clark, J. W., "Second Order Rate Equation for BOD." J. San. Engr. Div., ASCE, 91, SA1, 43-58 (1965).

41. Ross, G. A., "The Stanford Watershed Model: The Correlation of Parameter Values Selected by a Computerized Procedure With Measurable Physical Characteristics of the Watershed." University of Kentucky Water Resources Institute Research Report No. 35 (1970).

42. Streeter, H., and Phelps, E., "A Study of the Purification of the Ohio River." U. S. Public Health Service Bulletin No. 146 (1925).

43. Thayer, R. P., and Krutchkoff, R. G., "A Stochastic Model for Pollution and Dissolved Oxygen in Streams." Bulletin No. 22, Water Resources Center, Virginia Polytechnical Institute, Blacksburg, Va., 1-130 (1966).

44. Thomas, H. A., "Pollution Load Capacity of Streams." Water and Sewage Works, 95, 409-420 (1948).

45. "Three Projects on Illinois Rile Citizens' Groups." Tulsa World, July 14 (1974).

46. "Tulsa Tapping Illinois River Proposed." Tulsa World, January 17 (1969).

47. U. S. Dept. of Interior Geological Survey, "Surface Water Supply of the United States" Part 7, Cont. Series.

48. U. S. Dept. of Interior Geological Survey, "Water Resources Data for Oklahoma" Part 1, Cont. Series.

49. U. S. Dept. of Interior Geological Survey, "Quality of Surface Waters of the United States" Part 7, Cont. Series.

50. U. S. Dept. of Interior Geological Survey, "Water Resources Data for Oklahoma" Part 2, Cont. Series.

51. U. S. Dept. of Interior Geological Survey, "Surface Waters at Illinois River Basin in Arkansas and Oklahoma" (1959).

52. Velz, Clarence J., Applied Stream Sanitation. John Wiley and Sons, Inc., New York (1970).

53. Velz, C. J., and Cannon, John, "Drought Flow a Statewide Analysis." Proceedings, 16th Industrial Waste Conference, Purdue University, Lafayette, Indiana, 572-602 (1961).

54. "Water Quality and Pollutant Source Monitoring." Environmental Protection Agency. Federal Register, 39, August 28 (1974).

APPENDIX

APPENDIX A

COMPUTER PROGRAM FOR THE STREETER-PHELPS EQUATION

```
C     THE  "STREETER-PHELPS   EQUATION
C       THE UNITS ON THE VARIABLES
C       BOD=MG/L,  DO=MG/L,  Q=CFS,  TEMP=CENT,  VEL=FT/SEC,  DEPTH=FT.
C       DISTANCE=MILES.
C
C       BL=BOD.    DO=DISSOLVED OXYGEN.    Q=FLOW RATE.    TEM=TEMPERATURE
C       V=VELOCITY.    H=DEPTH.    DIS=DISTANCE    DOM=DOSSOLVED OXYGEN IN
C       THE INTERVAL.   SDO=SATURATED DISSOLVED OXYGEN.  PROB=THE PROBLEM
      DIMENSION BL(20),DO(20),Q(20),TEM(20),V(20),H(20),DIS(20),DOM(60)
     X ,SDO(20),PROB(20),TBL2(10),TO2(10),TA(10)
C
C
      READ(5,100)(PROB(I),I=1,20)
  100 FORMAT(20A4)
C
C
      WRITE(6,101)PROB
  101 FORMAT(1H1,20A4////)
      WRITE(6,30)
   30 FORMAT('     D.O. DEFICIT IS PLOTTED EVERY 2 MILES'/)
      READ(5,1)N2
          DO 600 L4=1,N2
C
      READ(5,1)M
C
C       THIS DO LOOP INCLUDES CALCULATIONS FOR EACH MINOR STREAM SYSTEM
C       L5=THE NUMBER OF THE SIMPLE STREAM SYSTEM
          DO 500 L5=1,M
C
C       N=THE NUMBER OF INFLUENTS TO THE STREAM + 1
      READ(5,1) N
    1  FORMAT(I5)
      READ(5,2) (BL(I),DO(I),Q(I),TEM(I),V(I),H(I),DIS(I),SDO(I),I=1,N)
    2 FORMAT(8F10.2)
C
          IF(L5.EQ.1) GO TO 300
          DO 301 J=1,N
C
          IF(BL(J).GT.3) GO TO 301
C
              BL(J)=TBL2(J)
              DO(J)=TO2(J)
              DIS(J)=TA(J)
  301 CONTINUE
  300         NM1=N-1
C       WRITING OUT IMPORTANT ORIGINAL DATA ABOUT THE STARTING RIVER(J)USE
      WRITE(6,102)DO(1),BL(1),Q(1),NM1,(DIS(I),I=1,NM1)
  102  FORMAT(' OF THE ORIGINAL STREAM '/' D.O.=',F5.2,' MG/L,  B.O.D.=',
     XF8.2,' MG/L,  Q=',
     XF8.2,' CFS '///,15,' INTERVALS O.D. DEFICIT PLOTTED FROM EFFLUENT
     XDISCHARGE'/' IN MILES',/(F6.2),///)
              A=Q(1)
C
C  THIS DO LOOP INCLUDES THE CALCULATIONS FOR EACH INTERVAL OF THE STREAM
          DO 80 I=1,NM1
              IP1=I+1
C       SUMMING THE FLOWS OF ALL EFFLUENTS PLUS THE ORIGINAL SOURCE
              A=A+Q(IP1)
C       FINDING THE AVERAGE VELOCITY AND AVERAGE DEPTH FOR AN INCREMENT OF
C       THE STREAM OR RIVER
              VAV=(V(I)+V(IP1))/2.
              HAV=(H(I)+H(IP1))/2.
C       THE TEMPERATURE IS CALCULATED AT THE POINT WHERE AN EFFLUENT OR ANOTHER
C       STREAM MEETS THE ORIGINAL STREAM, AND THE TEMPERATURE IS PROPORTIONAL TO
C       THE FLOW RATES
              TEMP=(TEM(I)*(A-Q(IP1))+TEM(IP1)*Q(IP1))/A
C USING  THE AVERAGE VELOCITY,DEPTH , AND TEMPERATUREC WE CALCULATE THE
C  COEFFICIENTS OF DEOXYGENATION AND REARATION (Y1 AND Y2)
      CALL VAL(Y1,Y2,VAV,HAV,TEMP)
              TIME=(DIS(I)*5280.)/(VAV*86400.)
C  THE DISSOLVED OXYGEN AND BOD ARE CALCULATED AT THE POINT OF DISCHARGE OF
C  A TRIBUTARY OR  A DISCHARGE INTO THE STREAM BY A COMMUNITY
          IF(L.GT.1) GO TO 15
              D1=(DO(I)*Q(I)+DO(2)*Q(2))/A
              BL1=(BL(I)*Q(I)+BL(2)*Q(2))/A
          GO TO 16
C       THE BOD AND THE DISSOLVED OXYGEN ARE IN PROPORTION TO THE FLOW RATES OF
C       THE RESPECTIVE STREAM OR EFFLUENT HAVING THAT BOD OR DISSOLVED OXYGEN
C       LEVEL
   15         D1=(D2*(A-Q(IPL))+DO(IPL)*Q(IPL))/A
              BL1=(BL2*(A-Q(IP1))+BL(IP1)*Q(IPL))/A
   16         C=DIS(I)*.5
              L=C
          IF(L.EQ.0) GO TO 19
          GO TO 21
   19         L=1
   21         LP1=L+1
              DOM(I)=SDO(I)-D1
C  THE BOD AND THE DISSOLVED ARE NOW CALCULATED AT THE END OF THE INTERVAL
              BL2=BL1*EXP(-Y1*TIME)
              F=((Y1*BL1)/(Y2-Y1))*(EXP(-Y1*TIME)-EXP(-Y2*TIME))
              G=DOM(I)*EXP(-Y2*TIME)
              DOM(LP1)=F+G
              D2=SDO(IP1)-DOM(LP1)
          IF(D2.GE.0) GO TO 22
              DOM(LP1)=SDO(IP1)
              D2=0
C    IN THIS DO LOOP THE DISSOLVED OXYGEN IS CALCULATED AT EQUAL INCREMENTS
C    ALONG THE STREAM
   22     DO 81 J=2,L
              Y=J
              TIM2=Y*(TIME/C)
              F=((Y1*BL1)/(Y2-Y1))*(EXP(-Y1*TIM2)-EXP(-Y2*TIM2))
              G=DOM(I)*EXP(-Y2*TIM2)
              DOM(J)=F+G
              TES=SDO(I)-DOM(J)
          IF(TES.GE.0) GO TO 81
              DOM(J)=SDO(I)
```

```
  81  CONTINUE
C   THE CRITICAL DISSOLVED OXYGEN DEFFICIT AND THE CRITICAL TIME ARE
C   CALCULATED FOR THE INTERVAL
                TEST=DOM(I)*(Y2-Y1)/(Y1*BL1)
            IF(TEST.GT.1)GO TO 201
               F=ALOG((Y2/Y1)*(1.-DOM(I)*(Y2-Y1)/(Y1*BL1)))
               G=1./(Y2-Y1)
               TIMCR=G*F
               F=((Y1*BL1)/(Y2-Y1))*(EXP(-Y1*TIMCR)-EXP(-Y2*TIMCR))
               G=DOM(I)*EXP(-Y2*TIMCR)
               DOCR=F+G
C  THE CRITICAL DISTANCE FROM THE POINT OF DISCHARGE IS NOW CALCULATED WHERE
C     THE DISSOLVED OXYGEN DEFICIT IS A MAXIMUM
               DISTCR=VAV*TIMCR*86400.
  201 WRITE(6,104)DO(IP1),BL(IP1),Q(IP1)
  104  FORMAT(' THE EFFLUENT OR TRIBUTARY'///' D.O.=',F5.2,' MG/L,  B.O.D.
     X=',F8.2,' MG/L      Q=',F8.2,' CFS',///)
       WRITE(6,106)SDO(I)
  106  FORMAT(' THE SATURATED DISSOLVED OXYGEN VALUE AT THE POINT OF DISC
     XHARGE =',F5.3,' MG/L'///)
       WRITE(6,105)Y1,Y2
  105  FORMAT(' COEFFICIENT OF DEOXYGENATION, Y1=',F6.3,/'COEFFICIENT OF
     XREAERATION,Y2=',F7.3,///)
C     THE RESULTS ARE WRITTEN OUT FOR TWO DIFFERENT CASES--1) WHEN THE EXISTS
C      A DISSOLVED OXYGEN DEFICIT MAXIMUM WITHIN THE INTERVAL  AND 2)  WHEN
C     THE MAXIMUM IS AT THE ENDD OF THE INTERVAL
            IF(TEST.GT.1)GO TO 17
           IF(TIMCR.GT.TIME) GO TO 17
           IF(TIMCR.LT.0) GO TO 17
       WRITE(6,50)DOM(I),DOM(LP1),BL1,BL2,DOCR,DISTCR,TIMCR
   50  FORMAT(' D.O. DEFICIT AT POINT OF DISCHARGE=',F5.2,' MG/L'/
     X ' D.O. DEFICIT AT END OF INTERVAL=',F5.2,' MG/L'/
     X ' B.O.D. AT POINT OF DISCHARGE=',F8.2,' MG/L'/
     X ' B.O.D. AT END OF INTERVAL=',F8.2,' MG/L'/
     X ' CRITICAL D.O. DEFICIT=',F5.2,' MG/L AT',F12.2,' FEET BELOW POIN
     XT OF DISCHARGE',F5.2,' DAYS DOWNSTREAM')
            GO TO 18
   17   WRITE(6,51) DOM(I),DOM(LP1),BL1,BL2
   51   FORMAT(' D.O. DEFICIT AT POINT OF DISCHARGE=',F5.2,' MG/L'/
     X ' D.O. DEFICIT AT END OF INTERVAL=',F5.2,' MG/L'/
     X ' B.O.D. AT POINT OF DISCHARGE=',F8.2,' MG/L'/
     X ' B.O.D. AT END OF INTERVAL=',F8.2,' MG/L')
   18   CALL GRAPH(DOM,L)
        WRITE(6,70)
   70   FORMAT(1H1)
   80   CONTINUE
        READ(5,1)L2
C
                TD2(L2)=D2
                TBL2(L2)=BL2
                TA(L2)=A
        WRITE(6,303)L5
  303   FORMAT(/////,' END OF SYSTEM NO.',I2,/////)
  500   CONTINUE
  600   CONTINUE
        STOP
        END
C
C
C
C
C
        SUBROUTINE VAL(Y1,Y2,VAV,HAV,TEMP)
C
C
        READ(5,1)ISW,ISQ,Y1,Y2
    1   FORMAT(2I5,2F10.2)
C       THE FIRST TEST VALUE IS A SWITCH WHICH WILL EQUAL 1 IF WE DO NOT NEED
C       TO CORRECT THE COEFFICIENTS VALUE TO OTHER THAN 20 DEGREES C
            IF(ISQ.EQ.1) GO TO 40
C       IF ISW EQUALS 1 , K2 HAS TO BE SUPPLIED ON A DATA CARD
            IF(ISW.EQ.1) GO TO 20
                Y2=(SQRT(.0000841*VAV*3600.)/(HAV**1.5))*24.
   20           Y1=Y1*1.047**(TEMP-20)
                Y2=Y2*1.024**(TEMP-20)
   40   RETURN
        END
C
C
C
C
C
        SUBROUTINE GRAPH(DOM,L)
C       THIS SUBROUTINE IS USED ONLY FOR AIDING IN READING AND INTERPRETING
C       THE DATA
C
C     THIS SUBROUTINE WILL TAKE THE ARRAY OF DISSOLVED OXYGEN DEFICITS IN AN
C     INTERVAL AND WRITE THEM OUT  ALONG WITH A GRAPH REPRESENTING THESE VALUES
C
        DIMENSION DOM(L),G(60,110),E(60)
        DATA AST/1H*/, BLANK/1H /
            DO 2 I=1,L
C        MAGNIFYING THE SCALE
                E(I)=10.*DOM(I)
                K=E(I)
            IF(K.EQ.0) GO TO 5
            DO 3 N=1,K
                G(I,N)=AST
    3   CONTINUE
    5           KP1=K+1
            DO 4 J=KP1,110
                G(I,J)=BLANK
    4   CONTINUE
C       WRITING OUT THE DISSOLVED OXYGEN LEVEL FOLLOWED BY A REPRESENTATIVE
C       NUMBER OF ASTERICKS
        WRITE(6,6) DOM(I),(G(I,J),J=1,110)
    6   FORMAT(1HO,F5.2,' MG/L',110A1)
    2   CONTINUE
        RETURN
        END
```

APPENDIX B

ANNUAL MINIMUM FLOWS AT WATTS, KANSAS, TAHLEQUAH, AND ELDON

ANNUAL MINIMUM FLOWS AT WATTS (07195500)

m	m/n+1	1-Day	7-Day	30-Day
1	.0527	147	151.2	241
2	.1053	118	145.1	217
3	.1579	92	113.6	184
4	.2106	88	101.3	175
5	.2632	88	91.3	118
6	.3158	86	91.3	116
7	.3683	68	90.7	115
8	.4211	67	80.0	113
9	.4737	60	75.0	105
10	.5264	52	71.8	104
11	.5790	51	64.0	100
12	.6316	46	55.0	97.4
13	.6843	41	53.0	73.5
14	.7369	39	46.7	69.9
15	.7895	33	34.4	56.5
16	.8421	30	32.7	44.2
17	.8948	10	13.8	20.9
18	.9474	10	11.1	14.9

ANNUAL MINIMUM FLOWS AT KANSAS (07196000)

m	m/n+1	1-Day	7-Day	30-Day
1	.0527	24	26.3	49.1
2	.1053	22	22.8	46.3
3	.1579	21	22.4	31.5
4	.2106	19	20.4	28.7
5	.2632	19	19.4	25.2
6	.3158	17	17.7	23.9
7	.3685	16	16.7	23.3
8	.4211	15	15.4	22.6
9	.4737	13	13.9	20.7
10	.5264	11	12.0	18.5
11	.5790	10	11.7	18.3
12	.6316	10	11.0	14.7
13	.6843	9.8	11.0	14.7
14	.7369	7	10.8	13.0
15	.7895	7	7.8	12.5
16	.8421	4	4.0	9.9
17	.8948	0.8	0.9	1.3
18	.9474	0.6	0.7	0.73

ANNUAL MINIMUM FLOWS AT TAHLEQUAH (07196500)

m	m/n+1	1-Day	7-Day	30-Day
1	.0257	206	221.0	380
2	.0513	183	188.1	309
3	.0770	182	187.7	255
4	.1026	174	186.6	242
5	.1282	152	159.4	224
6	.1539	144	154.3	215
7	.1795	141	149.0	214
8	.2052	132	147.1	207
9	.2308	122	140.0	175
10	.2565	113	126.0	162
11	.2821	109	116.2	158
12	.3077	107	115.0	155
13	.3333	103	113.2	154
14	.3590	102	110.0	152
15	.3847	100	109.8	142
16	.4103	92	108.1	138
17	.4359	91	100.8	130
18	.4616	89	94.1	125
19	.4872	87	93.5	124
20	.5129	87	92.4	124
21	.5385	83	86.4	121
22	.5641	79	84.4	121
23	.5898	78	83.6	121
24	.6154	78	82.3	117
25	.6411	77	81.0	115
26	.6667	72	73.1	113
27	.6923	69	72.1	105
28	.7180	61	65.1	93.5
29	.7436	58	60.6	84.5
30	.7693	51	51.7	78
31	.7949	38	40.7	62.5
32	.8206	38	39.7	49.6
33	.8462	30	33.0	45.7
34	.8718	6	32.0	45.6
35	.8975	3.6	6.6	10.5
36	.9231	1.1	2.4	7.1
37	.9488	1.0	1.4	5.4
38	.9744	0.1	0.1	3.2

ANNUAL MINIMUM FLOWS AT ELDON (07197000)

m	m/n+1	1-Day	7-Day	30-Day
1	.0385	42	46	77.8
2	.0770	41	43.3	64.9
3	.1154	37	38	55.5
4	.1539	36	37.4	50
5	.1923	31	33	44
6	.2308	30	31.1	40.3
7	.2693	27	28.4	39.7
8	.3077	23	24.8	35.3
9	.3462	21	22	33.4
10	.3847	19	20.4	32
11	.4231	18	20.4	31.4
12	.4616	15	17	28.4
13	.5000	13	14.4	25.3
14	.5385	12	13.6	18.1
15	.5770	11	11.1	17
16	.6154	10	11	16.9
17	.6539	9.3	9.6	12.8
18	.6923	8.5	9.3	12.6
19	.7308	7.8	8.7	12.4
20	.7693	6	6	11.7
21	.8077	4.4	5.1	10.2
22	.8462	2.6	2.7	6.6
23	.8847	2.2	2.4	3.2
24	.9231	2.2	2.4	3.1
25	.9616	1.8	1.8	2.0

APPENDIX C

MEAN DAILY FLOW PLOTS

Mean Daily Flow Plot (cfs) Illinois River near Tahlequah, Oklahoma, November, 1963

* = simulated

\+ = observed

Nov	25.8	258.0	2580.0	Simulated	Observed	Precip
1				73.5	44.0	.00
2				64.0	52.0	0.00
3				56.9	56.0	.14
4				55.5	52.0	.00
5				62.8	50.0	.05
6				64.9	56.0	0.00
7				63.9	56.0	0.00
8				65.1	58.0	0.00
9				64.8	60.0	0.00
10				65.0	64.0	0.00
11				63.2	64.0	.00
12				62.9	66.0	.01
13				61.4	66.0	0.00
14				60.7	66.0	0.00
15				60.0	66.0	0.00
16				62.0	66.0	0.00
17				75.4	68.0	0.00
18				81.9	76.0	0.00
19				62.9	86.0	1.05
20				53.6	86.0	0.00
21				69.5	82.0	.01
22				108.9	96.0	.31
23				127.1	110.0	0.00
24				120.8	116.0	0.00
25				116.7	108.0	0.00
26				113.7	106.0	0.00
27				105.6	102.0	0.00
28				99.1	98.0	0.00
29				93.7	94.0	0.00
30				88.0	90.0	0.00

Mean Daily Flow Plot (cfs) Illinois River near Tahlequah, Oklahoma, December, 1963-January, 1964. * = simulated
+ = observed

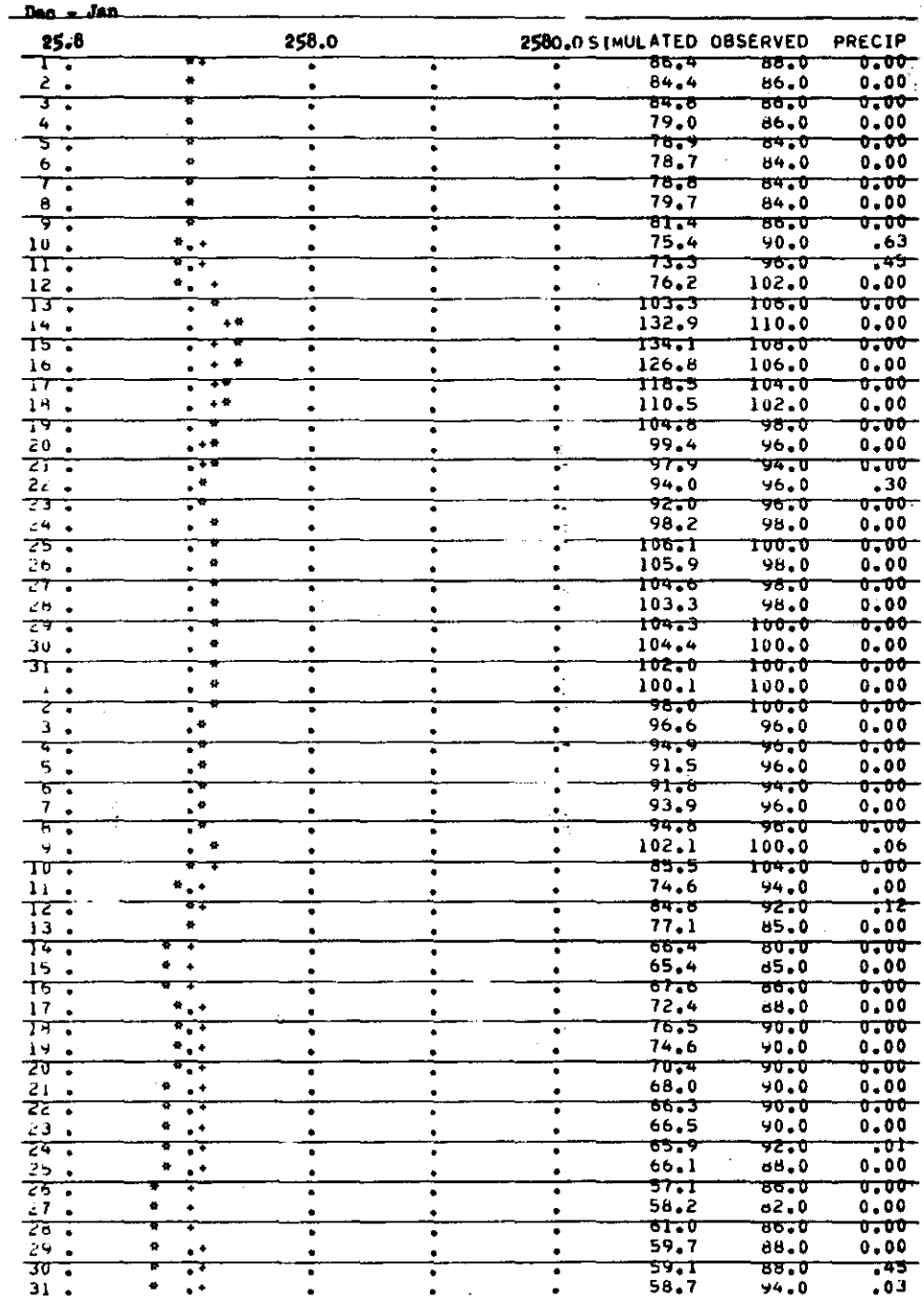

	SIMULATED	OBSERVED	PRECIP
1	86.4	88.0	0.00
2	84.4	86.0	0.00
3	84.8	86.0	0.00
4	79.0	86.0	0.00
5	78.9	84.0	0.00
6	78.7	84.0	0.00
7	78.8	84.0	0.00
8	79.7	84.0	0.00
9	81.4	86.0	0.00
10	75.4	90.0	.63
11	73.3	96.0	.45
12	76.2	102.0	0.00
13	103.3	106.0	0.00
14	132.9	110.0	0.00
15	134.1	108.0	0.00
16	126.8	106.0	0.00
17	118.5	104.0	0.00
18	110.5	102.0	0.00
19	104.8	98.0	0.00
20	99.4	96.0	0.00
21	97.9	94.0	0.00
22	94.0	96.0	.30
23	92.0	96.0	0.00
24	98.2	98.0	0.00
25	106.1	100.0	0.00
26	105.9	98.0	0.00
27	104.6	98.0	0.00
28	103.3	98.0	0.00
29	104.3	100.0	0.00
30	104.4	100.0	0.00
31	102.0	100.0	0.00
1	100.1	100.0	0.00
2	98.0	100.0	0.00
3	96.6	96.0	0.00
4	94.9	96.0	0.00
5	91.5	96.0	0.00
6	91.8	94.0	0.00
7	93.9	96.0	0.00
8	94.8	96.0	0.00
9	102.1	100.0	.06
10	85.5	104.0	0.00
11	74.6	94.0	.00
12	84.8	92.0	.12
13	77.1	85.0	0.00
14	66.4	80.0	0.00
15	65.4	85.0	0.00
16	67.6	86.0	0.00
17	72.4	88.0	0.00
18	76.5	90.0	0.00
19	74.6	90.0	0.00
20	70.4	90.0	0.00
21	68.0	90.0	0.00
22	66.3	90.0	0.00
23	66.5	90.0	0.00
24	65.9	92.0	.01
25	66.1	88.0	0.00
26	57.1	86.0	0.00
27	58.2	82.0	0.00
28	61.0	86.0	0.00
29	59.7	88.0	0.00
30	59.1	88.0	.45
31	58.7	94.0	.03

Mean Daily Flow Plot (cfs) Illinois River near Tahlequah, Oklahoma, February - March, 1964. * = simulated + = observed

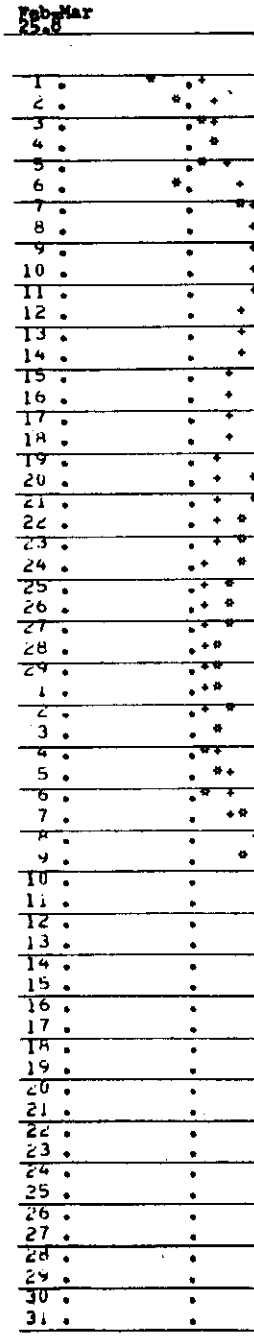

	STIMULATED	OBSERVED	PRECIP
1	58.0	94.0	.00
2	75.2	98.0	0.00
3	89.7	100.0	0.00
4	100.7	102.0	.40
5	92.1	122.0	1.03
6	76.7	128.0	.00
7	131.9	138.0	0.00
8	228.2	145.0	0.00
9	239.8	148.0	0.00
10	222.3	145.0	0.00
11	196.8	138.0	0.00
12	176.4	130.0	.30
13	175.1	132.0	.00
14	160.5	130.0	0.00
15	156.7	118.0	.07
16	167.9	116.0	.05
17	160.6	114.0	0.00
18	158.5	110.0	.04
19	157.0	108.0	.01
20	147.1	104.0	.00
21	141.0	100.0	.00
22	135.3	100.0	0.00
23	129.7	100.0	0.00
24	124.9	95.0	0.00
25	120.4	95.0	0.00
26	117.1	94.0	0.00
27	112.5	92.0	0.00
28	105.8	90.0	0.00
29	103.6	90.0	0.00
1	104.2	90.0	0.00
2	114.6	94.0	0.00
3	99.2	98.0	0.00
4	95.4	98.0	.53
5	103.1	112.0	0.00
6	93.7	116.0	.01
7	129.9	116.0	.26
8	166.3	136.0	.71
9	136.1	181.0	1.53
10	175.5	218.0	.01
11	827.9	357.0	0.00
12	951.7	477.0	0.00
13	856.2	530.0	0.00
14	764.5	535.0	0.00
15	642.5	464.0	0.00
16	538.8	405.0	0.00
17	486.6	352.0	0.00
18	425.0	316.0	.15
19	374.1	320.0	1.21
20	367.1	374.0	.00
21	922.8	446.0	.02
22	890.6	486.0	0.00
23	745.2	477.0	0.00
24	633.8	441.0	0.00
25	546.6	392.0	.00
26	496.0	348.0	0.00
27	446.9	320.0	0.00
28	406.3	296.0	.00
29	371.2	273.0	0.00
30	328.5	248.0	.03
31	302.1	238.0	0.00

Mean Daily Flow Plot (cfs) Illinois River near Tahlequah, Oklahoma, April - May, 1964. * = similated
+ = observed

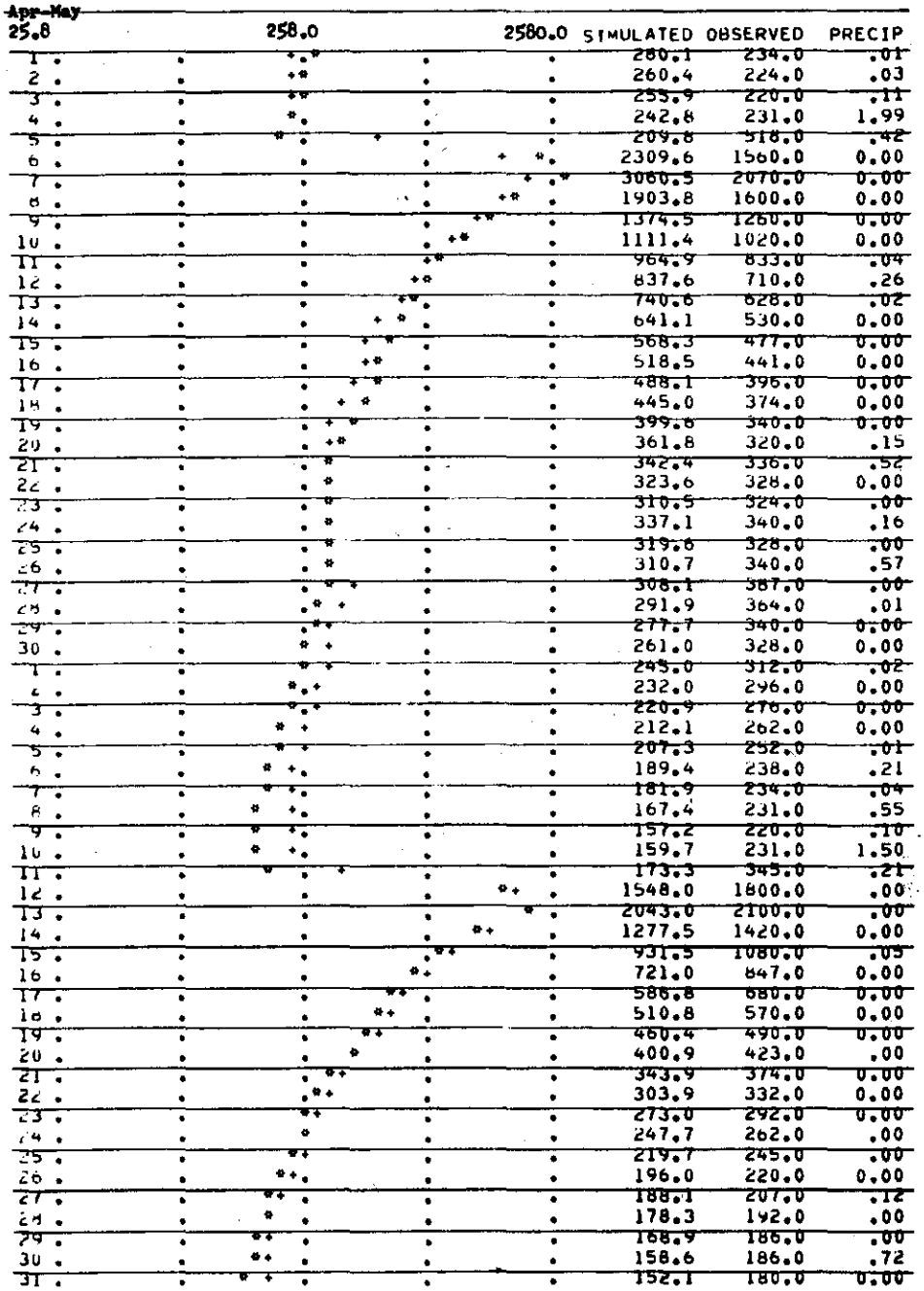

Apr-May 25.8	258.0	2580.0	SIMULATED	OBSERVED	PRECIP
1			280.1	234.0	.01
2			260.4	224.0	.03
3			255.9	220.0	.11
4			242.8	231.0	1.99
5			209.8	518.0	.42
6			2309.6	1560.0	0.00
7			3060.5	2070.0	0.00
8			1903.8	1600.0	0.00
9			1374.5	1260.0	0.00
10			1111.4	1020.0	0.00
11			964.9	833.0	.04
12			837.6	710.0	.26
13			740.6	628.0	.02
14			641.1	530.0	0.00
15			568.3	477.0	0.00
16			518.5	441.0	0.00
17			488.1	396.0	0.00
18			445.0	374.0	0.00
19			399.6	340.0	0.00
20			361.8	320.0	.15
21			342.4	336.0	.52
22			323.6	328.0	0.00
23			310.5	324.0	.00
24			337.1	340.0	.16
25			319.6	328.0	.00
26			310.7	340.0	.57
27			308.1	387.0	.00
28			291.9	364.0	.01
29			277.7	340.0	0.00
30			261.0	328.0	0.00
1			245.0	312.0	.02
2			232.0	296.0	0.00
3			220.9	276.0	0.00
4			212.1	262.0	0.00
5			207.3	252.0	.01
6			189.4	238.0	.21
7			181.9	234.0	.04
8			167.4	231.0	.55
9			157.2	220.0	.10
10			159.7	231.0	1.50
11			173.3	345.0	.21
12			1548.0	1800.0	.00
13			2043.0	2100.0	.00
14			1277.5	1420.0	0.00
15			931.5	1080.0	.05
16			721.0	847.0	0.00
17			586.8	680.0	0.00
18			510.8	570.0	0.00
19			460.4	490.0	0.00
20			400.9	423.0	.00
21			343.9	374.0	0.00
22			303.9	332.0	0.00
23			273.0	292.0	0.00
24			247.7	262.0	.00
25			219.7	245.0	.00
26			196.0	220.0	0.00
27			188.1	207.0	.12
28			178.3	192.0	.00
29			168.9	186.0	.00
30			158.6	186.0	.72
31			152.1	180.0	0.00

Mean Daily Flow Plot (cfs) Illinois River near Tahlequah, Oklahoma, June - July, 1964. * = simulated + = observed

June - July 25.8	258.0	2580.0	SIMULATED	OBSERVED.	PRECIP
1			163.8	180.0	0.00
2			185.2	177.0	.10
3			183.2	174.0	0.00
4			171.3	171.0	.26
5			162.1	168.0	.25
6			163.3	171.0	.01
7			155.6	168.0	.00
8			156.4	162.0	0.00
9			157.7	153.0	0.00
10			148.9	153.0	0.00
11			120.0	142.0	.00
12			93.5	128.0	1.49
13			83.5	123.0	1.13
14			99.9	125.0	0.00
15			257.3	153.0	0.00
16			347.6	189.0	.38
17			326.6	201.0	2.23
18			456.7	358.0	0.00
19			1636.3	1390.0	0.00
20			1231.8	1050.0	0.00
21			892.1	716.0	0.00
22			688.9	540.0	0.00
23			566.0	441.0	.46
24			500.9	374.0	0.00
25			445.6	316.0	0.00
26			395.9	266.0	0.00
27			351.4	234.0	0.00
28			312.5	223.0	.56
29			282.8	276.0	.06
30			262.6	262.0	0.00
[illegible]			248.3	217.0	.00
2			240.1	195.0	0.00
3			219.9	174.0	0.00
4			202.6	156.0	0.00
5			181.4	145.0	0.00
6			159.5	132.0	0.00
7			142.4	123.0	0.00
8			128.7	115.0	0.00
9			114.5	107.0	.13
10			108.1	103.0	0.00
11			102.5	95.0	.02
12			100.2	91.0	.02
13			99.3	89.0	.00
14			91.9	85.0	0.00
15			88.2	82.0	0.00
16			83.7	78.0	0.00
17			77.3	75.0	0.00
18			72.3	71.0	0.00
19			68.0	67.0	0.00
20			64.5	61.0	0.00
21			62.4	58.0	0.00
22			59.0	55.0	0.00
23			56.9	52.0	.12
24			55.2	51.0	0.00
25			55.4	48.0	.00
26			54.2	46.0	.02
27			50.8	45.0	.04
28			49.2	44.0	.12
29			48.3	42.0	0.00
30			48.0	40.0	0.00
31			47.6	39.0	0.00

Mean Daily Flow Plot (cfs) Illinois River near Tahlequah, Oklahoma, August - September, 1967. * = simulated
+ = observed

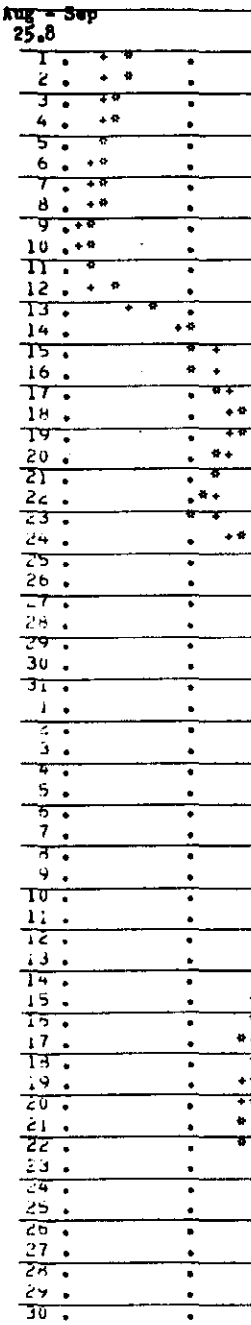

	SIMULATED	OBSERVED	PRECIP
1	47.1	38.0	0.00
2	43.5	37.0	0.00
3	41.2	36.0	0.00
4	39.7	35.0	0.00
5	38.0	35.0	0.00
6	37.5	34.0	.01
7	36.6	33.0	.00
8	35.1	32.0	.00
9	33.9	30.0	0.00
10	33.3	30.0	1.38
11	32.4	33.0	.01
12	40.0	32.0	.00
13	57.2	48.0	0.00
14	77.2	70.0	1.23
15	81.8	99.0	.34
16	79.4	103.0	0.00
17	101.4	111.0	0.00
18	123.9	119.0	.00
19	124.7	121.0	.00
20	108.8	113.0	0.00
21	98.2	105.0	.87
22	95.2	101.0	0.00
23	85.4	103.0	0.00
24	128.9	120.0	.00
25	194.0	188.0	.74
26	168.7	259.0	1.85
27	187.4	329.0	0.00
28	470.9	911.0	1.71
29	764.4	1230.0	.07
30	1139.2	1760.0	1.36
31	1183.8	1520.0	.01
1	1211.8	1520.0	.03
2	923.5	1160.0	0.00
3	694.0	840.0	0.00
4	564.7	639.0	0.00
5	497.2	510.0	.03
6	441.8	428.0	0.00
7	392.4	360.0	0.00
8	354.0	316.0	0.00
9	320.9	273.0	0.00
10	284.1	242.0	0.00
11	258.3	217.0	.03
12	231.1	192.0	0.00
13	210.3	177.0	0.00
14	193.7	162.0	0.00
15	173.9	153.0	.00
16	149.8	145.0	.09
17	135.6	142.0	.09
18	137.6	138.0	.01
19	143.6	132.0	0.00
20	149.8	135.0	.54
21	135.1	162.0	.74
22	126.7	196.0	.93
23	323.5	350.0	0.00
24	944.9	1220.0	0.00
25	870.3	1080.0	0.00
26	608.0	700.0	.41
27	491.1	525.0	.18
28	411.3	432.0	0.00
29	395.2	400.0	0.00
30	408.6	396.0	.00

Mean Daily Flow Plots (cfs) Illinois River near Watts, Oklahoma, October - November, 1964. * = simulated
+ = observed

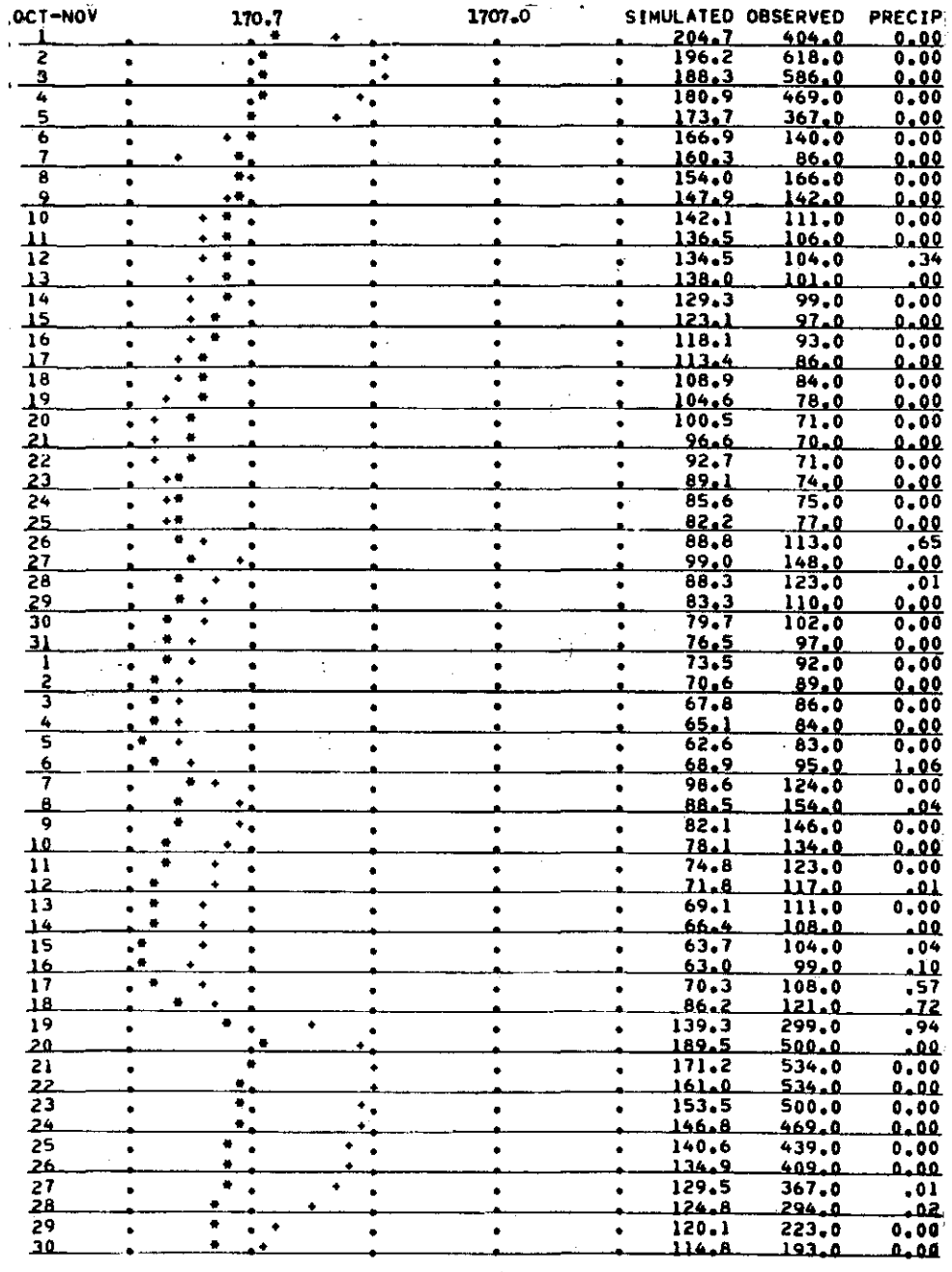

	SIMULATED	OBSERVED	PRECIP
1	204.7	404.0	0.00
2	196.2	618.0	0.00
3	188.3	586.0	0.00
4	180.9	469.0	0.00
5	173.7	367.0	0.00
6	166.9	140.0	0.00
7	160.3	86.0	0.00
8	154.0	166.0	0.00
9	147.9	142.0	0.00
10	142.1	111.0	0.00
11	136.5	106.0	0.00
12	134.5	104.0	.34
13	138.0	101.0	.00
14	129.3	99.0	0.00
15	123.1	97.0	0.00
16	118.1	93.0	0.00
17	113.4	86.0	0.00
18	108.9	84.0	0.00
19	104.6	78.0	0.00
20	100.5	71.0	0.00
21	96.6	70.0	0.00
22	92.7	71.0	0.00
23	89.1	74.0	0.00
24	85.6	75.0	0.00
25	82.2	77.0	0.00
26	88.8	113.0	.65
27	99.0	148.0	0.00
28	88.3	123.0	.01
29	83.3	110.0	0.00
30	79.7	102.0	0.00
31	76.5	97.0	0.00
1	73.5	92.0	0.00
2	70.6	89.0	0.00
3	67.8	86.0	0.00
4	65.1	84.0	0.00
5	62.6	83.0	0.00
6	68.9	95.0	1.06
7	98.6	124.0	0.00
8	88.5	154.0	.04
9	82.1	146.0	0.00
10	78.1	134.0	0.00
11	74.8	123.0	0.00
12	71.8	117.0	.01
13	69.1	111.0	0.00
14	66.4	108.0	.00
15	63.7	104.0	.04
16	63.0	99.0	.10
17	70.3	108.0	.57
18	86.2	121.0	.72
19	139.3	299.0	.94
20	189.5	500.0	.00
21	171.2	534.0	0.00
22	161.0	534.0	0.00
23	153.5	500.0	0.00
24	146.8	469.0	0.00
25	140.6	439.0	0.00
26	134.9	409.0	0.00
27	129.5	367.0	.01
28	124.8	294.0	.02
29	120.1	223.0	0.00
30	114.8	193.0	0.00

Mean Daily Flow Plots (cfs) Illinois River near Watts, Oklahoma, December, 1963 - January, 1974. * = simulated + = observed

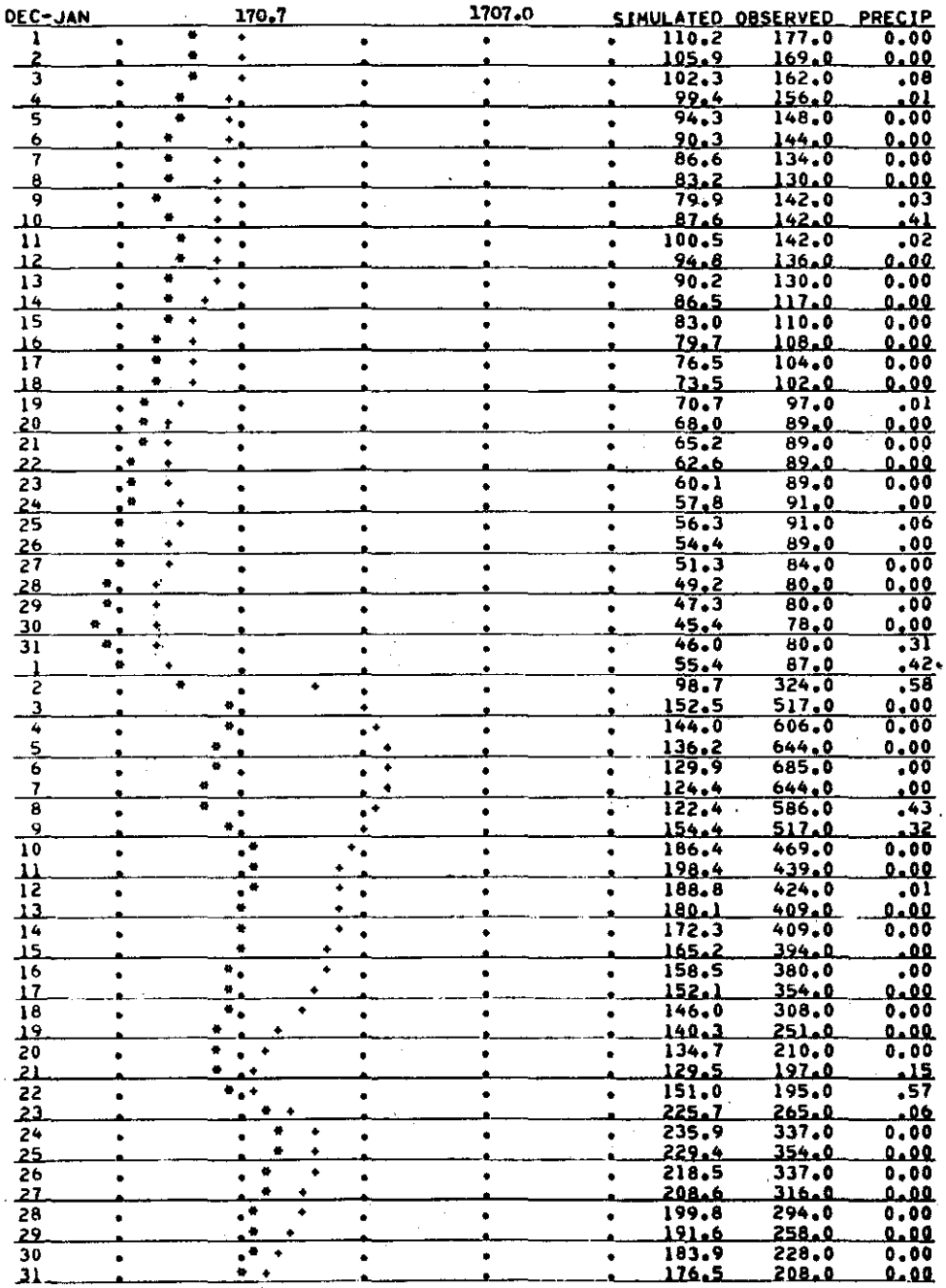

DEC-JAN	SIMULATED	OBSERVED	PRECIP
1	110.2	177.0	0.00
2	105.9	169.0	0.00
3	102.3	162.0	.08
4	99.4	156.0	.01
5	94.3	148.0	0.00
6	90.3	144.0	0.00
7	86.6	134.0	0.00
8	83.2	130.0	0.00
9	79.9	142.0	.03
10	87.6	142.0	.41
11	100.5	142.0	.02
12	94.8	136.0	0.00
13	90.2	130.0	0.00
14	86.5	117.0	0.00
15	83.0	110.0	0.00
16	79.7	108.0	0.00
17	76.5	104.0	0.00
18	73.5	102.0	0.00
19	70.7	97.0	.01
20	68.0	89.0	0.00
21	65.2	89.0	0.00
22	62.6	89.0	0.00
23	60.1	89.0	0.00
24	57.8	91.0	.00
25	56.3	91.0	.06
26	54.4	89.0	.00
27	51.3	84.0	0.00
28	49.2	80.0	0.00
29	47.3	80.0	.00
30	45.4	78.0	0.00
31	46.0	80.0	.31
1	55.4	87.0	.42
2	98.7	324.0	.58
3	152.5	517.0	0.00
4	144.0	606.0	0.00
5	136.2	644.0	0.00
6	129.9	685.0	.00
7	124.4	644.0	.00
8	122.4	586.0	.43
9	154.4	517.0	.32
10	186.4	469.0	0.00
11	198.4	439.0	0.00
12	188.8	424.0	.01
13	180.1	409.0	0.00
14	172.3	409.0	0.00
15	165.2	394.0	.00
16	158.5	380.0	.00
17	152.1	354.0	0.00
18	146.0	308.0	0.00
19	140.3	251.0	0.00
20	134.7	210.0	0.00
21	129.5	197.0	.15
22	151.0	195.0	.57
23	225.7	265.0	.06
24	235.9	337.0	0.00
25	229.4	354.0	0.00
26	218.5	337.0	0.00
27	208.6	316.0	0.00
28	199.8	294.0	0.00
29	191.6	258.0	0.00
30	183.9	228.0	0.00
31	176.5	208.0	0.00

Mean Daily Flow Plots (cfs) Illinois River near Watts, Oklahoma, February - March, 1964. * = simulated + = observed

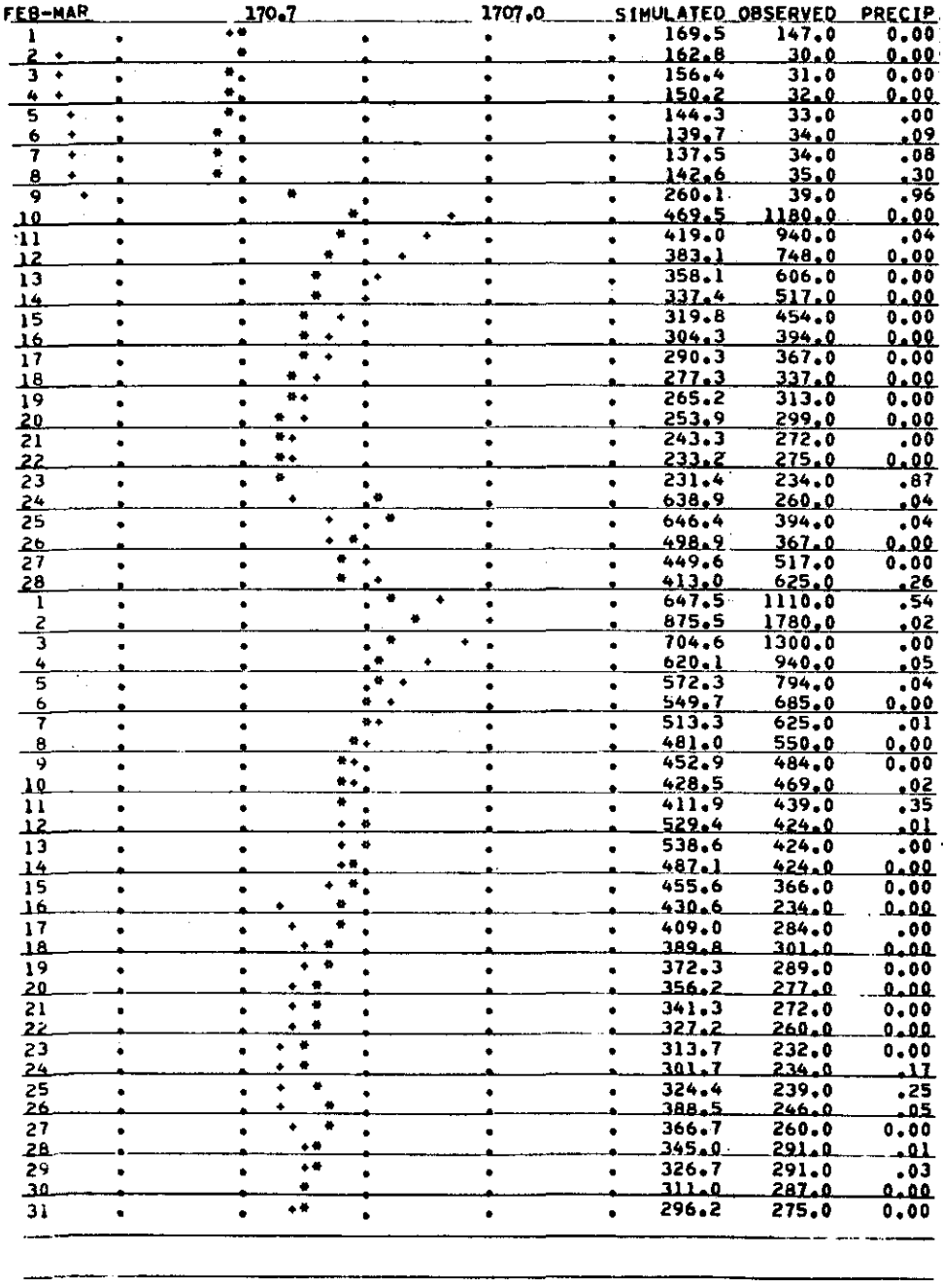

FEB-MAR	170.7	1707.0	SIMULATED	OBSERVED	PRECIP
1			169.5	147.0	0.00
2			162.8	30.0	0.00
3			156.4	31.0	0.00
4			150.2	32.0	0.00
5			144.3	33.0	.00
6			139.7	34.0	.09
7			137.5	34.0	.08
8			142.6	35.0	.30
9			260.1	39.0	.96
10			469.5	1180.0	0.00
11			419.0	940.0	.04
12			383.1	748.0	0.00
13			358.1	606.0	0.00
14			337.4	517.0	0.00
15			319.8	454.0	0.00
16			304.3	394.0	0.00
17			290.3	367.0	0.00
18			277.3	337.0	0.00
19			265.2	313.0	0.00
20			253.9	299.0	0.00
21			243.3	272.0	.00
22			233.2	275.0	0.00
23			231.4	234.0	.87
24			638.9	260.0	.04
25			646.4	394.0	.04
26			498.9	367.0	0.00
27			449.6	517.0	0.00
28			413.0	625.0	.26
1			647.5	1110.0	.54
2			875.5	1780.0	.02
3			704.6	1300.0	.00
4			620.1	940.0	.05
5			572.3	794.0	.04
6			549.7	685.0	0.00
7			513.3	625.0	.01
8			481.0	550.0	0.00
9			452.9	484.0	0.00
10			428.5	469.0	.02
11			411.9	439.0	.35
12			529.4	424.0	.01
13			538.6	424.0	.00
14			487.1	424.0	0.00
15			455.6	366.0	0.00
16			430.6	234.0	0.00
17			409.0	284.0	.00
18			389.8	301.0	0.00
19			372.3	289.0	0.00
20			356.2	277.0	0.00
21			341.3	272.0	0.00
22			327.2	260.0	0.00
23			313.7	232.0	0.00
24			301.7	234.0	.17
25			324.4	239.0	.25
26			388.5	246.0	.05
27			366.7	260.0	0.00
28			345.0	291.0	.01
29			326.7	291.0	.03
30			311.0	287.0	0.00
31			296.2	275.0	0.00

Mean Daily Flow Plots (cfs) Illinois River near Watts, Oklahoma, April - May, 1964. * = simulated + = observed

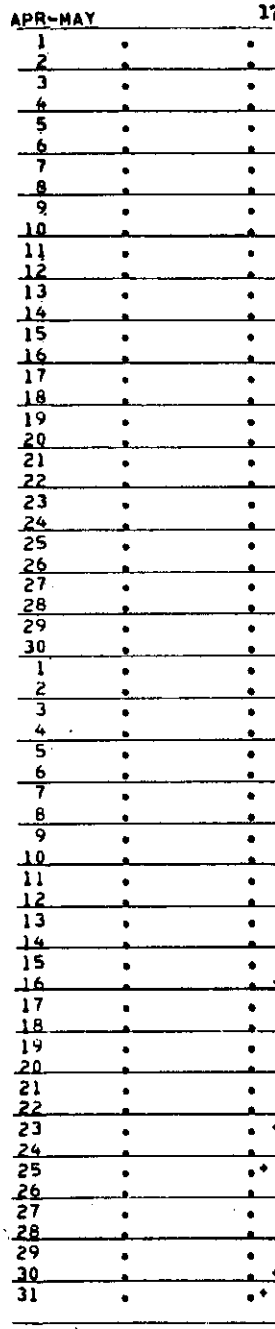

	SIMULATED	OBSERVED	PRECIP
1	283.0	260.0	0.00
2	711.8	352.0	1.74
3	4486.0	5000.0	.53
4	3017.5	3000.0	.07
5	2387.0	3500.0	1.42
6	5311.8	6950.0	.00
7	3494.3	3530.0	.06
8	2919.3	2620.0	.49
9	2723.1	2470.0	.01
10	2097.1	1710.0	.07
11	1750.8	1420.0	.13
12	1493.9	1240.0	0.00
13	1288.7	1020.0	.22
14	1257.6	915.0	1.14
15	2470.9	2660.0	.28
16	2296.6	2020.0	0.00
17	1722.7	1330.0	0.00
18	1462.5	1070.0	0.00
19	1281.5	915.0	0.00
20	1140.1	794.0	0.00
21	1026.2	727.0	0.00
22	932.8	498.0	0.00
23	855.1	550.0	0.00
24	789.7	517.0	.09
25	736.9	484.0	.09
26	688.6	500.0	.12
27	646.3	469.0	0.00
28	606.9	439.0	.00
29	573.3	409.0	0.00
30	543.5	380.0	0.00
1	516.5	367.0	0.00
2	491.8	354.0	0.00
3	469.0	329.0	0.00
4	447.9	277.0	0.00
5	428.2	260.0	.02
6	410.9	282.0	.11
7	394.8	277.0	0.00
8	376.4	279.0	.45
9	406.4	367.0	1.41
10	633.3	898.0	.04
11	686.3	816.0	.00
12	629.8	606.0	0.00
13	586.5	500.0	0.00
14	571.5	586.0	.37
15	580.6	360.0	.06
16	556.4	223.0	.11
17	530.0	294.0	0.00
18	505.3	270.0	.41
19	511.4	294.0	.01
20	518.5	299.0	.02
21	494.5	277.0	0.00
22	471.5	246.0	0.00
23	451.4	226.0	0.00
24	433.1	230.0	.03
25	416.3	186.0	.02
26	426.4	232.0	1.06
27	508.8	255.0	0.00
28	487.9	253.0	.08
29	459.6	228.0	0.00
30	435.8	204.0	0.00
31	416.4	193.0	.02

Mean Daily Flow Plots (cfs) Illinois River near Watts, Oklahoma, June - July, 1964. * = simulated + = observed

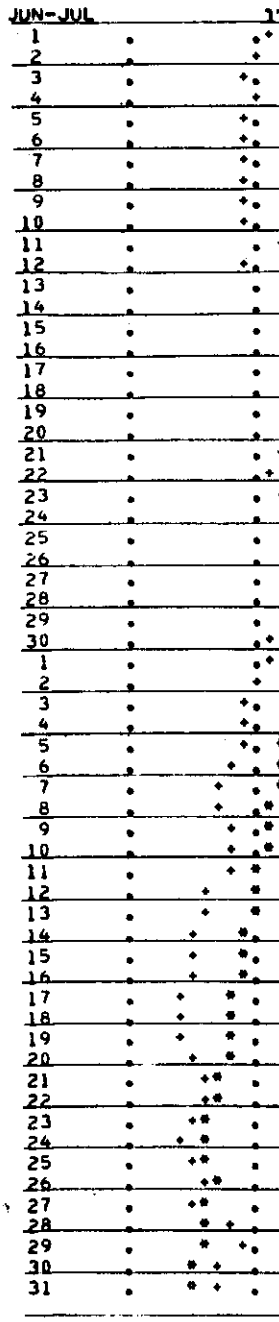

JUN-JUL	SIMULATED	OBSERVED	PRECIP
1	399.4	182.0	.00
2	382.7	169.0	.01
3	367.1	160.0	0.00
4	352.2	164.0	.00
5	338.2	158.0	.01
6	324.8	148.0	0.00
7	311.9	146.0	.03
8	311.1	146.0	.67
9	336.1	146.0	0.00
10	323.6	150.0	.49
11	332.5	205.0	.13
12	327.3	154.0	.43
13	334.4	290.0	.41
14	352.5	240.0	.40
15	347.3	898.0	.27
16	352.5	606.0	.00
17	335.8	367.0	0.00
18	320.4	313.0	0.00
19	306.8	253.0	0.00
20	294.3	228.0	0.00
21	296.4	204.0	.68
22	310.4	186.0	.52
23	325.7	204.0	.20
24	331.5	728.0	.29
25	336.1	706.0	.00
26	318.8	409.0	.00
27	304.2	282.0	0.00
28	291.3	275.0	0.00
29	279.4	251.0	0.00
30	268.3	199.0	0.00
1	257.6	182.0	0.00
2	247.4	177.0	0.00
3	237.7	156.0	0.00
4	228.8	154.0	.07
5	220.8	144.0	0.00
6	210.9	136.0	.08
7	204.9	128.0	.26
8	200.1	128.0	0.00
9	192.7	140.0	.12
10	183.3	140.0	0.00
11	174.6	130.0	.00
12	167.8	111.0	.10
13	162.5	106.0	0.00
14	156.2	97.0	.34
15	158.5	97.0	0.00
16	147.8	95.0	0.00
17	140.6	89.0	0.00
18	134.9	87.0	.13
19	131.8	86.0	.05
20	128.2	99.0	.00
21	120.7	108.0	.00
22	115.7	102.0	.01
23	111.2	95.0	0.00
24	106.6	87.0	0.00
25	104.2	101.0	.74
26	120.7	111.0	0.00
27	109.6	99.0	.21
28	109.5	130.0	.30
29	109.4	148.0	0.00
30	99.2	126.0	0.00
31	94.6	115.0	0.00

Mean Daily Flow Plots (cfs) Illinois River near Watts, Oklahoma, August - September, 1964. * = simulated
+ = observed

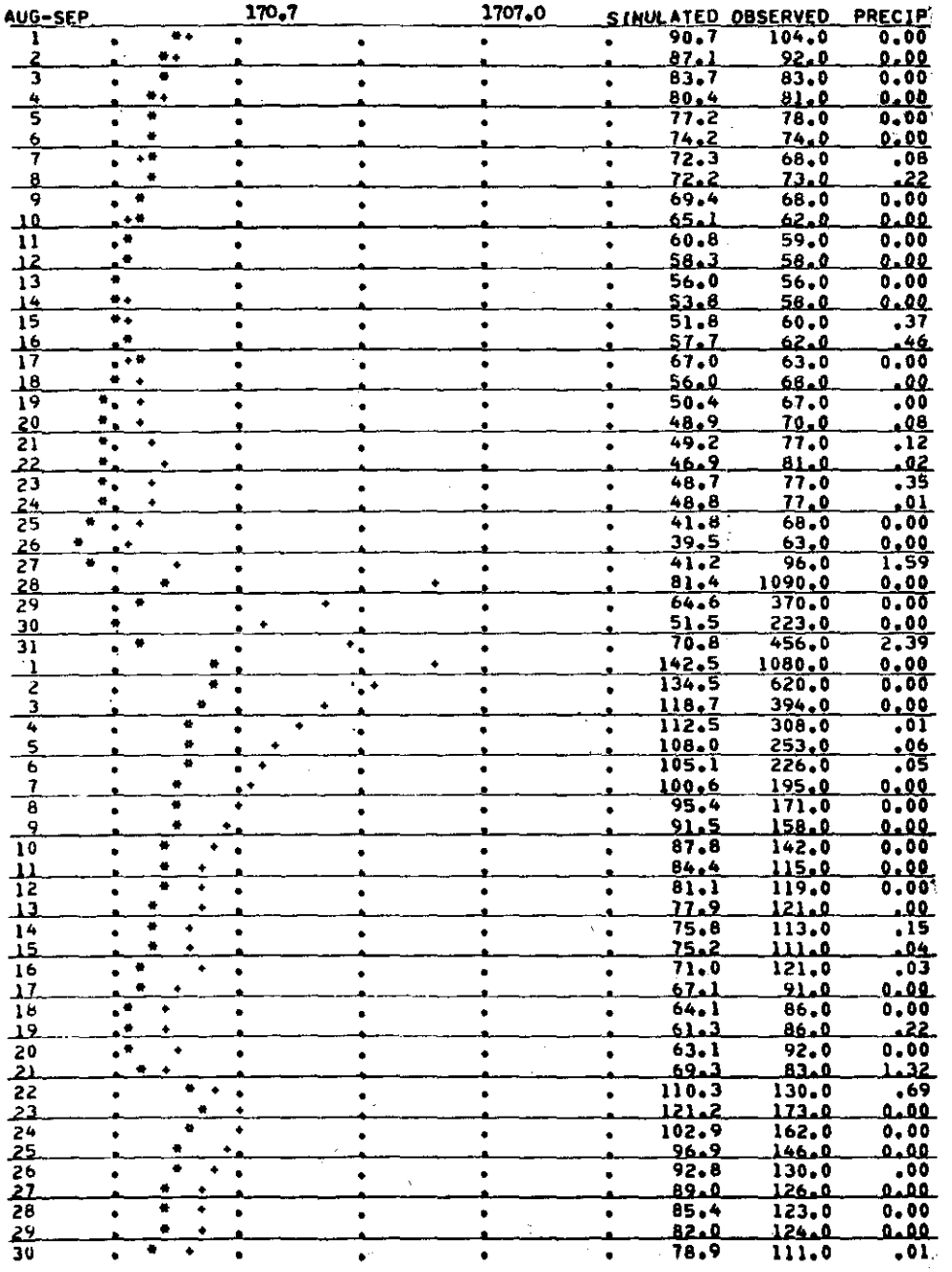

	SIMULATED	OBSERVED	PRECIP
1	90.7	104.0	0.00
2	87.1	92.0	0.00
3	83.7	83.0	0.00
4	80.4	81.0	0.00
5	77.2	78.0	0.00
6	74.2	74.0	0.00
7	72.3	68.0	.08
8	72.2	73.0	.22
9	69.4	68.0	0.00
10	65.1	62.0	0.00
11	60.8	59.0	0.00
12	58.3	58.0	0.00
13	56.0	56.0	0.00
14	53.8	58.0	0.00
15	51.8	60.0	.37
16	57.7	62.0	.46
17	67.0	63.0	0.00
18	56.0	68.0	.00
19	50.4	67.0	.00
20	48.9	70.0	.08
21	49.2	77.0	.12
22	46.9	81.0	.02
23	48.7	77.0	.35
24	48.8	77.0	.01
25	41.8	68.0	0.00
26	39.5	63.0	0.00
27	41.2	96.0	1.59
28	81.4	1090.0	0.00
29	64.6	370.0	0.00
30	51.5	223.0	0.00
31	70.8	456.0	2.39
1	142.5	1080.0	0.00
2	134.5	620.0	0.00
3	118.7	394.0	0.00
4	112.5	308.0	.01
5	108.0	253.0	.06
6	105.1	226.0	.05
7	100.6	195.0	0.00
8	95.4	171.0	0.00
9	91.5	158.0	0.00
10	87.8	142.0	0.00
11	84.4	115.0	0.00
12	81.1	119.0	0.00
13	77.9	121.0	.00
14	75.8	113.0	.15
15	75.2	111.0	.04
16	71.0	121.0	.03
17	67.1	91.0	0.00
18	64.1	86.0	0.00
19	61.3	86.0	.22
20	63.1	92.0	0.00
21	69.3	83.0	1.32
22	110.3	130.0	.69
23	121.2	173.0	0.00
24	102.9	162.0	0.00
25	96.9	146.0	0.00
26	92.8	130.0	.00
27	89.0	126.0	0.00
28	85.4	123.0	0.00
29	82.0	124.0	0.00
30	78.9	111.0	.01